EXPERIMENTAL INVESTIGATION OF CENOSPHERE EPOXY SYNTACTIC FOAM COMPOSITES

Thesis

Submitted in partial fulfillment of the requirements for the degree of

DOCTOR OF PHILOSOPHY

by

KIRAN SHAHAPURKAR

DEPARTMENT OF MECHANICAL ENGINEERING

NATIONAL INSTITUTE OF TECHNOLOGY KARNATAKA,

SURATHKAL, MANGALORE – 575025

AUGUST, 2018

D E C L A R A T I O N

I hereby *declare* that the Research Thesis entitled **"EXPERIMENTAL INVESTIGATION OF CENOSPHERE EPOXY SYNTACTIC FOAM COMPOSITES"** which is being submitted to the **National Institute of Technology Karnataka, Surathkal** in partial fulfillment of the requirements for the award of the Degree of **Doctor of Philosophy** in **Department of Mechanical Engineering** is a *bonafide report of the research work carried out by me*. The material contained in this Research Thesis has not been submitted to any University or Institution for the award of any degree.

Register Number   : **155108ME15F06**

Name of the Research Scholar   : **KIRAN SHAHAPURKAR**

Signature of the Research Scholar :

<div align="center">Department of Mechanical Engineering</div>

Place   : **NITK, Surathkal**

Date   :

C E R T I F I C A T E

This is to *certify* that the Research Thesis entitled **"EXPERIMENTAL INVESTIGATION OF CENOSPHERE EPOXY SYNTACTIC FOAM COMPOSITES"** submitted by **Mr. KIRAN SHAHAPURKAR** (**Register Number: 155108ME15F06**) as the record of the research work carried out by him, is *accepted as the Research Thesis submission* in partial fulfillment of the requirements for the award of degree of **Doctor of Philosophy.**

Research Guides

Dr. Mrityunjay Doddamani

Assistant Professor

Department of Mechanical Engineering

Dr. G. C. Mohan Kumar

Professor

Department of Mechanical Engineering

Chairman – DRPC

Date:

ACKNOWLEDGEMENT

ABSTRACT

Polymer matrix composites provide lower weight structures and result in improved efficiency and performance in transportation applications. Thermosetting polymers when used with suitable hollow reinforcing constituents, higher specific properties can be achieved that cater to variety of applications. Development of syntactic foams with cenospheres serves dual purpose of beneficial utilization of industrial waste fly ash and reduction in the component cost in addition to weight reduction. In the present study, LAPOX L-12 epoxy resin is used as the matrix material and fly ash cenospheres (hollow microspheres) in as received and silane modified conditions are used as filler. Manual stirring method is employed for developing cenosphere/epoxy syntactic foams with as received and surface treated cenospheres in 20, 40 and 60 volume %. With increasing cenosphere content, density of untreated and silane treated foams decreases. Influence of cenosphere surface treatment and volume fraction of cenospheres in epoxy matrix on compression, quasi-static compression, flexural, tensile, dynamic mechanical analysis, wear and erosion properties are investigated in this work.

Effect of arctic conditions on the compressive and flexural response of cenosphere/epoxy syntactic foams is dealt to understand the behavior of foams under extreme conditions. Samples are conditioned under arctic environment at a temperature of -60°C. Compression and flexural tests are then conducted at room temperature as well as at in-situ -60°C on the conditioned samples and compared against unconditioned samples tested at room temperature. For the case of unconditioned samples, compressive strength decreased whereas compressive modulus increased with increasing cenosphere volume fraction for both surface modified and as received cenospheres. For the arctic conditioned samples, a reduction in compressive modulus and significant increase in strength is observed for untreated and treated syntactic foams as compared to their unconditioned counterparts. Increase in flexural modulus is noted while a decrease in flexural strength is observed as compared to neat resin at room temperature with increasing filler content for both untreated and treated cenosphere reinforced syntactic foams. For the case of arctic

exposed samples, an apparent increase in flexural modulus is observed as compared to room temperature tested cenospheres/epoxy syntactic foams. In addition, an apparent increase in the flexural strength is noted under arctic environment.

Room temperature quasi-static compressive response is investigated at different strain rates. The energy absorption of syntactic foams increases with increase in cenosphere content. Compressive modulus of untreated and treated syntactic foams is observed to be higher than that of neat epoxy sample at the same strain rate. Silane treated foams exhibit higher modulus. Yield strength of untreated and treated foams decreases as compared to neat epoxy. Tensile modulus of both untreated and treated syntactic foams increases with increase in cenosphere volume fraction as compared to neat epoxy. Strength values of syntactic foams show decreasing trend as compared to neat epoxy. Treated syntactic foams registered better results as compared to untreated ones. Storage modulus increases with increasing cenosphere content and decreases with increasing temperature. Loss modulus of syntactic register lower values as compared to neat epoxy, while damping is noted to be increasing. Syntactic foams with treated cenospheres reveal higher values of damping for all the volume fractions. Treated syntactic foams render higher stiffness and damping as compared to untreated syntactic foams and neat epoxy at elevated temperatures. Wear rate decreases with increasing cenosphere content at all the tested conditions. Specific wear rate decreases significantly with increasing applied loads. Further, coefficient of friction decreases with higher filler loading and filler surface modifications. Wear debris is analysed further and disc temperature is also reported.

Erosion behavior is studied at room temperature for 30 to 90° impact angles and 30 to 60 m/s velocities. Results show a strong dependence of impact angle and velocity on erosion rate of syntactic foams. With increasing cenosphere content erosion rate decreases for all impact angles. Erosion rate decreases with increasing impact angle and with decreasing velocity. Structure-property correlations of all the investigated properties are presented with the help of exhaustive SEM images to understand underlying mechanisms. Finally, the potential of using the evaluated properties are presented in the form of property map. These property maps provide guidelines to

industrial practioners and researchers in selecting appropriate materials based on the envisaged applications.

CONTENTS

LIST OF FIGURES

LIST OF TABLES

ABBREVIATIONS

APTS   : Amino propyl tri ethoxy silane

ASTM   : American Society for Testing and Materials

DGEBA   : Diglycidyl Ether of Bisphenol A

EDS   : Energy Dispersive Spectroscopy

FTIR   : Fourier Transform Infrared spectroscopy

PMC   : Polymer Matrix Composite

SEM   : Scanning Electron Microscope

SF   : Syntactic Foam

XRD   : X-ray Diffraction

NOMENCLATURE

ρ	Density of the composite	kg/m^3
ρ_f	Density of the filler	kg/m^3
V_f	Volume fraction of filler	%
ρ_m	Density of the matrix	kg/m^3
V_m	Volume fraction of matrix	%
ϕ_V	Void content	%
ρ^{th}	Theoretical density	kg/m^3
ρ^{exp}	Experimental density	kg/m^3
E_z^c	Compressive modulus	MPa
F_z^c	Compressive ultimate strength	MPa
E_{fM}	Flexural modulus	MPa
σ_{fS}	Flexural strength	MPa
V	Sliding velocity	m/s
w_t	Wear rate	mm^3/km
W	Wear volume	mm^3
W_C	Start of wear volume	mm^3
W_B	End of wear volume	mm^3
D	Sliding distance	km
D_C	Start of sliding distance	km
D_B	End of sliding distance	km
w_r	Wear resistance	km/mm^3
w_s	Specific wear rate	mm^3/km-N
F	Applied force	N
F_T	Tangential force	N
F_N	Normal force	N
μ	Coefficient of friction	----
T_g	Glass transition temperature	°C
T_{max}	Maximum use temperature	°C

$Tan\ \delta$	Damping factor	-----
E'	Storage modulus	MPa
E''	Loss modulus	MPa
E_r	Erosion rate	g/g
v	Impact velocity	m/s
k	Velocity component	----
ε	Erosion efficiency	%
H	Hardness	Pa

1   INTRODUCTION

1.1   Composite Materials

Ever increasing demands for high performance facilities with modern technology necessitates looking for new materials. Achieving such enhanced performance standards with one material is a difficult and a challenging task. Thereby novel materials are processed by combining two or more conventional materials called as composite materials to provide exclusive blend of properties that cannot be achieved from any single conventional material. Composite material is defined as "macroscopic combination of two or more different materials with a distinguishable interface between them" (Gauthier 1995). Composites are generally prepared by incorporating certain reinforcement such as fibers or particles in a matrix material. Composite materials offer advantages such as higher strength, enhanced modulus, bending stiffness and chemical resistance. According to specific design requirements, directional and spatial properties of composites can be effectively employed to tailor essential properties. Composite materials are extensively used in applications of aeronautics and space sector due to their lightweight and high strength properties. Almost all modes of transportation and sports equipment use substantial amount of composites. Particulate reinforced composites are widely used in developing lightweight composites catering to aerospace, automotive and marine applications.

1.2   Particulate Composites

Particulate composites are used as core materials in sandwich composites. Reinforcement of particulate fillers in epoxies leads to several useful properties such as reduced density, increased impact strength, desired magnetic and electrical properties, high damage tolerance and reduced cost. These properties make particulate composites suitable for use in weight sensitive applications such as aircraft structures and damage prone applications such as packaging. Sandwich structures having particulate filled composite materials as core particularly give the advantage of high specific compressive strength and bending stiffness.

1.3 Filler Materials

A variety of particles are used as fillers in composites (Norbert 1988). Purpose of using fillers are from reducing the cost of expensive polymeric components to modification in strength, magnetic, electrical or fire retardant properties and density changes as demanded by the envisaged applications. Large number of materials can be selected as fillers for the polymers, which include particles of minerals, metals, ceramics, polymers and also some industrial wastes (Gupta et al. 2001). Some common examples of filler materials are particles of alumina, silica, hollow and solid particles of glass, wood chips, fly ash and carbon black. Selection of materials is mainly based on the desired properties of the composite. The shape of the filler particles plays an important role in determining the properties of the composite; hence, particles are normally classified based on their shapes. Some of the common shapes are spherical, cubical, blocks, flaky and fibrous. The surface area is different for the same volume of these shapes, which affects the size of the interfacial region between the particle and the matrix resin. For each of these shapes the stress concentration factor would be different due to their different corner radius of curvature and aspect ratios. Spherical particulate fillers are more popular compared to the other types. Use of hollow spherical particles, known as cenospheres, has increased considerably in recent years in the production of core materials of low density and high damage tolerance. Such low density materials are classified as close cell structured foams and are known as "Syntactic Foams". Density values of syntactic foams can be tailored over a wide range by changing the material or density of cenospheres.

1.4 Syntactic Foams

Syntactic foams are known for their high specific compressive strength, low moisture absorption and excellent damping properties. They are used as a core material in sandwich composites for weight sensitive structural applications. These foams are multi-functional composite materials due to their broad range of mechanical properties coupled with vibration damping characteristics, fire performance and ability to be fabricated in functionally graded configurations. These materials were developed in the 1960s as buoyancy aid materials for deep sea applications (Wright 1991). Presently they are used in aircraft, spacecraft and marine structures (Bardella and Genna 2001). One of the major advantages of syntactic foams is their ability to be designed and fabricated according to the physical and mechanical property

2

requirements of the application. Depending upon the service conditions, the matrix resin can be chosen from a wide range of thermosetting and thermoplastic resins. Similarly, cenospheres of polymer, ceramic or metal can be chosen (Feldman 1993, Lawrence 1966). Other parameters that can be varied are the volume fractions of the matrix and cenospheres in the structure.

There are two methods of changing the density of syntactic foams to directly influence their properties. The first method is to change the cenosphere volume fractions and the second one being different internal and outer radii cenospheres for given filler loading. Among these, the second method gives great design flexibility as any change in properties of syntactic foam can be related to just one parameter, the internal radius of cenospheres.

Considering the applications of syntactic foams in aeronautics and space applications, it is important to establish the effect of the radius on the mechanical properties of syntactic foams. Nevertheless, for naturally available hollow fillers like in fly ash cenospheres, first method is most feasible. In the present work syntactic foams having fly ash cenospheres in polymeric matrix are developed, analyzed and structure-property correlations are discussed.

1.4.1 Structure of Syntactic Foams

Syntactic foams have two phases in their structure, namely matrix resin and fly ash cenospheres. Figure 1.1 presents micrograph exhibiting structure of syntactic foam. Micrography is performed on the as-cut surface of syntactic foam specimen. Cenospheres embedded in the matrix resin are clearly visible from the micrograph.
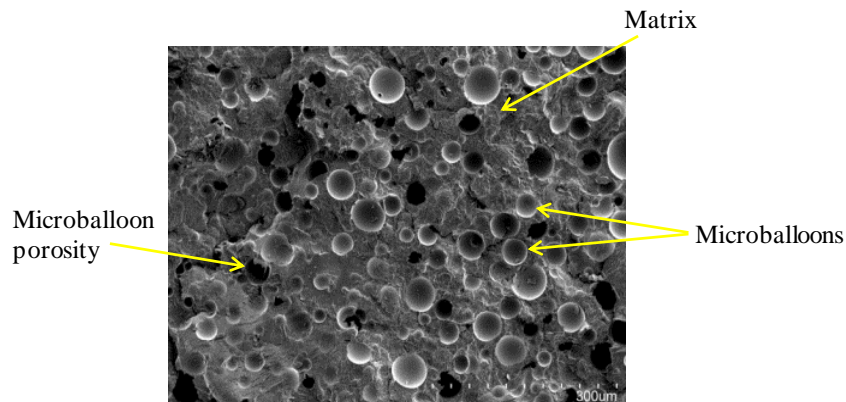
Figure 1.1 Syntactic foam structure.

3

The two phase structure is schematically presented in Figure 1.2a. During the fabrication process, air is inevitably trapped into the structure of syntactic foams and is present as open cell structured porosity. This entrapped air is termed as voids and makes syntactic foams three phase materials. Figure 1.2b shows three phase structure. In the present work, the fabricated syntactic foams have three phased structures.

2-Phase

3-Phase

(a)

(b)
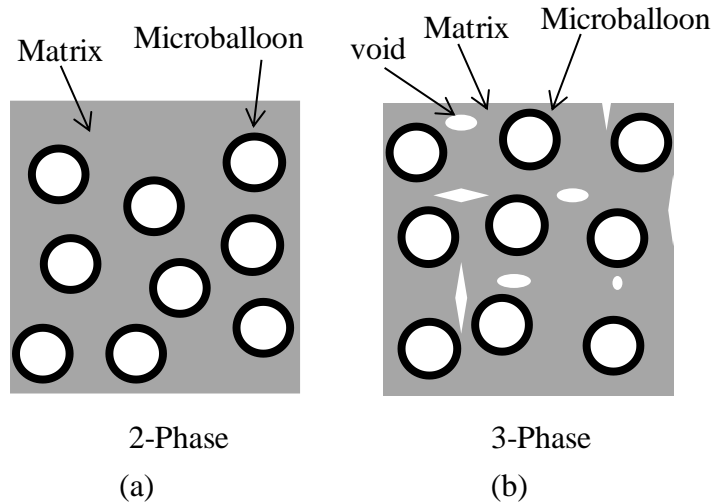
Figure 1.2 Representation of syntactic foams (a) two phase and (b) three phase.

1.4.2 Processing of Syntactic Foams

Every material system has unique physical, mechanical and processing characteristics. A suitable manufacturing method must be chosen to transform the material to its final form. Processes used for the fabrication of parts prepared from composite materials have evolved in the later twentieth century from skilled labour operations to sophisticated microprocessor systems having automatically controlled equipment. Hand lay-up techniques or spray-up in open molds are used by early pioneers to form the final system by combining raw materials and cured at ambient temperature.

Advantages of polymer matrix composites have steered these synthetic materials to enter almost every other market worldwide, from consumer products, automotive and marine to primary structural elements of aircraft and bridges. Such extensive growth in product applications commanded corresponding growth in materials technology, design approaches, and fabrication processes (Seidel 2012).

In case of fabricating syntactic foam composites, processing route must be carefully designed to reinforce hollow particles to avoid particle breakage and unintentional effect of higher matrix porosity by steadying gas bubbles in polymer matrix. The processing methods need to be efficient enough in helping wetting of reinforcement by the matrix resin, breaking clusters without damaging reinforcement and attaining uniform distribution of reinforcement in the resin material.

Figure 1.3 presents commonly used fabrication method for thermoset based syntactic foams. In this method, a two-step mixing process is used. Reinforcement (hollow microballoons) is added to the neat resin and thoroughly mixed until the slurry of consistent viscosity is obtained in first step. In the second step, the hardener or catalyst is added to the resin and stirred slowly. The mixture is cast into the molds and cured as per the resin.

Resin + hollow microballoons   Resin + hollow microballoons
+ hardener
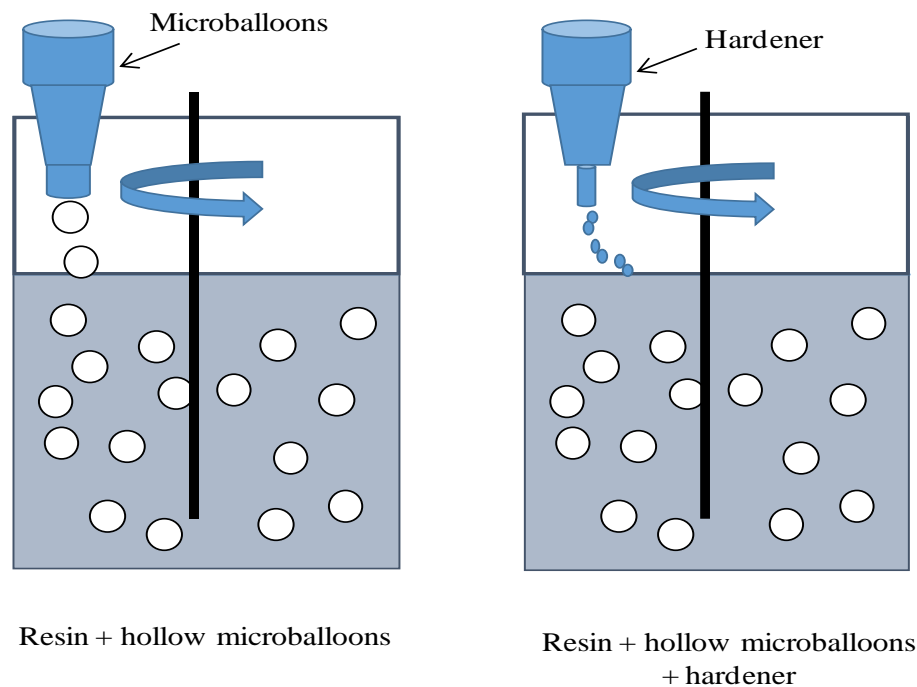
Figure 1.3 Illustration of syntactic foam fabrication steps (Gupta et al. 2013).

1.5   Role of interface and its modification

Interfacial bonding between reinforcement and matrix plays a very vital role in transferring load from matrix to cenospheres. Surface modification of the constituents might improve the

performance of these SFs owing to better compatibility. Improvement in the morphology and resulting properties of the composite can be attained by using additives in the form of compatibilizer. Interfacial energy between the constituents reduces due to compatibilization resulting in increased adhesion. Generally, adding compatibilizer results in finer dispersion, alongside more regular and stable morphologies resulting in higher stiffness, strength and impact toughness of the resultant composites.

A key region that influences mechanical properties of the composite is the matrix/reinforcement interface (Guru et al. 2015). A series of phenomena takes place at such interfaces. The structure of interface and the stresses developed during different stages of processing and services have a bearing on the fracture and failure of the composite. Hence it is essential to consider the interfaces in detail and examine their effect on the composite properties, so as to alter the properties to suit one's need in the end product. Good interfacial bonding is essential to have effective load transfer from matrix to the filler. The interfacial characteristics can be improved in different ways; chemical treatment is one such effective method. Reinforcing materials such as fly ash cenospheres contain oxides like Al_2O_3, SiO_2 and Fe_2O_3 which form links to hydroxyl groups during their contact with moisture and convert into water molecule (Rugele et al. 2017). The presence of water, additionally, reduces the wettability of the reinforcement as it lowers the surface energy. Coatings that function as coupling agents are expected to raise the effective surface energy of the reinforcement. The coupling agents are primarily aimed at creating a bridge between the oxide groups on the surface of filler and molecules of the matrix (Ranney et al. 1974).

General formula of silane coupling agents is $R-Si-X_3$, wherein this multifunctional molecule reacts with filler surface on one side and polymer phase on the other. In these 'X' group represent hydrolysable and thereby hydrolysis silane to corresponding silanol (R-OH) in the presence of aqueous solution. These silanol molecules and water molecules compete with each other to form hydrogen bonds with the hydroxyl groups that are strongly bonded to the reinforcement surface (Hull and Clyne 1996). Once the reinforcement is dried, the free water is taken away and condensation takes place both at silanol/surface junction and between the adjacent silanol particles. The resultant is a polysiloxane (X-R-Si (OH)$_3$) coating bonded to the

filler/reinforcing surface offering an array of 'R' functional groups to the environment. These open functional groups involve in curing reaction with the polymer matrix and establish a bond (Hull and Clyne 1996). Besides improving the bonding and the mechanical properties, the coupling enhances the electrical, thermal and magnetic properties due to increased effective contact at the interface. Another important feature is the increased resistance to environmental effects. The bonding also serves to reduce the effect of hostile environments at the reinforcement causing degradation and thus retains useful mechanical properties of the composite in spite of its exposure to such environments.

Silane treatments help in better wetting while those wherein dirt or greasy/oily layers envelope the fillers, the effectiveness of the medium to wet reinforcements/fillers reduces (Farinha et al. 2000). Their presence also affects the properties including mechanical behavior. The mechanical property of polymer-cenosphere composite is lower attributed to poor interfacial interactions between the hydrophilic surface of cenospheres and hydrophobic polymer (Guhanathan et al. 2001).

However, surface treated cenosphere is found to improve the interfacial interactions (Thongsang and Sombatsompop 2006). A mechanism of interaction between Silane-69 (Bis (3-triethoxy silyl) propyl tetrasulfide) coupling agent and fly ash (Nabil et al. 2004), is shown in Figure 1.4.

Surface modified fly ash
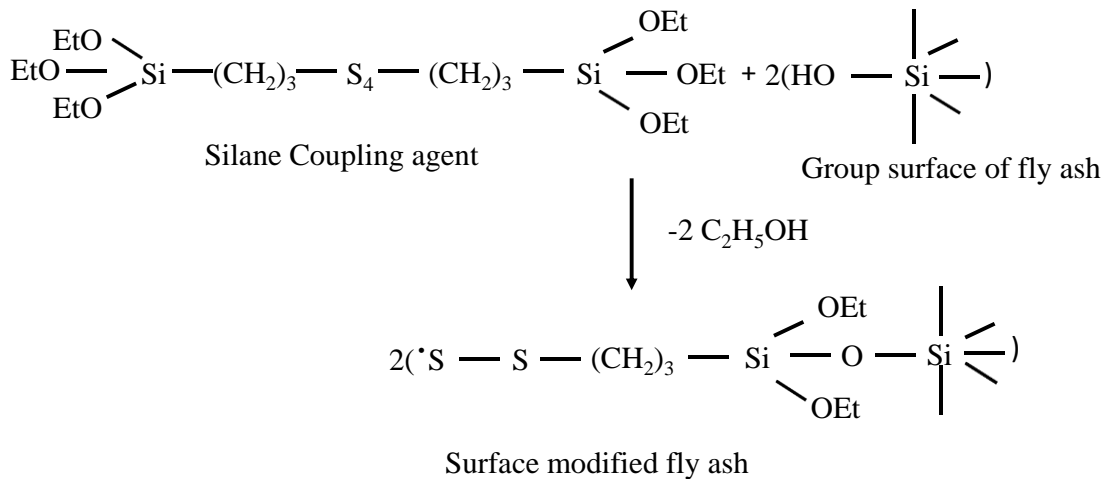
Figure 1.4 Reaction between Silane-69 coupling agent and fly ash.

Effect of surface treated fly ash on the mechanical properties of HDPE as compared to conventional calcium carbonate filler reveal increase in tensile strength on addition of fly ash (Atikler et al. 2006). However, higher increase is noticed when modified fly ash is used with 30% filler content. The decrease in elongation at break is higher for ash filled composites when compared to calcium carbonate ones. The decrease in property is higher in case of treated fly ash.

Mechanical behavior of Mica/Epoxy composites is investigated to study the effect of silane and zirconate coupling agents (Bajaj et al. 1992). Tensile modulus and flexural strength are improved by the surface treatment. Properties of silica filled styrene-butadiene rubber composites are enhanced through plasma surface modification of silica (Kulkarni and Kishore 2002). Scanning electron microscopy revealed improved filler dispersion post plasma and silane treatment. Mathew et al. (2004) reported that the fly ash filled epoxy composite presented better strength in compression post exposure to aqueous media but the surface treated fly ash fillers in epoxy exhibited reduction in compression strength. Ramakrishna et al. (2006) concluded that the toughened epoxy/fly ash composites revealed improved compressive and impact strength. However, the tensile strength decreased while modulus increased with increase in fly ash content (Ferreira et al. 2010, Sachinkumar et al. 2018, Srivastava and Shembekar 1990). Surface modifications are crucial and influence mechanical behavior to a greater extent.

1.6 Polymer Matrix

Polymers are long chain organic molecules or macromolecules with many desirable properties such as high ductility, ease of forming and non-corrosiveness. A wide variety of such materials are available to a designer. Two such classes are thermosetting and thermoplastic polymers. Their initial target applications were in aerospace and later became viable alternative material in the sporting, automotive and in construction industries (Gokhale et al. 2011, Mallik et al. 2011). In thermosetting polymers, there are covalent cross bonds (cross link) between molecules, in addition to Van der Waals forces. Owing to these cross bonds, a thermosetting polymer remains rigid on heating. Thermoplastic polymers can be re-shaped by repeated

heating and cooling without losing their properties. They soften on heating and become rigid on cooling. On the other hand, thermosets remain rigid during reheating till they are converted into char. This difference in behavior on heating is due to the relatively weak Van der Waals forces acting between the molecules of thermoplastic polymers. On heating, the bonds between the molecules weaken substantially and the material becomes soft and yieldable.

Thermosetting epoxy resin is one of the most frequently used polymeric matrix material. They are available in a wide range of varieties from low viscosity liquids to high melting solids and can be tailored quite amenable to a range of modifications and processes. They offer high strength, lower shrinkage, ease of curing by a variety of chemical agents, superior electrical insulation, good adhesion and soaking of surfaces. Such properties make them ideal to be used in composites. Cross linking of epoxide groups (one oxygen and two carbon atoms) takes place in epoxy resins. For use at elevated temperatures, epoxy resins can be cured by adding chemical agents to yield an inflexible molecular structure. Epoxies are primarily employed for composite applications in the following classes – phenolic glycidyl ethers, aromatic glycidyl amines and cycloaliphatics. The most commonly used epoxy is diglycidyl ether of bisphenol A (DGEBA) which is a type of phenolic glycidyl ether. The chief curing agents used as hardeners for epoxy resins are amines, amine derivatives or anhydrides. Some chemicals called modifiers can be utilized to alter the mechanical and physical functionality of cure or uncured resins. These include rubbers, thermoplastics, fillers, flame retardants and pigments.

Though PMCs have higher initial material costs, low cost ones could be developed from using fillers in plastics with low cost environmental pollutants like cenospheres. A boom in the consumption of plastic in India is experienced with the economic liberalization since 1991. Plastic consumption in India has more than doubled from 0.85 million tons during 1990-91 to 1.79 million tons during 1995-96. Demand for commodity plastics is growing at the rate of 15% per year (Shekhar 2012). With such a drastic growth prevailing in the consumption of plastic, thermosetting syntactic foam composites with naturally available in abundance filler such as fly ash cenospheres may be an essential requirement to avoid concerns regarding plastic management and environmental linked fly ash disposal issues.

1.7 Literature review

Syntactic foams are lightweight composites and used prominently in weight saving applications. However, the extent to which these can be tailored to yield a target mechanical performance strongly depends on the resultant effective properties and more importantly relating these properties to its microstructure. Therefore investigating mechanical, thermal and other relevant properties for a given microstructure and its spatial distribution plays an important role in the design and development of syntactic foam. A number of reviews dealing with various aspects of syntactic foams under different loading conditions have been published in recent years and are presented in tabular form herewith. Notations used to represent the summary of literature are as follows:

ρ	Density	kg/m^3
$d_{\mu m}$	Particle diameter	μm
d_{nm}	Particle diameter	nm
Φ_w	Filler content	weight %
Φ_v	Filler content	volume %
η	Radius ratio	-
T$_g$	Glass transition temperature	°C
ε	Erosion efficiency	-
k	Velocity exponent	-

Table 1.1 Literature survey on mechanical behavior of composites subjected to Arctic conditions.

Author	Reinforcement	Matrix	Remarks
Dutta (1994)	*Glass fiber*	Polyester	• Change in the mechanical properties is attributed to the induced residual stresses within the composite as a result of thermal expansion mismatch between its constituents and the stiffening of the polyester matrix at low temperature. • The yield strength at -48°C increases by about 17% as compared with room temperature samples. Both theoretical prediction and experimental results illustrate that low temperature is beneficial. • At low temperature, compressive strength and stiffness of the sample increases while progressive thermal cycling reduces the brittleness and improves impact durability.
Dutta (1988)	*Glass fiber*	Polyester	• Compressive strength increases by 17.6% for sample at -60°C as compared to room conditioned sample. Failure of the samples is more catastrophic for low temperature ones. • Higher energy absorption is observed before failure for low temperature as compared with room temperature sample.
Jia et al. (2018)	*Carbon fibre* ρ : 1800 Φ_v : 50	Vinylester	• All the specimens exhibit a linear elastic regime followed by a stress drop. The specimens break catastrophically at -60°C, -

			20°C, 25°C, while at other temperatures the specimens show clear post break strength.
			• Composites become stronger and tougher at lower temperatures under three-point bending load. Brittle behavior of the polymer matrix is due to lower temperatures, higher modulus and smaller ultimate tensile strain.
			• Compared to effect of the matrix properties change, effect of the thermal stress is secondary.
Prusty et al. (2015)	*Glass fiber* (3K) $d_{\mu m}$: 15, Φ_v : 50 *Multi walled carbon nano tube* d_{nm} : 5-6 Length : 5μm	Epoxy Lapox L-12 and hardener K-6	• Extent of matrix hardening is higher due to carbon nanotubes incorporation. • Decrease in temperature from 20°C to -80°C, modulus of the samples increases by 13% whereas strength increases by 77% for glass epoxy composites. • For composites filled with carbon nano tubes, modulus increases by 17% while the strength improves by 29% as the temperature is decreased from 20°C to -80°C.
Sanchez Saez et al. (2002)	*AS4 carbon fibre* Φ_v : 60	Epoxy 3501-6	• Flexural stiffness of laminate grows as the temperature rises. • Strength diminishes from 1297 to 984 MPa (24% reduction) as the temperature decreases from room temperature to -150°C. Slight change in stiffness is observed between 30°C and - 60°C.

Table 1.2 Literature survey on compressive behavior.

Author	Reinforcement	Matrix	Remarks
Jayavardhan and Doddamani (2018)	*Glass microballoons* ρ : 200, 270, 350 Φ_v : 20, 40, 60	High density polyethylene	• Modulus and yield strength values are strain rate sensitive displaying rise with increasing strain rates. Foams with higher density at 60 vol.% of glass microballoons show higher modulus and yield strength. • Neat HDPE present lower specific modulus as compared to syntactic foams. Wall thickness of microballoons has a dominant effect on the properties.
Labella et al. (2014)	*Fly ash cenospheres* ρ : 980, 950, 900, 835 Φ_v : 30, 40, 50, 60	Vinyl ester and methyl ethyl ketone peroxide	• Neat sample displays higher strength as compared to all the syntactic foams. Foams with 60 vol.% filler reveals the lowest strength. • Modulus of all the syntactic foams is higher as compared to neat resin. Foams with 40 vol.% filler shows an increase in modulus by 42% as compared to neat resin. • Compared to all the syntactic foams, neat resin shows 12-19% higher specific strength and 50-70% lower specific modulus.
Poveda et al. (2013)	*Glass hollow particles* ρ : 220, 460	Epoxy DER332 and hardener DEH24	• Exposure to moisture does not affect the quasi-static compressive modulus of samples but decrease in about 30% strength is noted.

	$d_{\mu m}$: 35, 40 Φ_v : 30, 50 *Carbon nano fibres* ρ : 1950, Φ_w : 1		• All the samples exhibit moisture absorption between 0.75 and 2% except for syntactic foam with low density and highest glass particle content.
Swetha and Kumar (2011)	*Glass microballoons* η : 0.98, 0.97, 0.94 ρ : 150, 220, 460 Φ_v : 0, 10, 20, 30, 40, 50, 60	Epoxy Araldite GY257 and curing agent Aradur HY951	• Increase in microspheres volume fraction show decreasing trend for modulus and strength values while it increases as the wall thickness of the microspheres increase. • Failure behaviour of foams is dictated by the nature of stress-strain curves that in turn depends on the wall thickness of microspheres. • Energy absorption capacity increases with increase in the microspheres volume fraction up to 50%.
Gupta et al. (2010)	*Glass microballoons*, η : 0.97, 0.96, 0.95, 0.94 ρ : 220, 320, 370, 460	Vinyl ester and methyl ethyl ketone peroxide	• Compressive modulus of syntactic foams is comparable to neat resin. Specific moduli for all the syntactic foams composites are 10-47% higher than neat resin. • Microballoons with η < 0.955 result in significant improvement of mechanical properties.

Wouterson et al. (2005)	*Glass microballoons (K15* ρ : 150; $d_{\mu m}$: 71 *(K46)* ρ : 250; $d_{\mu m}$: 70 *Phenolic microspheres* ρ : 460; $d_{\mu m}$: 43.6 Φ_v : 0, 10, 20, 30, 40, 50	Epoxy Epicote 1006	• Modulus and strength of all the composites register lower values as compared with neat epoxy samples. • Composites with K46 microspheres present upper modulus and yield strengths as compared to K15 and phenolic microspheres. • Improvement of properties for K46 type composites is attributed to their better thickness to radius ratio.
Gupta et al. (2004)	*Cenospheres* η : 0.92, 0.91, 0.89, 0.88, 0.86 ρ : 200, 320, 370, 380, 460	Epoxy DER332 with DEH24 hardener	• Decrease in radius ratio increases compressive strength and modulus by 58.33 and 41.28% respectively for flat wise compression samples. • Compared to edgewise test samples, flat wise tested samples show an increase in peak compressive modulus and strength by 18.86 and 12.5% respectively.
Gupta and Woldesenbet (2003)	*Borosilicate glass microballoons (S22)*	Epoxy DER332 and triethylene	• At room temperature, S22 and K46 syntactic foams present moisture absorption below 1%. At 70°C, S22 type syntactic foam absorbed 6.7 and 2.5% moisture whereas 3.9 and 1.9% moisture

| | ρ : 205; $d_{\mu m}$: 75
 Borosilicate glass microballoons (K46)
 ρ : 460; $d_{\mu m}$: 80
 Φ_v : 65 | tetramine hardener | was absorbed for K46 type syntactic foam in deionized and salt water, respectively.

 • For the same type of syntactic foams, wet samples show decrease in modulus as compared to dry samples.

 • Decrease in modulus by 49 and 68% for low and high temperature deionised water respectively is observed for S22 samples, while it decreases by 51 and 65% respectively for low and high temperature salt water.

 • For K46 samples modulus decreased by 48% and 57% for low and high temperature deionised water respectively, while it decreased by 64 and 60% respectively for low and high temperature salt water.

 • No difference is observed in peak compressive strength for low temperature specimens as compared to the dry specimens. |
| Gupta et al. (2002) | *Glass microballoon*
 ρ : 254
 $d_{\mu m}$: 80
 E-glass fibers: 6 mm | Epoxy LY5052 with HY5052 hardener | • Compressive strength of reinforced syntactic foam decreases by 34.49 and 44.51% for fibers oriented in parallel and perpendicular loading direction respectively.

 • Compressive strength in flat wise orientation decreases by 37.9% as compared to edgewise orientation. |

Gupta et al. (1999)	*Glass microballoons* ρ : 250 $d_{\mu m}$: 10-100 E-glass fibers: 6 mm	Epoxy Araldite LY5052 and hardener HY5052	• Addition of fibers into the resin before incorporating microballoons in the system yields castings with a void content lower than 4%. • Cast slabs with lower void content possess high compressive strength.

Table 1.3 Literature survey on flexural behavior.

Author	Reinforcement	Matrix	Remarks
Zeltmann et al. (2015)	*Glass microballoons* ρ : 220, 460 Φ_v : 15, 30, 50 *Carbon nano fibres* Φ_w : 1, 2, 5	Epoxy resin DER 332 with triethylene tetramine hardener	- As compared to neat resin, all the nanocomposites present higher moisture uptake. 18% higher moisture absorption is observed by all the syntactic foams as compared to neat resin samples. - Strength of dry conditioned neat resin is higher than all other samples. The strength of neat resin sample reduces considerably to 53 MPa due to weathering. - Composite with 1 wt.% of CNF shows highest fracture strength of 96.9 MPa. - Composites with 2 and 5 wt.% of CNF show higher strength after weathering. Higher CNF content is observed to have 27% increase in strength after immersion as compared to dry composite. - Modulus of dry specimens is almost the same for neat sample and all CNF/epoxy composites. Maximum change in modulus of 61 % is observed for composites with higher density and volume fraction with 1 wt.% CNF as compared to as-fabricated material.

Labella et al. (2014)	*Fly ash cenospheres* ρ : 980, 950, 900, 835 Φ_v : 30, 40, 50, 60	Vinyl ester and methyl ethyl ketone peroxide	• Syntactic foams register higher modulus and lower strength as compared to neat resin samples. • Syntactic foam with 60 vol.% of cenospheres show a maximum decrease in strength by 73% whereas modulus increases by 47%. • Due to early failure commencing from the cenosphere particles, failure strain of all the syntactic foams is lower as compared to neat resin samples.
Thakur and Chauhan (2014)	*Cenosphere* ρ : 970, 670, 660 $d_{\mu m}$: 2 d_{nm}: 900, 400 Φ_w : 10	Vinyl ester with HY951 hardener	• Enhancement in strength is observed with reduced size of particles. • Vinyl ester composite filled with 400 nm sized cenospheres show 27.11% higher strength as compared with 900 nm (15.25%) and 2 µm (10.16%) cenosphere filled composites.
Jena et al. (2013)	*Cenosphere (CS300)* ρ : 450-800 $d_{\mu m}$: 60-94 Φ_w : 0, 1.5, 3, 4.5, 6, *Bamboo fiber* ρ : 950	Epoxy L12 with K6 hardener	• Strength increases by 32, 9 and 11.2% in 3, 5, 7-layered bamboo-epoxy composite. • Strength decreases by 8.97% as cenosphere content increases to 3 wt. % in 9-layered bamboo-epoxy composite. • Strength increases by 30.6, 9.09 and 14.75% for 1.5, 3 and 4.5 cenosphere wt.% while decreases to 24.4% for 6 wt.% in 3, 5, 7 and 9-layered bamboo-epoxy composites respectively.

Tagliavia et al. (2010)	*Glass microballoons* ρ : 220, 320, 370, 460 Φ_v : 30, 40, 50, 60	Vinyl ester and methyl ethyl ketone peroxide hardener	• Trends between modulus and volume fraction are not similar for all the microballoon wall thickness. • Thin-walled particles show decrease in modulus from 2850 to 2350 MPa whereas thicker-walled particles present an increase in the elastic modulus from 3650 to 3800 MPa with increase in the volume fraction that exceeds the modulus of neat resin. • All the syntactic foams present higher specific modulus than neat resin samples. • Strength of the composite decreases as the resin content decreases. • Absence of debris on the fracture surface indicates brittle failure from the tensile side of the sample.
Gupta et al. (2008)	*Glass microballoon (S22, S32, K37, K46)* ρ : 220, 320, 370, 460 Φ_v : 30, 40, 50, 60 η : 0.9703 - 0.9356	Epoxy DER332 with DEH24 hardener	• Modulus and strength of functionally graded syntactic foams decreases by 39.5 and 34.18% as η and filler content increase. • Radius ratio type functionally graded syntactic foams reveal that with increasing microballoon volume fraction, strength and modulus decreases by 52 and 13% respectively.

Wouterson et al. (2005)	*Glass microballoons (K15)* ρ : 150; $d_{\mu m}$: 71.5 *Glass microballoons (K46)* ρ : 250; $d_{\mu m}$: 70 *Phenolic microspheres (BJO-093)* ρ : 460; $d_{\mu m}$: 43.6 Φ_v : 0, 10, 20, 30, 40, 50	Epoxy Epicote 1006	• Modulus and strength of all the composites register lower values as compared with neat epoxy samples except for strength values of K46 samples that present higher strength owing to large reduction in strain rate. • Specific strength attains a least value around 40-50% of filler content. • With increasing filler content, K46 type samples demonstrate an increase in modulus. • K15 type samples present no change in modulus whereas phenolic microspheres samples show decrease in modulus with increase in microballoon filler content.

Table 1.4 Literature survey of tensile behavior.

Author	Reinforcement	Matrix	Remarks
Singh and Siddhartha (2015)	*Cenospheres* ρ : 670, 650, 640 d_{nm} : 900, 600, 300 Φ_w : 10	Polyester resin with methyl ethyl ketone peroxide catalyst	• Strength increases to the tune of 11% with decreasing particle size. • Strength for 300 nm particle reinforced composite is observed to be 16% higher compared to neat polyester.
Thakur and Chauhan (2014)	*Cenosphere* ρ : 970, 670, 660 $d_{\mu m}$: 2 d_{nm} : 900, 400; Φ_w : 10	Vinylester with HY951 hardener	• Marginal improvement in strength by 2.56% is observed for 400 nm cenosphere reinforced composites. • Volume fraction of void for 2μm, 900 nm and 400 nm is 9.4529, 8.0904 and10.434 respectively.
Jena et al. (2013)	*Cenosphere* (CS300) ρ : 450-800; $d_{\mu m}$: 60-94 Φ_w : 0, 1.5, 3, 4.5, 6; *Bamboo fiber* ρ : 950	Epoxy L12 with K6 hardener	• Increase in strength by 20 and 9% for 1.5 and 3 cenosphere wt.% and decrease in strength by 17.5 and 42.8% for 4.5 and 6 cenosphere wt.% respectively for 3, 5, 7 and 9-layered bamboo–epoxy composites is observed compared to neat samples. • Increase in strength by 25.4, 6.5 and 4.1% for 3, 5, and 7-layered bamboo-epoxy composite while 23.5% decrease in strength is observed for 6 wt. % cenosphere post seven layers.

Yu et al. (2012)	*Ceramic microsphere* ρ : 600-800; $d_{\mu m}$: 130 Φ_v : 0, 10, 20, 30, 40, 50	Epoxy E51 with PA651 hardener	• With the increase of filler content, strength and failure strain decrease to 61.65 and 58% respectively, compared to neat resin.
Gupta et al. (2010)	*Glass microballoons,* η : 0.97, 0.96, 0.95, 0.94 ρ : 220, 320, 370, 460	Vinyl ester and methyl ethyl ketone peroxide	• Higher tensile modulus is observed with high density syntactic foams as compared to neat resin. For the same syntactic foam compositions, tensile modulus is 15-30% higher than the compressive modulus. • Specific modulus of syntactic foams is 50-75% higher as compared to neat vinyl ester resin.
Dimchev et al. (2010)	*Glass microballoon* ρ : 254, 328, 377, 465; Φ_v : 30, 40, 50 *Carbon nano fibers* ρ : 1950	Epoxy DER332 with DEH24 hardener	• Strength and modulus of syntactic foams, shows 20-50% and 10-20% rise respectively owing to the presence of nanofibers. • With respect to the microballoon wall thickness and volume fraction, the trends in tensile properties are similar with and without nanofiber addition.

Nikhil and Ruslan (2006)	*Glass microballoons (3M)* ρ : 220, 320, 380, 460 Φ_v : 30, 40, 50, 60 η : 0.9702, 0.9565, 0.9474, 0.9356	Epoxy DER332 and hardener DEH24	• Increase in microballoon volume fraction from 30 to 60% decreases the strength in the range of 25-60% for various types of foams. • Strength is lower by 60-80% for all types of syntactic foams as compared to neat resin. • Modulus increased by 48.59% with the increase in microballoon density from 220-460 kg/m^3 for a 30% volume percentage of filler. • The modulus is found to increase in the range of 30-90% with the increasing microballoon density. Lower radius ratio microballoons performed better in both strength and modulus.
Wouterson et al. (2005)	*Glass microballoons (K15)* ρ : 150; $d_{\mu m}$: 71.5 *Glass microballoons (K46)* ρ : 250; $d_{\mu m}$: 70 *Phenolic microspheres (BJO-093)* ρ : 460; $d_{\mu m}$: 43.6 Φ_v : 0, 10, 20, 30, 40, 50	Epoxy Epicote 1006	• Modulus and strength of all the composites containing K15 and phenolic microspheres register lower values as compared with neat epoxy samples. • K46 microsphere samples possess higher strength values till 20 vol.% of microspheres as compared to neat sample, thereafter the strength values decrease. However, the modulus increases with increase in filler content as compared to neat sample.

Table 1.5 Literature survey on Dynamic Mechanical Analysis.

Author	Reinforcement	Matrix	Remarks
Zeltmann et al. (2016)	*Cenospheres* ρ : 750; $d_{\mu m}$: 63 Φ_v : 0, 60	High density polyethylene HD50MA180	• Addition of cenospheres improves the storage modulus for all the temperatures studied. Temperature at which the storage modulus drops below the 20 MPa threshold is improved by about 5°C in the syntactic foam, indicating greater thermal stability compared to the matrix resin. • The loss modulus of the syntactic foam is greater than the neat resin at all temperatures studied. • The damping increases with increasing temperature. The increase is most drastic as the melting temperature is approached.
Shunmugasamy et al. (2013)	*Glass microballoons* ρ : 220, 320, 460 Φ_v : 30, 40, 50, 60	Vinyl ester and methyl ethyl ketone peroxide	• At sub-zero and room temperatures, increase in microballoon wall thickness at similar volume fraction results in increase of storage modulus. • In the flow region after T_g, the storage modulus is lower for the neat resin by 76-96% than any syntactic foam. In this region, storage modulus increases with the microballoon wall thickness. • The room temperature loss modulus and damping parameter is found to vary linearly with the density of syntactic foams.

			• Presence of glass microballoons helps in increasing the retention of mechanical properties of syntactic foams at temperatures beyond T_g. • T_g increases with the microballoon volume fraction. • Addition of microballoons leads to 14-66% decrease in damping as compared to neat resin as well as increase in the storage modulus of the syntactic foams post T_g.
Das and Satapathy (2011)	*Cenospheres (CS 300)* ρ : 450-800 $d_{\mu m}$: 60-300	Polypropylene REPOL H110MA	• Improvement in the energy dissipation and storage modulus of the composite is observed with 10 wt.% and up to 30 wt.% of cenosphere. • Increase of storage modulus is higher with increasing cenosphere content at lower/sub-zero temperatures in the range -25 to 0°C. However, such an increase is not so evident at higher temperatures.
Hu and Yu (2011)	*Hollow particles* ρ : 130 $d_{\mu m}$: 80-110 Φ_v : 5, 10, 15, 20, 25	Epoxy resin E-44, hardener hexamethylene diamine, diluents glycidyl	• Addition of polymer particle leads to higher loss factor. • Loss factor of neat epoxy and syntactic foams containing 10% hollow particles in the range of -20 to 90°C present two relaxation peaks namely, α relaxation peak corresponding to T_g of the samples.

		methacrylate and butyl acrylate	• Minimum of the peaks correspond to β relaxation peaks related to the local motion of molecular chains. • Value of α relaxation peaks of all foams shifts to larger loss and the shape of peaks becomes wider as compared with pure resin. • Peak of syntactic foams for the both relaxation peaks shift to a higher temperature.
Tagliavia et al. (2009)	*Glass microballoons* ρ : 220, 320, 380, 460 η : 0.97, 0.956, 0.947, 0.936 Φ_v : 30, 40, 50, 60	Vinyl ester and methyl ethyl ketone peroxide	• Increase in the microballoon wall thickness results in enhanced storage modulus while storage modulus is not monotonically related to microballoon volume fraction. • Foams with thick-walled particles benefit from increase in volume fraction. • As the volume of resin decreases, the loss tangent of syntactic foams decreases owing to the brittle behavior of glass microballoons and the prominent viscoelastic behavior of the resin.
Lin et al. (2009)	*Glass microballoons* ρ : 220, 320, 380, 460 Φ_v : 30, 40, 50, 60	Epoxy DER 332 and hardener based on amine	• Thermal stability is increased by increasing microballoon wall thickness while it is relatively less sensitive to microballoon volume fraction.

			• Presence of ceramic content in the microstructure of syntactic foam lowers the coefficient of thermal expansion as compared to the matrix material. • Microballoon volume fraction has a prominent effect on the glass transition temperature whereas the effect of wall thickness is less significant. • Change in T_g is mainly attributed to the volume fraction of constituents indicating that the interfacial effects prominently affect the T_g of the composite.
Jian et al. (2009)	*Fly ash cenosphere* ρ : 600-700 Φ_v : 0, 30, 40, 50, 70	Epoxy E-51, catalyst tolylene-2-4-di-isocyanate and polyethylene glycol accelerator	• Damping capacity is enhanced by fly ash addition attributed to increase in frictional damping and hollow structure of fly ash particles. • Influence of matrix viscoelasticity is higher whereas frictional energy dissipation is comparatively lesser for cenosphere volume fraction less than 30%. • Between 30 to 50 vol.%, impact of frictional energy dissipation is as significant as that of matrix viscoelasticity. At 70 vol.%, the contribution of matrix viscoelasticity decreases sharply owing to the extreme dilution effect of the fly ash to the matrix.

| Sankaran et al. (2006) | *Glass microspheres* ρ : 254 $d_{\mu m}$: 80 | Epoxy DGEBA with amine hardener | • Storage modulus decreases with increase in temperature of both the foam as well as neat resin. • Syntactic foams present higher T_g as compared to neat resin attributed to reinforcing hollow microballoons affecting the mobility of polymeric chains in the interphase region between matrix and filler. • Composition of polymer composites is the key factor in determining the damping. However, interaction between filler and matrix also affect damping behavior. • Large decrease in room temperature damping values of the syntactic foams as compared to neat resin is attributed to the presence of higher volume percentage of rigid glass microballoons. |

Table 1.6 Literature survey on dry sliding wear behavior.

Author	Reinforcement	Matrix	Remarks
Imani et al. (2018)	*Surface modified nano silica powders* $d_{\mu m}$: 200-300 Φ_w : 23 Wax containing microcapsules (WMC) Φ_w : 2.5, 5, 10	Epoxy E51 and curing agent Aldibur HE600	• Improvement in wear resistance and decrease in the coefficient of friction is attained by maintaining a proper ratio of silica nano particles and WMCs. • Specific wear rate reduces to the tune of 3 times (1.05×10^{-4} - 4.39×10^{-7} mm^3/Nm) and 10 times reduction in coefficient of friction (0.72–0.07) for silica/WMC/epoxy composites as compared to neat epoxy samples. • Reduction in wear of samples containing WMC is attributed to formation of thin and continuous transfer film on the steel ball surfaces.
Doddamani et al. (2017)	*Walnut shell powder* ρ : 1520 Φ_w : 10, 20, 30	Epoxy LAPOX L-12 and hardener K6	• Walnut shell is effective in enhancing wear resistance of composites. Composites with 30 wt.% walnut shell particles show higher wear rate and lower coefficient of friction. • Wear rate increases with increase in applied force while reverse trends are observed with specific wear rate and coefficient of friction. • Wear rate decreases while coefficient of friction increases with increase in filler content of walnut powder.

			• Wear rate and coefficient of friction decreases with increase in velocity and sliding distance. • Applied force is the important parameter on wear and friction behavior of the composites as compared to other parameters.
Manakari et al. (2015)	*Cenospheres* ρ : 920 $d_{\mu m}$: 63 Φ_v : 0, 20, 40, 60	Epoxy LAPOX L-12 and hardener K6	• Increase in the applied load increases wear rate whereas specific wear values and coefficient of friction decreases. However, reverse trends are observed with increase in volume fraction of cenosphere. • Sliding velocity as well as sliding distance decrease wear and specific wear rate.
Pattanaik et al. (2016)	*Fly ash (Class C)* Φ_w : 10, 20, 30, 40 $d_{\mu m}$: 27.26	Epoxy LY556 and hardener HY951	• Nanometer size particle reduces the friction and wear of composites. • Applied normal load is the most influential parameter on the increase in wear, frictional force and coefficient of friction followed by fly ash content, track diameter, speed and time.
Chauhan and Thakur (2013)	*Cenosphere* ρ : 400 - 600 Φ_w : 2, 6, 10 $d_{\mu m}$: 2 d_{nm} : 400, 900	Vinylester resin and hardener HY 951 and accelerator	• Submicron sized particles are more effective in refining the wear resistance as compared to the micro sized particles. • Composites with 6 wt.% of submicron sized particles are optimum to lower the specific wear rate.

			• Highest wear rate is observed at 0.65×10^{-5} mm^3/Nm for an applied load of 10 N, velocity of 1.9 m/s and particles of 2 μm. Lowest wear of 1.8×10^{-6} mm^3/Nm at an applied load of 70 N, velocity of 1.9 m/s and particles of 400 nm size. • Composites with cenospheres of 400 nm are most effective in reducing coefficient of friction and specific wear rate.
Singh and Siddhartha (2015)	*Cenosphere* ρ : 640, 650, 670 d_{nm} : 300, 600, 900 Φ_v : 10	Polyester resin, hardener methyl ketone peroxide and cobalt naphthalene accelerator	• Cenospheres filled with 300 nm size composites shows highest wear resistance. • Composites with submicron size cenosphere particles show lower coefficient of friction and specific wear rate as compared to neat polyester. • Coefficient of friction and specific values of composites with cenospheres decrease with increase in load and sliding speed while increases with higher sliding distances.
Chand et al. (2011)	*Fly ash cenospheres* Φ_w : 10, 15, 20 $d_{\mu m}$: 355	Low density Polyethylene (LDPE) 16MA400	• Increase in sliding velocity and cenosphere content increases wear at constant applied load and sliding distance. • Resistance of LDPE/cenosphere foam to wear greatly enhances on silane modification of cenospheres. • 10 wt.% of silane modified cenosphere/LDPE foam shows the maximum resistance to wear.

Barpanda and Kulkarni (2009)	*Fly ash (Class C)* ρ : 900	Epoxy LAPOX-L12 and K6 hardener	• Higher fly ash content decreases the severity in the wear loss. • Wear loss increases with sliding speed and the increase is quite significant in case of neat epoxy system. • Micrography of wear surface reveals matrix flow and surface cracks for samples with lower fly ash content. • Wear surface features are fly ash content and sliding velocity dependent.
Ray and Gnanamoorthy (2007)	*Cenosphere (F class)* Φ_w : 40, 50	Vinyl ester resin FB-701, hardener methyl ketone peroxide and co-naphthalene and N, N-dimethyl aniline accelerator	• Neat epoxy shows 443% higher weight loss as compared to 40 wt.% cenospheres composites. • With increase in the sliding distance, wear rate of neat epoxy increases. • Neat epoxy presents the highest coefficient of friction. • Syntactic foam with 40 wt.% cenosphere particles reveal lower weight loss, coefficient of friction and linear wear as compared with composites having 50 wt.% of cenospheres.

Table 1.7 Review of erosion studies.

Author	Reinforcement	Matrix	Remarks
Jena et al. (2016)	*Cenosphere* ρ : 450 – 800 $d_{\mu m}$: 60-94 Φ_w : 1.5, 3, 4.5, 6 *Bamboo fibre* ρ : 950 width : 4.5 mm thickness : 1.5 mm	Epoxy L-12 and hardener K6	• Addition of cenospheres to bamboo epoxy composite reduces its erosion rate. • ε of the composites varies from 10 to 22, 6 to 12, and 3 to 8% for impact velocities of 33, 48, and 70 m/s, respectively. Lower erosion efficiency of cenosphere filled bamboo epoxy composite as compared with the bamboo epoxy composite is noted. All composites show semiductile erosive wear behavior. Maximum erosion resistance is observed for composite with 33 wt.% of fibre and 6 wt.% of filler.
Ranjan and Alok (2015)	*Linz-Donawitz slag (LD slag)* ρ : 1750 $d_{\mu m}$: 90-100 Φ_w : 0, 7.5, 15, 22.5, 30	Epoxy LY556 and hardener HY951	• Addition of LD slag increases the void fraction due to inadequate wetting of the fillers by the matrix material. • Presence of dissolved gases in the matrix during mixing and stirring further increases void content. Micro-hardness considered as one of the significant factors for determining erosion, increases with increase in the filler content. • Rise in the LD slag content from 7.5 to 30 wt.% increases hardness from 10.60 to 27.94 Hv. Velocity and filler content are found to be major control factors for reducing the erosion.

Rao et al. (2015)	*Graphite* *$d_{\mu m}$: 40-60* *Φ_w : 0, 2, 4, 6* *Bidirectional* *plain-woven* *carbon fabric* *ρ : 200*	Epoxy L-12 and hardener K5	• Erosive rate increases from 0 to 4 wt.% while decreases for 6 wt.% graphite filled composites. • For all the samples, maximum erosion takes place at 45° impinging angle. Graphite filled composites register lower erosion resistance as compared with unfilled composites.
Dalbehera and Acharya (2015)	*Cenospheres* *(CS300)* *Φ_w : 5, 10, 15, 20* *E-glass fibre*	Epoxy LY556 and hardener HY951	• Semiductile behavior is exhibited by all the samples. Cenosphere filled with 20 wt.% provide improved erosion resistance compared to 10 and 15 wt.% samples. • ε is 12% for low percentage (5 wt.%) of particulate filler while it decreases to 9.72, 8.6 and 5.72% for 10, 15 and 20 wt.% respectively, indicating better erosion resistance at higher filler content cenospheres.
Gaurav and Alok (2015)	*Glass* *microballoons* *ρ : 1628* *$d_{\mu m}$: 100* *Φ_v : 0, 10, 20, 30*	Epoxy LY556 and hardener HY951	• Density of the foam increases with addition of microballoon particles. With increase in filler content from 0 to 30 wt.%, hardness of the sample increases from 0.085 to 0.586 GPa • Impact velocity, glass microballoon content and impinging angle in decreasing order are recognised as important factors affecting the erosion behavior. Composites with hard and solid glass microspheres help in improving the resistance to erosion.

Bagci and Imrek (2011)	*Glass fibre* $d_{\mu m}$: 17 *Boric acid* $d_{\mu m}$: 150	Epoxy	• All test specimens reveal maximum erosion at 30° impinging angle, representing ductile behavior. Rate of erosion decreases with increase in impingement angle. • Addition of boric acid registers three to four times higher erosion as compared to neat sample. • Samples with 45°/45° fibre directions are more wear resistant than samples with 0°/90° fibre direction.
Mohan et al. (2012)	*Ultrahigh molecular weight polyethylene* (UHMWPE) $d_{\mu m}$: 5-26 *Bidirectional Kevlar-49 woven fabric* ρ : 2600	Epoxy bifunctional resin (LY5052) and hardener cyclo aliphatic amine	• Incorporation of UHMWPE in aramid epoxy (A-E) composites improves erosion resistance. Matrix micro cracking, fibre matrix debonding, fibre breakage and material removal are recognized as the basic wear mechanism for thermoset composites. • Maximum erosion occurs at 60° impinging angle revealing semiductile behaviour. Composites with fillers resist the damage from the erodent and provide a good lubricating action during erosion lowering weight loss.
Satapathy et al. (2009)	*Labito-Rohita fish scale* Length : 6-8 mm Width : 1 mm Φ_w : 5, 10, 15	Epoxy LY556 and hardener HY951	• Composites show higher erosion resistance as compared to neat epoxy. Particulate filled composites exhibit semi ductile erosion behavior for low impact velocity whereas ductile erosion response is observed with high impact velocity.

Harsha and Jha (2008)	*Uni-directional E-glass fibre* ρ : 1700 $d_{\mu m}$: 10-12 *Bi-directional E-glass fibre* ρ : 1460; $d_{\mu m}$: 10-12 *Uni-directional carbon fibre* ρ : 1210; $d_{\mu m}$: 10-12	Epoxy CY 205 and hardener HY 951	• Bi-directional glass fibre epoxy composite show better wear resistance as compared with unidirectional fibre composites. • Steady-state erosion of epoxy and its composites increases with increase in velocity from 25 to 60 m/s by about 31-95%. • Composites show peak erosion rate at 60° impingement angle at a velocity of 25 m/s. • In the present study, k varies in the range of 1.68-3 and ε varies from 1 to 24% at different impact velocities indicating semi-ductile behavior.
Srivastava and Pawar (2006)	*Fly ash* ρ : 3385 $d_{\mu m}$: 105 Φ_w : 2, 4 *Cross fly E-glass fibre sheet*	Epoxy CY205 and hardener HY951	• Micro hardness of samples decreases with increase in load. Presence of flyash content in the composite decreases the hardness and density of the samples. • Erosive wear of fly ash filled samples is lower as it restricts fibre matrix debonding. Samples without any filler show the highest erosion rate owing to weak bonding strength. • Erosion rate displays power law behaviour with velocity, where k varies from 1.6 to 5.Influence of impingement angle exhibits semiductile erosive wear behaviour with maximum wear rate at 60° impingement angle. ε varies from 0.178 to 6%.

From this literature, it is very clear that the environmental pollutant like fly ash cenospheres has not been explored fully to synthesize and develop thermosetting based syntactic foams using mechanical mixing technique.

- Work on surface modified Cenosphere/Epoxy syntactic foams are not reported in the literature.
- Most of the testing is done at room temperature conditions while studies based on low temperature testing of syntactic foams is not explored well.
- Tribological and erosive behavior of syntactic foams with respect to surface modification and varying filler content of cenospheres are not investigated.

Hence, present work deals with the development and characterization of eco-friendly and lightweight Cenosphere/Epoxy syntactic foams to address the aforementioned issues and to develop utilitarian foams beneficial to the society.

1.8 Motivation of work

Fly ash is a waste by-product produced in abundance by combustion of coal in thermal power stations. The main constituents of fly ash are silicon dioxide, iron oxide and aluminium oxide. Fly ash possesses severe environmental threat by polluting the surrounding atmosphere and land fill burden for its disposal. Increase in the production of fly ash year by year from coal thermal power plants poses a serious problem in terms of its safe dumping and utilization. Use of fly ash as fillers in polymer composites is appreciated from both economic and commercial point of view. Some studies have pointed to the excellent compatibility between fly ash and polymers. Few researchers have also shown the advantageous of utilizing treated fly ash in a wide variety of polymer matrices. The present work is focused on studying the possibility of manufacturing thermosetting syntactic foams using conventional casting route.

Fly-ash/polymer composites provide a significant opportunity to science and technology and pose significant challenges for future work in polymer composite field. Such fly ash filled polymer composites possess attractive mechanical, thermal,

electrical properties, better dimensional stability and are cost effective. Motivation for pursuing this topic is summarized as below.

- Waste utilization.
- Lower environmental pollution.
- Reduction in consumption of polymers.
- Eco friendly processing.
- Durable components.

Based on the above points, objectives are laid down and are presented in the following sections.

1.9   Objectives and scope of the work

From the foregoing literature survey, it is understood that the research reports on development of low cost thermoset based syntactic foams are hardly available. Hence, development and performance analysis of a low cost fly ash filled polymer resin system is proposed in the present investigation. The perusal of syntactic foam literature review prompted a thorough and systematic study on these composites by performing experimental characterization for various physical and mechanical properties. Therefore the work undertaken pursues the following objectives

- Incorporating environmental pollutant cenosphere filled epoxy resin (Lapox L-12) as a syntactic foam using open mold casting technique at room temperature.
- Processing of as received (untreated) and silane treated cenosphere reinforced epoxy syntactic foam composites.
- Influence of filler volume fraction and their surface modification on physical (Density and Void content) and mechanical properties (Compression, Quasi-static compression, Flexural, Tensile, Dynamic mechanical analysis, Dry sliding wear and Solid particle erosion) of the developed composites will be analyzed.
- To study the micrographs of as cast and fractured samples for structure-property correlations.

Scope of the present work includes, conventional casting of cenosphere (as received and silane treated) reinforced epoxy syntactic foam composites with cenosphere

varying as 20, 40 and 60% by volume. FTIR spectroscopy, X-ray diffractogram and particle size analysis are carried out on fly ash cenospheres. Cast samples are analyzed using micrographs for cenosphere dispersion in matrix resin. Experimental densities are reported for all the samples.

Such cast samples are tested initially for compressive response under room temperature and arctic environment. Further, quasi-static compression, flexure, tensile dynamic mechanical analysis, dry sliding wear and erosion behaviors are discussed with focus on filler content variation and surface modification effects.

1.10 Outline of the thesis

The systematic study carried out with respect to above objectives is presented in the thesis. A brief skeletal structure of the thesis is.

Chapter 1. Intends to provide necessary details of the research on syntactic foam composites along with an exhaustive literature survey followed by objective and scope of the work.

Chapter 2. Focuses on the constituents used for thermosetting syntactic foam composites, surface treatment details, fabrication route adopted and testing methodology.

Chapter 3. Compressive behavior of room and arctic conditioned samples is reported.

Chapter 4. Quasi static room temperature response is presented.

Chapter 5. Flexural behavior (room and arctic conditioned) of samples is reported.

Chapter 6. Tensile behavior of samples is discussed in this chapter.

Chapter 7. Dynamic mechanical analysis of samples is reported to study the effect of damping ability and the variations observed with respect to temperature.

Chapter 8. Dry sliding wear behavior is characterized and the results are presented here.

Chapter 9. Erosion of samples is reported in this section.

MATERIALS AND METHODS

2.1 Constituents

In the present work, hollow fly ash cenospheres (filler) and Lapox L-12 epoxy (matrix) is used to prepare lightweight thermosetting syntactic foam composites. Details about these constituents are dealt with in the sections to follow.

2.1.1 Fly ash cenospheres

Fly ash cenospheres of CIL 150 grade used as filler is procured from M/S Cenosphere India Ltd., Kolkata, West Bengal, India. Cenospheres are used in as received condition (Figure 2.1a), without any surface treatment. Table 2.1 presents the physical, chemical and sieve analysis details of fly ash cenospheres in as received condition. These cenospheres are primarily made up of alumina, silica, calcium oxide and iron oxides as observed from this table.

Table 2.1 Physical, chemical and sieve analysis details of cenospheres[*].

Physical properties		Chemical analysis		Sieve analysis	
True particle density	920 kg/m^3	SiO_2	52-62%	+ 30 # (500μm)	Nil
Bulk density	400 – 450 kg/m^3	Al_2O_3	32-36%	+ 60 # (250μm)	Nil
Hardness (MOH)	5 – 6	CaO	0.1-0.5%	+100 # (150μm)	Nil
Compressive strength	0.00176 – 0.00274 MPa	Fe_2O_3	1-3%	+150 # (106μm)	0-6%
Shape	Spherical	TiO_2	0.8-1.3%	+ 240 # (63μm)	70-95%
Packing factor	60-65%	MgO	1-2.5%	+ 240 #	0-30%
Wall thickness	5-10% of shell dia.	Na_2O	0.2-0.6%		
Color	Light grey – light buff	K_2O	1.2-3.2%		
Melting point	1200 – 1300 ºC	CO_2	70%		
pH in water	6 – 7	N_2	30%		
Moisture	0.5% max.				
Loss on ignition	2% max.				
Sinkers	5% max.				
Oil absorption	16 – 18 g/100g				

[*]As provided by the supplier.

2.1.2 Matrix

Lapox L-12 epoxy resin with K-6 hardener, supplied by M/S Atul, Valsad, Gujarat, India is the matrix resin used and is shown in Figure 2.1b. Lapox L-12 is a liquid, unmodified epoxy resin of medium viscosity that can be used with various hardeners for making composites. K-6 hardener is a low viscosity room temperature curing liquid hardener. Table 2.2 presents the properties of epoxy resin and hardener.

(a)   (b)

Figure 2.1 (a) Cenospheres and (b) Epoxy resin and hardener used for SF preparation.

Table 2.2 Properties of epoxy resin and hardener.

Description	Unit	Value
Epoxy resin (LAPOX L-12)		
Color	GS	0.8
Epoxy value	Eq./kg	5.35
Viscosity at 25 °C	MPa	11850
Volatile content at 105 °C/h	%	0.4
Hydrolysable chlorine	wt. %	0.08
Marten's value	°C	150
Hardener (K-6)		
Color	GS	0.8
Viscosity at 25 °C	MPa	10
Pot life at 80 °C	s	4140
Gel time at 80 °C	s	7080

2.2 Surface modification of cenospheres

Silane coating on cenospheres is carried out using 3-Amino propyl triethoxy silane (APTS), procured from M/S Sigma Aldrich, Bangalore, India. In syntactic foams, the volume fraction and size of cenospheres can alter the overall mechanical properties. Apart from the volume fraction and size, the interaction between cenospheres and epoxy plays a major role in load transfer mechanism between the constituents (Guhanathan et al. 2001).

Mechanical properties of cenosphere reinforced polymer composites are inferior owing to poor interfacial interactions between the hydrophilic cenosphere surface and hydrophobic polymer. Silane coupling agents are usually used as adhesion promoters between inorganic filler and organic matrix. In the present work, cenospheres are surface treated with silane by mixing 50 g of cenospheres into 100 ml solution of water/ethanol (20:80 wt.%). Further, 2% by volume of APTS is added into the solution and continuously stirred for 30 minutes at 80°C in a microwave reactor (Enerzi microwave systems, Bangalore, India). The resultant product is filtered, washed at least three times using a mix of water/ethanol and then dried in an oven to extract the coated cenospheres.

2.3 FTIR spectroscopy, X-ray diffractograms and Particle size analysis

Cenospheres are analyzed by FTIR spectroscopy (JASCO 4200, Japan, Automated Total Reflection mode, wave number 4000 to 650 cm^{-1}) to confirm the silane coating. X-ray diffractograms are determined for 2Ө values using DX GE-2P, JEOL, Japan having Nickel filter material with scanning speed of 2°/min and Cu Kα (λ=1.514A°) radiation. Particle size and shape analysis is carried out using a Sympatec (Pennington, NJ) QICPIC high speed image analysis system. The particles are dispersed using the RODOS and VIBRI systems, which aerosolize a stream of particles in a jet of compressed air.

A pulsed laser illuminates the particles as they pass a camera that images the particles at 175 frames/sec. For each particle imaged, the equivalent diameter is calculated as

the diameter of a sphere having a projected area equal to the projection captured by the camera. Five runs of each particle type are conducted and the values presented are averaged from these runs, with weight according to the number of particles in each run. Approximately 375,000 and 550,000 particles are measured for untreated and treated particles, respectively (Bharath Kumar et al. 2016, Bharath Kumar et al. 2016).

2.4 Sample preparation

Syntactic foams are fabricated by mixing desired volume fraction of cenospheres with Lapox L-12 epoxy resin and K-6 hardener at room temperature. The mixture is gently stirred to obtain a homogeneous and uniform slurry, followed by adding 10 wt.% hardener and finally mixture is degassed prior to casting into the aluminum molds (Figure 2.2). The cast slabs are cured at room temperature for 24 hours and post cured at 90°C for 3 hours. Three different syntactic foams with varying cenosphere content of 20, 40 and 60 vol.% in epoxy matrix are fabricated. This procedure is adopted for both as received and silane treated cenospheres. Additionally, neat specimens, i.e., without any filler in the matrix, are also prepared for comparison.

Samples are named according to the convention EXX-Y, where E denotes epoxy resin, XX is the volume fraction of cenospheres (20, 40 and 60%) and Y represents filler modification condition (U denotes untreated and T represents treated cenospheres). Cast slabs are trimmed using diamond saw cutter to confirm the dimensions as mentioned in ASTM standard. The densities of all the samples are measured using the procedure as outlined in ASTM D792-13 . Theoretical density is computed using rule of mixture and is given by,

$$\rho = \rho_f V_f + \rho_m V_m \tag{2.1}$$

where, ρ and V are density and volume fraction, respectively. Subscripts f and m denote filler and matrix, respectively. Furthermore, the void content (ϕ_V) is estimated using theoretical (ρ^{th}) and experimental (ρ^{exp}) densities and is given by (Gupta et al. 2004, Tagliavia et al. 2010),

$$\Phi_V = \frac{\rho^{th} - \rho^{exp}}{\rho^{th}} \qquad\qquad (2.2)$$

Figure 2.2 Mold used for sample preparation.

2.5 Density measurement

ASTM D792-13 standard is espoused to measure the density of all the fabricated specimens. The densities of five specimens are measured and the average values and standard deviations are reported.

2.6 Arctic conditioning

There is no standard for arctic exposure studies and therefore, a procedure for specimen conditioning is developed in-house, which is similar to the initial conditioning for water intake measurements as mentioned in ASTM C272-01 and ASTM D5229-15 standards. Prior to any type of conditioning and testing, the syntactic foams are oven dried for 24 hours to eliminate moisture content absorbed during processing, if any. Further, five samples for each volume fraction for both untreated and treated categories are placed in a freezer, which is maintained at -60°C.

All specimens are then conditioned for 57 days, after which the specimens are mechanically tested under in-situ arctic conditions (-60°C). The procedure followed to

obtain the mechanical properties for the syntactic foam samples is discussed in the following section.

2.7 Compression testing at room and arctic temperatures

All the specimens are mechanically tested in compression at room (30°C) and arctic temperatures (-60°C) using Zwick (Zwick Roell Z020, ZHU) Universal Testing system as depicted in Figure 2.3. A crosshead displacement rate of 1.3 mm/min is applied on 12.7×12.7 mm face of each specimen following the ASTM D695-15 standard. Compressive modulus and ultimate strength are calculated using (Garcia et al. 2017),

$$E_z^c = \frac{(P_{0.00x2} - P_{0.00x1})h}{(\delta_{0.00x2} - P_{0.00x1})A} \; ; \; F_z^c = \frac{P_{max}}{A} \tag{2.3}$$

where, $P_{0.00x}$ is the applied force at a given deflection, h is the specimen mean height, $\delta_{0.00x}$ is the recorded deflection value, A is the cross-sectional area and P_{max} is the ultimate force prior to failure.
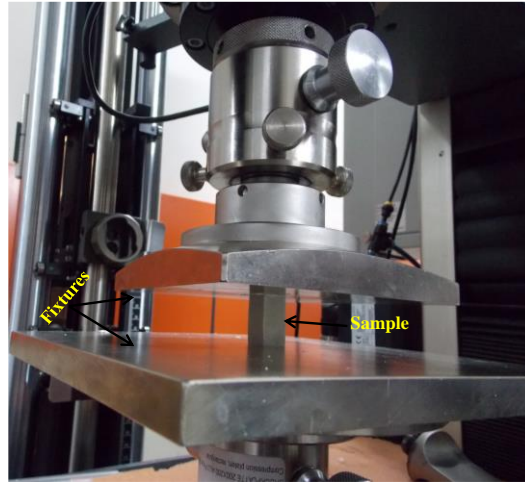
Figure 2.3 Compression test setup with sample in place.

2.8 Quasi-static compression test

The quasi-static compression tests are conducted using a Zwick (Zwick Roell Z020, ZHU) computer controlled universal test system with 20 kN load cell. The test is conducted at an initial strain rate of 10^{-3}, 10^{-2} and 10^{-1} s^{-1} corresponding to cross-head displacement velocity of 0.001, 0.01 and 0.1 mm/min respectively. The criteria for end

of the test is set at 20 kN load. The data is analyzed using an in-house developed MATLAB code. Compressive modulus and strength are calculated for all the specimens. The compressive strength is defined by the peak stress at the end of the elastic region. At least five samples of each volume fraction are tested to check for repeatability.

2.9 Flexural test

The flexural testing is performed in three-point bend configuration using a computer controlled Zwick (Zwick Roell Z020, ZHU) machine having a load cell capacity of 20 kN as depicted in Figure 2.4. Flexure test is conducted as per (ASTM D790-17) standard at both room (30°C) and arctic condition (-60°C). A pre-load of 0.1 MPa is set and crosshead displacement rate is maintained at 1.4 mm/min. All specimens have span length of 52 mm to maintain 16:1 span length/thickness ratio. Five replicates of each volume fraction for both untreated and treated configurations are tested and average values are reported for analysis. Tests are continued until the specimen failure and the stress-strain data is acquired. The flexural modulus is calculated by,

$$E_{fM} = \frac{L^3 m}{4bd^3} \tag{2.4}$$

where L is the support span (mm), b is the width of beam (mm), d is the thickness of beam (mm) and m is the slope of the tangent to the initial straight-line portion of the load-deflection curve. The flexural stress is estimated by (Garcia et al. 2017),

$$\sigma_{fs} = \frac{3PL}{2bd^2} \tag{2.5}$$

Where P is the load (N) at a given point on the load-deflection curve. The reported flexural strength values are taken post fracture for comparison.
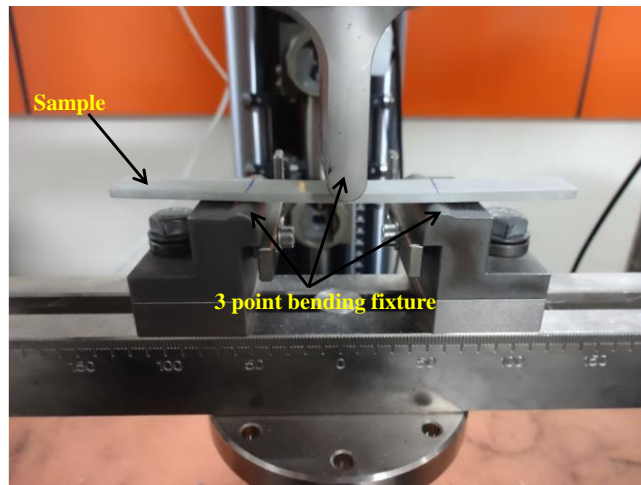
Figure 2.4 Three point bending test setup.

2.10 Tensile testing

A computer controlled universal test system (Z020 Zwick Roell, USA) with 20 kN load cell is used for tensile testing as shown in Figure 2.5. Samples with dimension of narrow width –13 mm, length of the narrow section – 57 mm, overall width – 19 mm, and overall length – 165 mm are considered. All the samples have a gage length of 50 mm and distance between grippers is maintained at a distance of 115 mm. A constant crosshead displacement rate is maintained at 5 mm/min during the tests (ASTM D638-14). The test is conducted till the fracture of the sample. The acquired load and displacement data are used to calculate the stress and strain, respectively. Average modulus and strength values of five specimens for each sample are reported.

2.11 Dynamic Mechanical Analysis

Dynamic mechanical analysis is carried out using TA Instruments (New Castle, DE) Q800 DMA (Figure 2.6a). Specimens of recommended dimensions 7×4×50 mm are tested in the dual cantilever configuration with a span length of 40 mm (Figure 2.6b). Testing is conducted in the strain control mode with a maximum displacement of 25 µm. DMA is conducted to study the behavior of the syntactic foams at high temperature using the temperature sweep mode at constant frequency. In the temperature sweep test, the temperature is ramped from 28 to 175 °C at a rate of 1°C/min with the deformation occurring at a constant frequency of 1 Hz. Testing is stopped once the storage modulus

reaches a value of 20 MPa to prevent total melting of the specimen. At least five specimens of each type are tested in this phase.
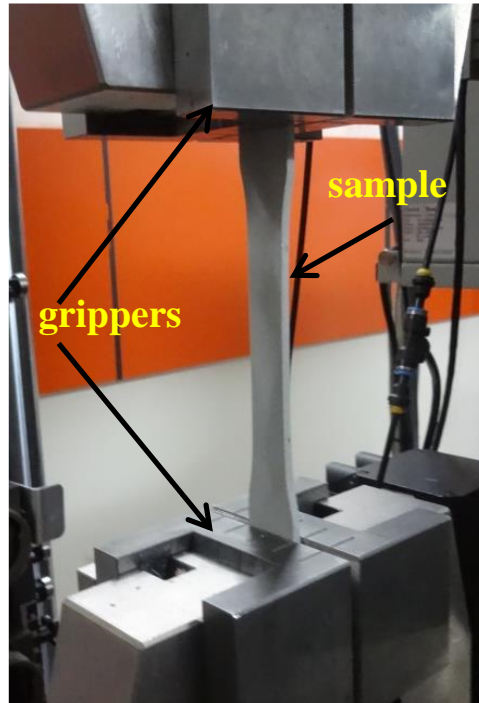
Figure 2.5 Tensile test setup.

(a)   (b)

Figure 2.6 (a) DMA setup and (b) Test configuration.

2.12 Dry sliding wear testing

Wear test in dry mode is conducted at ambient conditions as outlined in ASTM G99-05 using tribometer (TR-20LF-PHM400-CHM600) procured from DUCOM, Bangalore, India (Figure 2.7). EN-31 disc having 62HRC hardness is used for investigating wear response of all the prepared samples. The tests are carried out on 120 mm diameter track with 318 and 795 rpm corresponding to 2 and 5 m/s sliding velocities. Table 2.3 shows the parameters and their values used for the wear experiments.
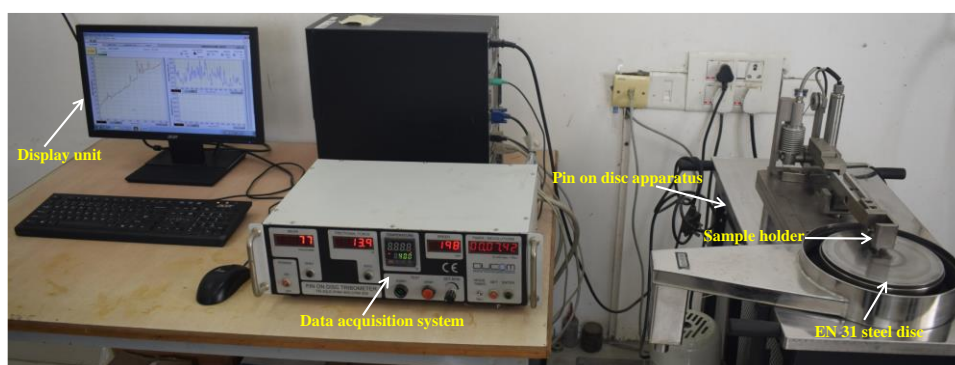
Figure 2.7 Pin on disc tribometer setup with data acquisition system.

Table 2.3 Wear parameters used in the present investigation (Doddamani et al. 2017, Manakari et al. 2015).

Input parameters		Output parameters
Cenosphere content, (vol. %)	0, 20, 40 and 60	Wear rate (mm^3/km)
Cenosphere morphology	Untreated and treated	Specific Wear rate (mm^3/N-km)
Load, F (N)	30 and 50	Coefficient of friction
Sliding velocity, V (m/s)	2 and 5	Disc Temperature (°C)
Sliding distance, D (km)	3, 5 and 7	

Sliding velocity, applied load and sliding distances are represented as V_a, F_b and D_c. Subscripts a, b and c represent respective values of the parameters. The width of the

wear track is 12±0.01 mm. Disc is polished with SiC paper (600 grit) prior to each test for maintaining constant surface roughness value of 0.11 μm. The sample with dimensions of 12×12×25.4 mm is clamped firmly in the sample holder and test is carried out. Frictional force and height loss are recorded. Pin cross-sectional area is used to compute the volume loss. Sliding distance is calculated from sliding speed and time elapsed. Wear rate (w_t) is determined by,

$$w_t = \frac{W_C - W_B}{D_C - D_B}$$

(2.6)

Wear rate varies with applied normal load and is independent of sliding distance. Wear resistance (w_r) is reciprocal of wear rate and is given by,

$$w_r = w_t^{-1}$$

(2.7)

Specific wear rate (w_s) accounts for the load carrying capacity and is computed using,

$$w_s = \frac{w_t}{F}$$

(2.8)

Coefficient of friction (μ) is defined as,

$$\mu = \frac{F_T}{F_N}$$
(2.9)

where, subscripts C and B corresponds to end and start of steady-state wear. F_T and F_N represents tangential force and normal force respectively. Temperature of the steel disc after the completion of each wear test is measured using a thermocouple (CMPH – x, HAMI THERM, Netherlands). Energy Dispersive Spectroscopy (EDS) (JSM 6380LA, JEOL, Japan) is done on the wear debris to identify the prominent wear mechanism.

2.13 Solid particle erosion

Erosion tests are performed under conditions as outlined in ASTM G76-13 standard using a test rig (Figure 2.8) procured from DUCOM, Bangalore, India. Compressed dry air is used to accelerate 5 g of erodent particles per minute to strike the test sample. Erosion test parameter values are listed in Table 2.4 and are chosen based on the literature (Satapathy et al. 2009, Srivastava and Pawar 2006).

Figure 2.8 Erosion test setup.

Table 2.4 Erosion test parameters (Satapathy et al. 2009, Srivastava and Pawar 2006).

Erosion parameters	Parameter	Value
Constants	Erodent	Silicon carbide
	Erodent size (μm)	250
	Erodent shape	Angular
	Test temperature (°C)	Room temperature
	Erodent mass flow rate (g/s)	0.0833
	Nozzle to sample distance (mm)	10
	Nozzle diameter (mm)	1.5
	Nozzle length (mm)	86
Variables	Impingement angle (°)	30, 45, 60, 90
	Impact velocity, v (m/s)	30, 45, 60
	Cenosphere content (vol. %)	0, 20, 40, 60

Specimen surface is cleaned with acetone to remove the impurities. Subsequently all the specimens are weighed to an accuracy of 0.001 mg using a precision electronic balance (BSA223S, SARTORIUS, Germany). The specimens are firmly fixed in the sample holder and then the tests are carried out for 5 minutes at a predetermined erodent velocity and then the specimen weight loss is recorded. The test is continued and the weight is recorded every 2 minutes until the steady state of weight loss is achieved (ASTM G76-13). Total time of test is recorded to estimate erosion rate (ratio of sample weight loss to weight of eroding particles) (Harsha and Jha 2008). At least 5 specimens are tested for each test condition and the average values are reported. 3D profiles of the eroded samples are obtained using optical profilometry (ZETA-20, ZETA instruments, USA).

2.14 Imaging

Scanning electron microscope (JSM 6380LA, JEOL, Japan) is used for micro structural analysis. All the samples are sputter coated using JFC-1600 auto fine coater (JEOL, Japan). Nikon D7000 camera with Nikkor 35 mm F1.8G lens is used for optical imaging. Tokina AT-X pro 100 mm F2.8D macro lens is used for imaging fractured features.

3 ROOM AND ARCTIC ENVIRONMENT COMPRESSIVE RESPONSE

3.1 FTIR and XRD analysis

Fly ash cenospheres used in the present study are used in as received (untreated) and silane modified (treated) conditions. FTIR results for untreated and silane treated cenospheres are presented in Figure 3.1a. The spectrum confirms the presence of a silane surface layer and the –C–H– stretching of propyl group is seen at 2929 cm^{-1}. XRD diffraction results of as received and silane modified cenospheres is shown in Figure 3.1b. Untreated and treated fly ash cenospheres has a main peak at 2θ value of 26.6 and 26.04 and other numerous small peaks manifesting mainly metal oxides, predominantly SiO_2 and $3Al_2O_3$ respectively.
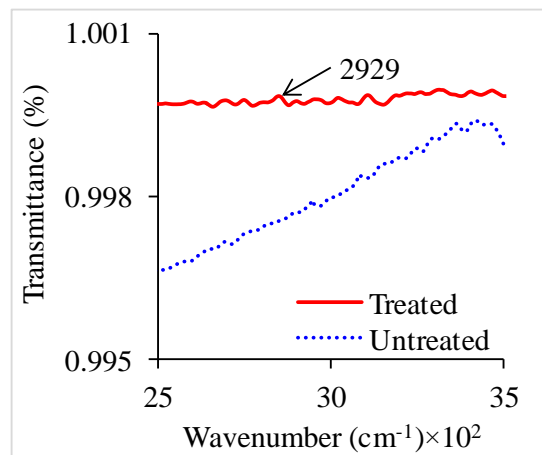
(a)
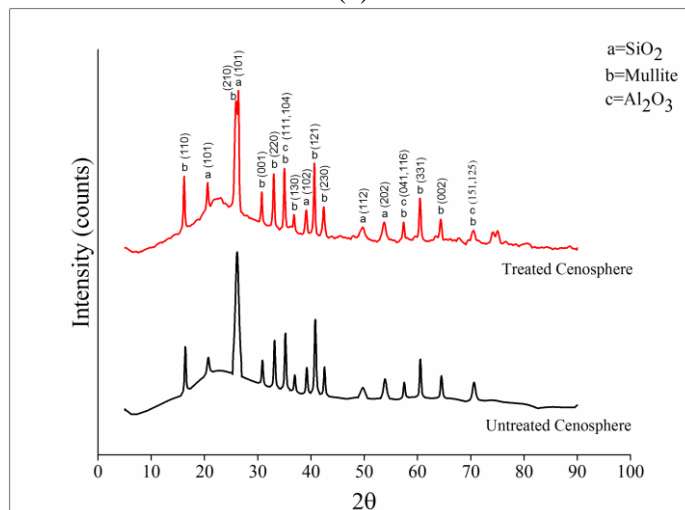
(b)

Figure 3.1 (a) A section of the FTIR spectra of untreated and silane treated cenospheres (Bharath Kumar et al. 2016) and (b) X-ray difftractogram of cenospheres.

54

3.2 Particle size analysis

Figure 3.2 presents micrographs of untreated and treated cenospheres respectively. The coating layer is not visibly identifiable in the micrographs due to its small thickness, despite, FTIR results (Figure 3.1a) confirm the silane presence on cenospheres. Surface morphology is not uniform for fly ash cenospheres due to variations in sphericity and presence of numerous defects as seen from these micrographs. One such broken cenospheres is micrographed at higher magnification and is presented in Figure 3.2c. Porosity in the cenosphere walls and irregular wall thickness is clearly evident from the micrograph, which might lead to lower mechanical properties as compared to non-porous ones. Such variations lead to deviation of the experimental investigation from that predicted by empirical and/or mathematical models.

(a)   (b)

(c)
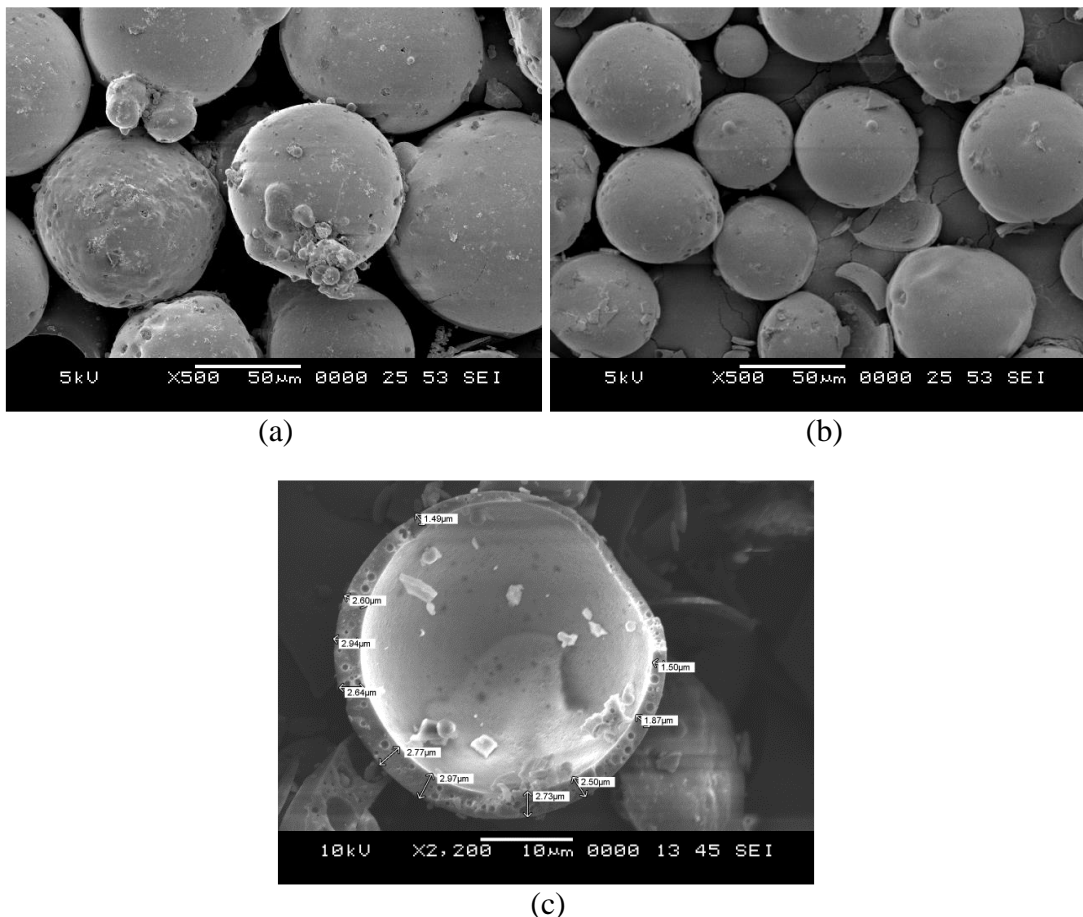
Figure 3.2 Cenosphere micrographs of (a) untreated (b) treated and (c) one broken treated particle.

Particle size distribution of untreated and treated cenospheres and their results are presented in Figure 3.3. It can be observed that the volume weighted mean particle size for untreated and treated particles are 99.5 and 110.2 μm respectively. Broader peak is seen in case of treated particles. Untreated and treated cenospheres registered X_{50} median particle sizes of 76.3 and 98.1 μm, respectively confirming an increase in average diameter owing to silane treatment. Densities of as received and treated cenospheres are measured to be 920 and 1000 kg/m^3.

Sphericity of cenospheres is observed to be in the range of 0.6-0.85 (Bharath Kumar et al. 2016). Deviation from '1', a perfectly spherical particle, might be due to surface defects as observed in Figure 3.2a. Shift in the curve of treated particles in the plot (Figure 3.3) can also be attributed to particle coating.

From Figure 3.3, considerable extension is seen at the tail end of the curve for the treated particle indicating a small amount of cluster formation. Shear forces induced during stirring is expected to disperse some of these clusters formed, if any.
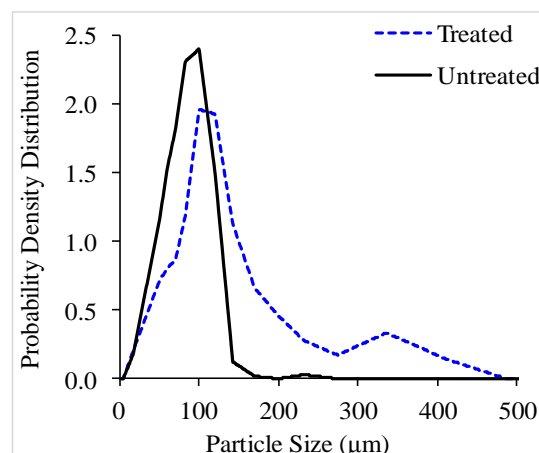
Figure 3.3 Particle size analysis of untreated and treated cenospheres (Bharath Kumar et al. 2016, Bharath Kumar et al. 2016).

3.3 Fabrication of specimens

Synthesizing of syntactic foam composites with uniform dispersion of cenospheres, minimum cluster formation and particle failure in the matrix during processing is a

challenging task. Manual stirring approach (Figure 1.3) is used in the present work to prepare cenosphere/epoxy foams. Micrographs of as cast cenospheres/epoxy foams are presented in Figure 3.4. Uniform dispersion of hollow cenospheres both, untreated and treated in the matrix is observed in Figure 3.4a and Figure 3.4b demonstrating the feasibility of using manual stirring for developing such syntactic foam composites.

Further, clusters are not seen to be formed for the foams with treated cenospheres (Figure 3.4b) as anticipated from Figure 3.3. Clusters are expected to be broken effectively due to shear forces induced owing to stirring of the cenospheres/epoxy slurry as mentioned earlier. Interfacial adhesion between the epoxy resin and the as received cenospheres is seen to be poor as seen in Figure 3.4c.

Silane modification of cenospheres shows good adhesion between the constituents (Figure 3.4d). Improvement in the interfacial bonding is expected to improve the load transfer from the matrix to the particle and improve the properties of syntactic foams. Load transfer between filler and the matrix along with failure mechanism are governed by interface topology.

Flexural and tensile properties are strongly affected by the interfacial bonding strength (Bharath Kumar et al. 2016, Bharath Kumar et al. 2016, Yusriah and Mariatti 2013, Zhang and Ma 2010) as interfacial cracks tend to form under such conditions. However, in compression, the mechanical properties are less sensitive to interfacial adhesion (Aureli et al. 2010, Tagliavia et al. 2010). Nevertheless, non-uniform layer of coating makes comparison of mechanical properties to be challenging (Tagliavia et al. 2010), and is beyond the scope of the present work.

(a)   (b)

(c)   (d)
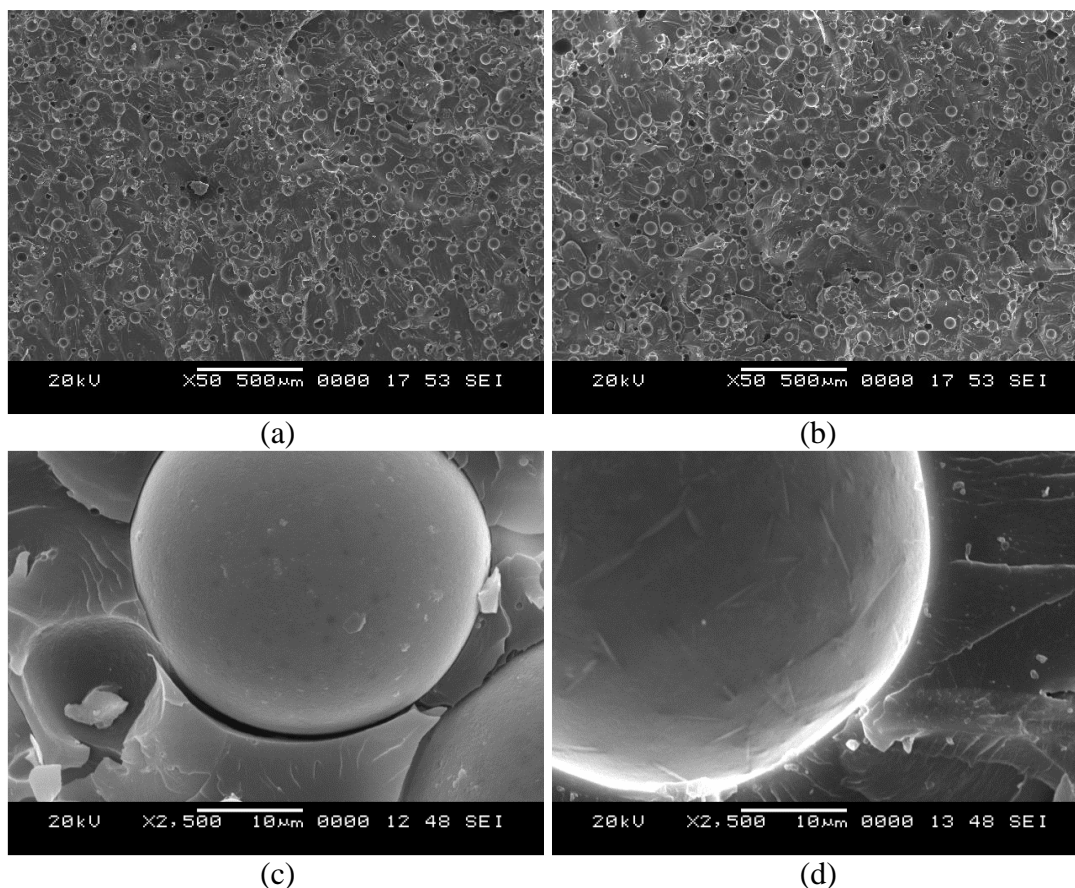
Figure 3.4 Micrographs of (a) E20-U (b) E20-T foams showing uniform dispersion of cenospheres (c) Lack of bonding for E20-U and (d) good interfacial bonding in E20-T is noted.

3.4 Density

Quality and the mechanical properties of the syntactic foam composites depend on the survival of the hollow cenospheres and the void content due to entrapped air during processing. Thereby, it is necessary to quantify and correlate these parameters with the properties being investigated. Table 3.1 presents shore hardness, density and void content estimations. Hardness of syntactic foams increases with increase in content of cenospheres for both untreated and surface treated cenospheres and is higher than that of the neat epoxy for all the syntactic foams. Improved interfacial bonding promoted by silane treatment of cenospheres has resulted in increased hardness of the specimens at comparable cenosphere content. Theoretical densities are computed using Equation 2.1, which are higher compared to experimental ones as seen from Table 3.1. Reduction in the density of composites determined experimentally as compared to the theoretical

58

ones is attributed primarily due to presence of hollow fly ash particles in resin and partially owing to air entrapment in matrix during the process of mechanical mixing of cenospheres in the resin. The presence of very few entrapped air pockets is observed in representative samples as presented in Figure 3.4a and Figure 3.4b, which are characteristic of typical syntactic foams. Such entrapped air is undesired as it adversely affects the mechanical properties and is referred as voids. The void content (ϕ_V) is calculated using Equation 2.2. As seen from Table 3.1, the void content appears to increase with increase in filler content except at highest filler loading. The presence of such voids further reduces the matrix content. The amount of matrix present at 60 vol.% filler loading is much lesser compared to other compositions resulting in much lower void content. Density of foams with treated cenospheres registered higher density values for all the compositions prepared. Silane coating on as received cenospheres increases the effective mean diameter, thereby increasing their density. Narrow variations in standard deviations are observed affirming consistency in specimen processing.

Table 3.1 Hardness, density and void volume fraction of syntactic foams.

Material	Shore Hardness	ρ^{th} (kg/m^3)	ρ^{exp} (kg/m^3)	ϕ_V (%)	Weight saving potential (%) compared to 'E0'
E0	64±1.28	-------	1192.00±23.84	0.34	-------
E20-U	68±1.36	1137.60	1129.63±22.59	0.70	5.23
E40-U	74±1.48	1083.20	1064.72±21.29	1.71	10.68
E60-U	78±1.56	1028.80	1028.36±20.56	0.05	13.73
E20-T	73±1.46	1153.60	1133.14±22.66	1.78	4.94
E40-T	77±1.54	1115.20	1073.92±21.47	3.70	9.91
E60-T	83±1.66	1076.80	1055.65±21.11	1.98	11.44

Further, weight saving potential is estimated as compared to neat epoxy samples, and values are listed in Table 3.1. Lower densities of syntactic foams with untreated cenospheres noted to have better weight saving. Specific mechanical properties are worth investigating for exploiting these lightweight cenosphere/epoxy foams in naval applications. It would be an interesting task to understand and analyze the effect of arctic environment on such abundantly available untreated/treated hollow fly ash cenospheres to propose suitable applications.

3.5   Compressive modulus and strength

Figure 3.5 presents stress-strain curves for all types of cenosphere/epoxy syntactic foams in compression including neat epoxy samples. The unconditioned (dry) neat resin and syntactic foams show similar stress-strain profiles until peak stress, which consists of a linear elastic region followed by a strain softening region that is characterized by stress drop. Upon further loading the specimens in compression, the stress starts rising again in neat epoxy samples upto around 15% strain value after which it starts to drop until final fracture. The post peak increase in stress is faster and significantly higher in the case of neat resin, whereas for syntactic foams it depends on the volume fraction and surface modification of hollow fillers. In both treated and untreated syntactic foams, the strain at final fracture decreases with increasing cenosphere volume fraction.
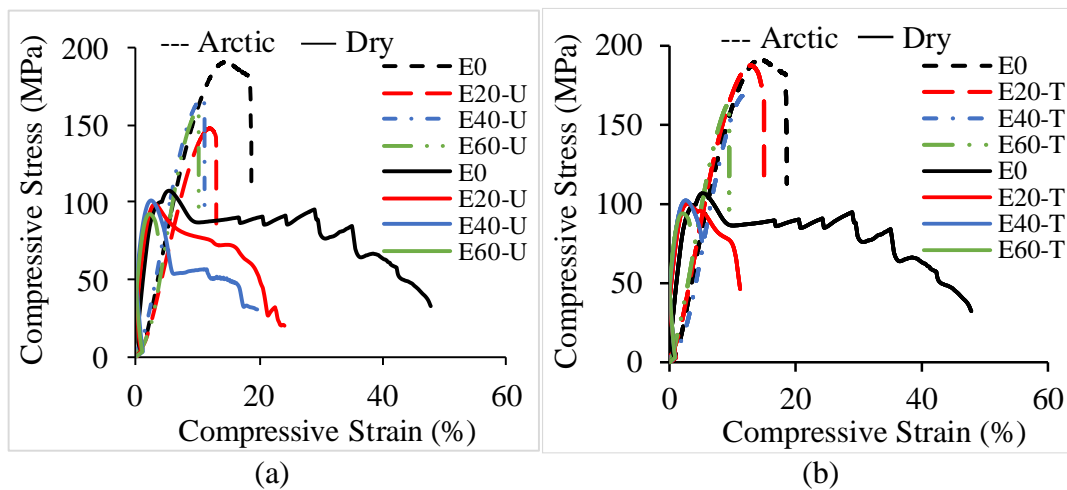
Figure 3.5 Representative stress-strain curves in compression of neat epoxy and their syntactic foams with (a) untreated and (b) treated cenospheres.

For the case of arctic exposed samples, both treated and untreated cenospheres/epoxy foams demonstrated a brittle behaviour. Upon reaching a maximum load carrying capacity, a slight decrease in stress is observed before complete failure of the samples. The compression rate is held constant in this experimental study at the ASTM standard recommended value, as the stress–strain behavior can potentially be a strain rate dependent phenomena (Bardella 2001, Boyce et al. 1988). From Figure 3.5, it can be noted that all syntactic foam compositions do not show a stress plateau, which is seen as a typical feature for most types of syntactic foams, including epoxy and aluminum

matrix syntactic foams (Balch and Dunand 2006, Woldesenbet et al. 2005). In case of epoxy syntactic foams with relatively brittle microballoons, once the maximum load carrying is reached, the stress value decreases without much deformation till the final fracture (Swetha and Kumar 2011). Further, lower temperatures induce behavioral changes in the matrix making them more stiff and strong. In the presence of stiffer cenospheres, such an effect of matrix hardening when exposed to arctic conditions affects plateau stress to a greater extent (Lord and Dutta 1988, Rivera and Karbhari 2002). In the current study, the syntactic foams tested under in-situ arctic conditions failed catastrophically after reaching the maximum compressive stress value. Therefore, the samples are not subjected to further compressive loading beyond this point.

Compressive modulus is determined from the slope of the initial linear region of the stress-strain response and is presented in Figure 3.6a. It is observed that compressive modulus increases with increasing filler content, for both untreated and treated fillers. Significant rise is observed for EXX-T foams with higher filler content. Also, the compressive modulus values are significantly higher in syntactic foams as compared to that of the neat epoxy. Further, the specific moduli (modulus divided by the foam density) for EXX-T composites are 26-81% higher than the neat epoxy as exhibited in Figure 3.6b. Significant advantage over the neat epoxy in terms of weight saving can be achieved if EXX-T foams are used in compressive loading conditions.

Compressive strength is defined as the first peak in the stress-strain response. Figure 3.6c shows the compressive strength values, where it is observed that an increasing cenosphere content in both EXX-U and EXX-T configurations decreases compressive strength. Compressive strength values of all the foams tested are lower compared to neat epoxy samples. Nevertheless, results for specific compressive strengths (compressive strength divided by density) for all the foam compositions are comparable or marginally higher than that of the neat resin.
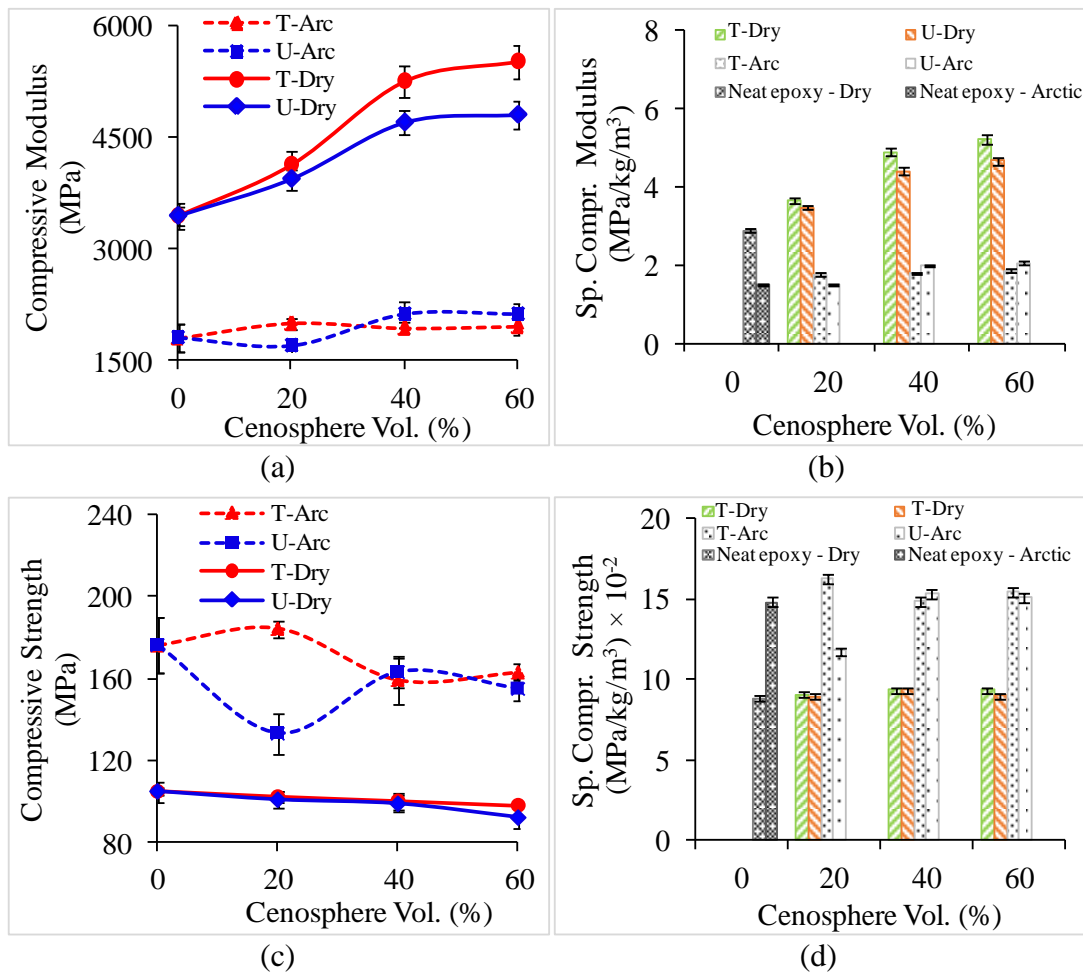
Figure 3.6 Experimentally measured compressive (a) modulus (b) specific modulus (c) strength and (d) specific strength of syntactic foams.

For the arctic conditioned samples, both treated and untreated cenospheres/epoxy foams manifest a brittle behaviour in their stress-strain response. By comparing the arctic conditioned samples to the unconditioned (dry) samples, a decrease in compressive modulus of elasticity by 47-57% and 47-65% is observed for untreated and treated cenosphere/epoxy foams respectively (Table 3.2). On the other hand, the compressive strength value increased by 32-68% for untreated cenospheres and 59-80% for treated cenospheres. Exposure to arctic condition increases the strength due to the matrix hardening (Rivera and Karbhari 2002, Swetha and Kumar 2011). Lower temperatures induce a change in matrix strength and stiffness making them more stiff and strong as they are cooled (Rivera and Karbhari 2002). Pre-conditioning of samples to arctic temperature appears to have degraded the foams due to cyclic change in

temperature, thereby, causing a reduction in the compressive modulus. However, in-situ arctic condition introduced more strength into the syntactic foams due to matrix hardening. On the other hand, hygrothermal studies on syntactic foams by (Gupta and Woldesenbet 2003) reveal considerable decrease in modulus without significant change in the compressive strength at lower temperature owing to plasticization resulting from moisture infusion.

Table 3.2 Compressive modulus and Strength properties of syntactic foams.

Material	30°C		-60°C	
	Strength (MPa)	Modulus (MPa)	Strength (MPa)	Modulus (MPa)
E0	104.88±2.01	3443.46±119.78	176.26 ±13.57	1807.48 ±179.13
E20-U	100.79±3.79	3939.28±137.03	133.01 ±9.98	1701.09 ±50.92
E40-U	98.79±4.10	4697.47±165.68	163.03 ±6.96	2125.45 ±171.09
E60-U	92.06±5.53	4800.71±197.21	154.87 ±5.67	2124.40 ±156.44
E20-T	102.29±3.14	4132.08±179.78	184.41 ±4.01	2001.20 ±80.54
E40-T	100.26±4.03	5253.51±206.85	159.48 ±11.82	1937.16 ±76.13
E60-T	98.11±0.62	5518.09±231.88	163.10 ±3.91	1959.14 ±107.00

3.6 Micrographic analysis of fractured samples

Fracture features of neat epoxy and syntactic foams with two volume fractions of cenospheres are compared in Figure 3.7. Prominent shear crack and excessive plastic deformation marks are observed in neat epoxy sample (Figure 3.7a). Syntactic foams containing 20 vol.% cenospheres deform with fewer cracks than those containing 60 vol.% ones for EXX-U and EXX-T configurations. The failure features of these specimens are similar to those observed in the literature (Gupta et al. 2001).

Shear cracks form and propagates with fragment formation from the sidewalls. Brittleness of the foams increases at higher filler loadings due to inclusion of relatively brittle cenospheres in epoxy matrix. At E60, excessive crushing of constituents and specimen cracking are observed for foams with untreated and treated cenospheres respectively as seen in Figure 3.7d and Figure 3.7e.
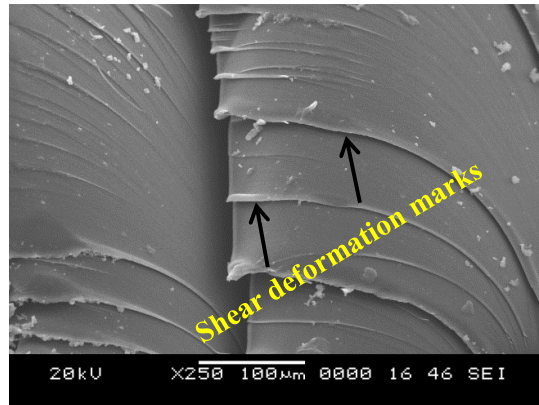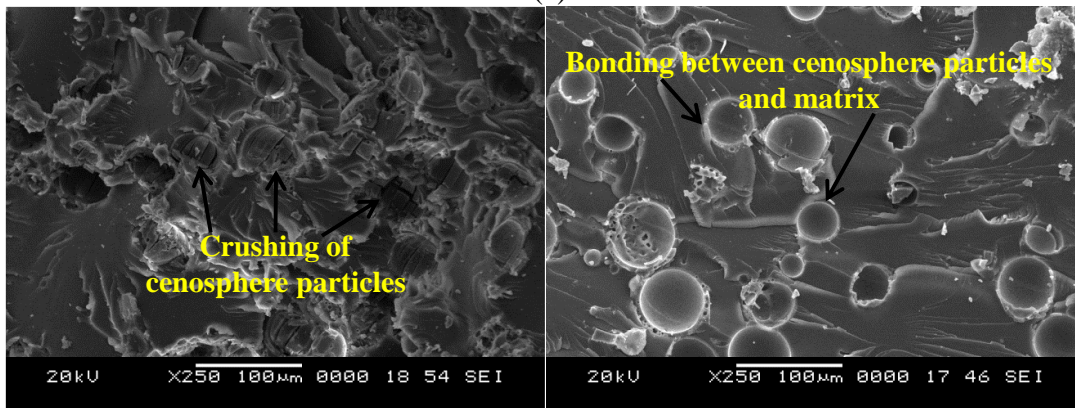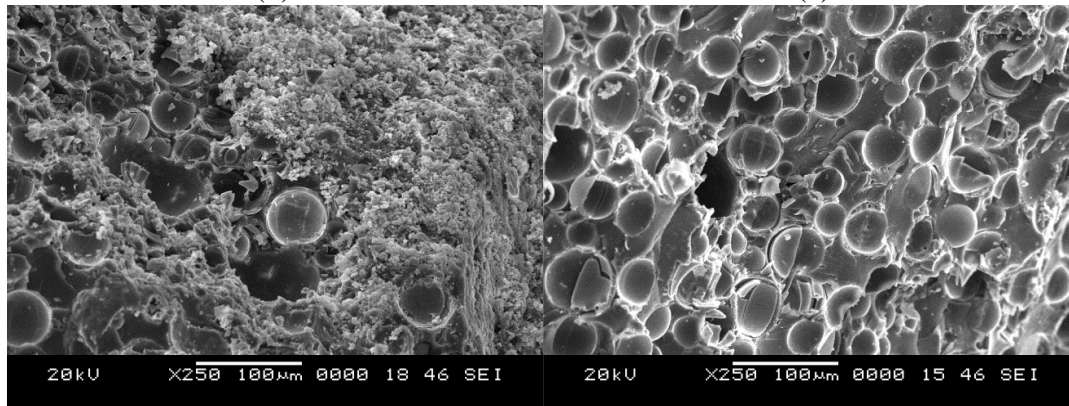
Figure 3.7 Micrographs of (a) Neat epoxy resin (b) E20-U (c) E20-T (d) E60-U and (e) E60-T post compression room temperature tests.

In addition, the stress–strain curves of unconditioned EXX-T type syntactic foams show lower fracture strain values compared to unconditioned EXX-U. Relatively higher brittleness owing to silane coating on cenospheres increases overall brittleness of composite foams reducing the fracture strain for EXX-T. Nevertheless, in case of coated cenospheres, mean particle diameter appears to influence the higher stiffness of

the composites resulting in earlier crack initiation in the direction of compression. This might lead to formation of relatively larger fragments in EXX-T. Such situations are preferred while designing core for sandwich structures. In case of arctic exposed samples, fracture strain values are similar between EXX-T and EXX-U type syntactic foams.

Fracture surfaces of representative syntactic foams are shown in Figure 3.8 and Figure 3.9, where extensive cenosphere damage is observed during compressive fracture of the EXX-U material. Such extensive fracture of brittle reinforcing media, similar to microballoons, has also been observed in epoxy matrix syntactic foams (Gupta et al. 2002). On the other hand, EXX-T foams manifest lesser cenosphere damage in combination with matrix damage at both lower and higher cenosphere volume fractions. This shift in failure mechanism is an indication of effective transfer of stresses between cenospheres and the matrix, which is attributed to good interfacial bonding between the constituents due to silane treatment. Though the interfacial strength has not been explicitly measured at the microscale for these samples, the existence of silane coating has been determined through FTIR as shown in Figure 3.1a.
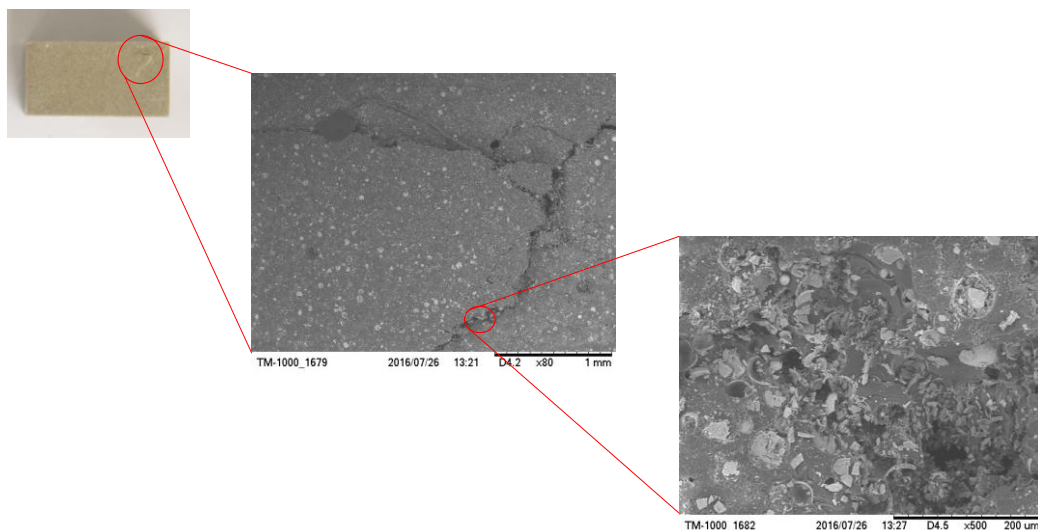
Figure 3.8 E40-U compression specimen schematic post arctic condition tests.
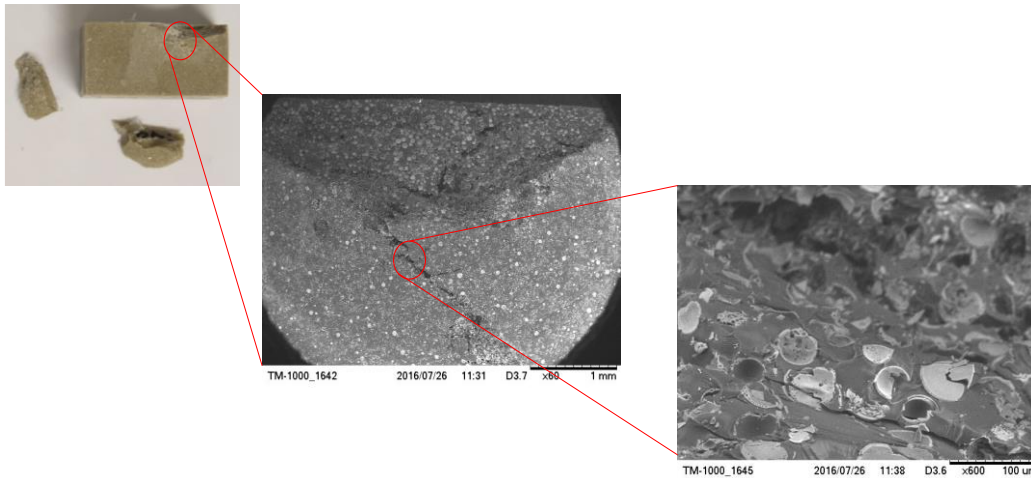
Figure 3.9 E40-T compression specimen schematic post arctic condition tests.

For E60-T specimen, majority of the cenospheres are partially fractured retaining their original location resulting in higher strength values compared to E60-U foam. Though the compressive strength shows decreasing trend with increasing filler content, specific values are comparable or marginally better than the neat resin counterparts. Such situations are highly desirable in structural components used in marine applications.

Conclusions

Compressive properties of untreated and treated cenosphere/epoxy foams under room and arctic temperatures are discussed in the present chapter. It is observed that the cenosphere/epoxy foams with untreated and treated fillers manifest lower strains to failure under compressive loading at room temperature conditions as compared to neat epoxy samples. All foam compositions show an increase in compressive modulus compared to that of the neat resin. The results show that epoxy matrix syntactic foams with treated cenospheres have promise for structural application at room temperatures. Significantly higher specific compressive moduli and marginally higher specific strength make treated cenosphere/epoxy (EXX-T) foams a viable material for marine applications.

Further, these foams are subjected to compressive loading at -60°C to explore the feasibility of using them in arctic environment. Similar to room temperature tested samples, all cenosphere/epoxy foams with treated and untreated fillers exposed to arctic

conditions demonstrated a lower failure strains compared to neat epoxy, but also compared to its unconditioned counterpart. It is observed that for in compression, the modulus of elasticity decreased for arctic specimens compared to the unconditioned (dry) specimens. However, an overall increase in compressive strength is observed when tested under in-situ arctic condition. After examining the behaviour of all samples, it is noted that the conditioning of specimens under extreme low temperatures caused the material to reduce their compressive modulus. Also, the syntactic foams behaved in a brittle manner causing drastic failure under in-situ compression testing.

4 QUASI-STATIC COMPRESSION BEHAVIOR

4.1 Quasi-static compressive stress-strain curves

Quasi-static compressive stress-strain curves of all the samples at different strain rates are presented in Figure 4.1. All the samples exhibit similar stress-strain profiles until peak stress is reached. Drop in stress at the end of the initial linear elastic region followed by a stress plateau region is observed which resembles typical characteristic of foams and porous materials. Similar behavior is observed for epoxy and vinyl ester matrix syntactic foams (Gupta et al. 2006, Swetha and Kumar 2011). Since epoxy resin is brittle in nature, stress drop is observed at the end of the initial linear elastic region followed by a stress plateau (Gupta et al. 2010,Wouterson et al. 2005, Zhang et al. 2014). This drop of stress is attributed to the successive failure of brittle particles in the matrix owing to stress concentration in the confined regions around broken particles (Kim et al. 2000). Stress plateau observed in cenosphere/epoxy syntactic foams is not witnessed for HDPE syntactic foams (Bharath Kumar et al. 2016). Peak stress values are seen to be decreasing drastically with decreasing strain rates for EXX-U foams as compared to EXX-T foams. Peak stress values of E20-T foam are comparable to neat epoxy response. Further, EXX-T foams are seen to be performed better as compared to EXX-U foams as seen from Figure 4.1 implying surface modification influence on quasi-static compressive response.

Figure 4.2 shows a schematic representation of stress strain curves for the samples. The representative curve can be divided into three regions namely linear elastic region, plateau region and densification region. In the elastic region, the sample is subjected to a uniform deformation resulting in a linear elastic region. The stress attains a maximum value and consequently reaches a constant value as the load increases resulting in the plateau region. The peak stress indicates crack instigation in the matrix (Figure 4.1). Once the crack formation takes place, sustained deformation at constant stress is observed conforming to the energy absorbed by the samples under compression. Energy absorption is attributed to the fragmentation of cenospheres that expose the hollow space within cenospheres to accommodate the compression material (Gupta et

al. 2006). Stress level starts to increase again when substantial amount of cenospheres are crushed in compression representing densification region.
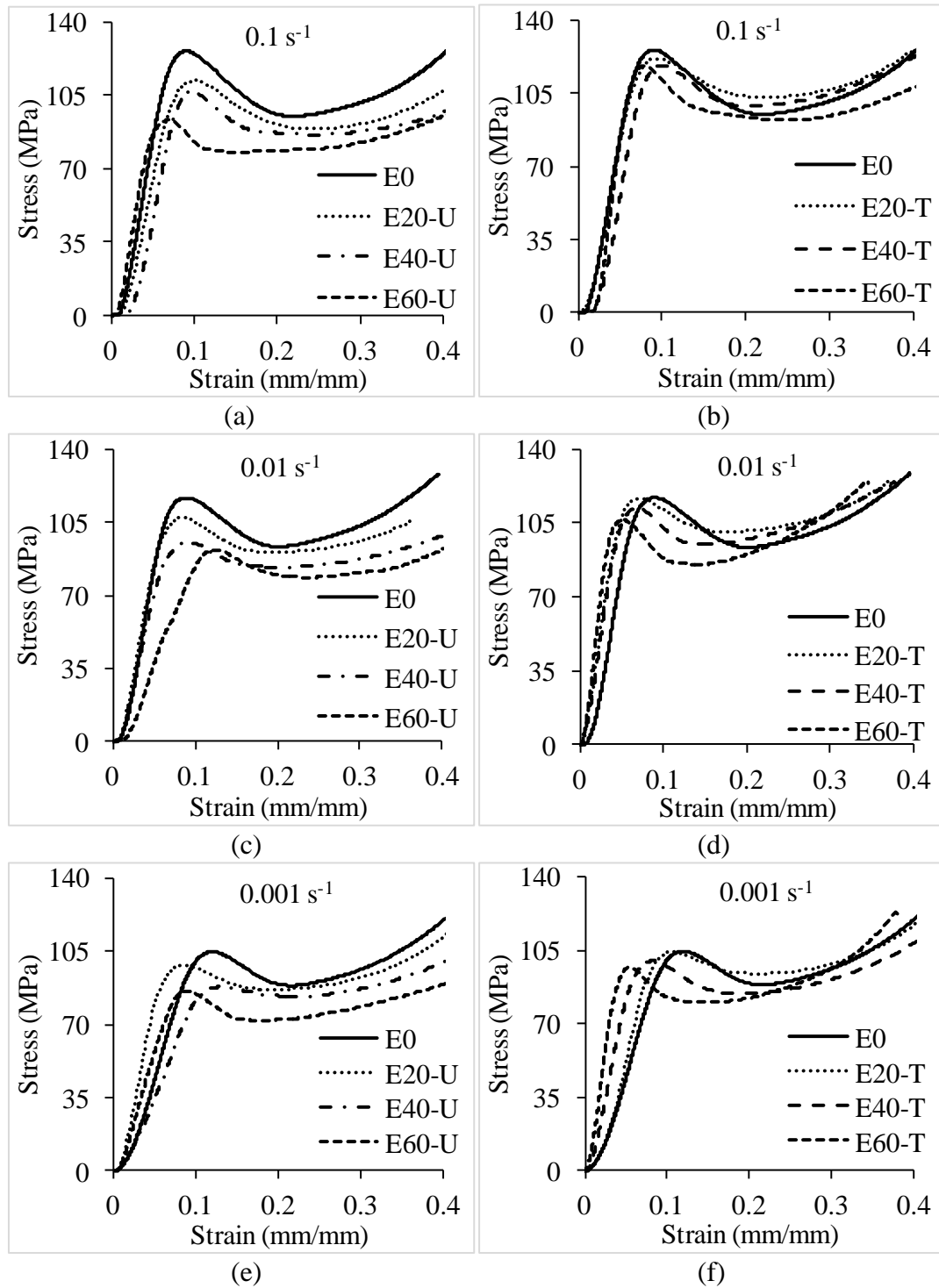
Figure 4.1 Stress-strain curves of samples for different strain rates.
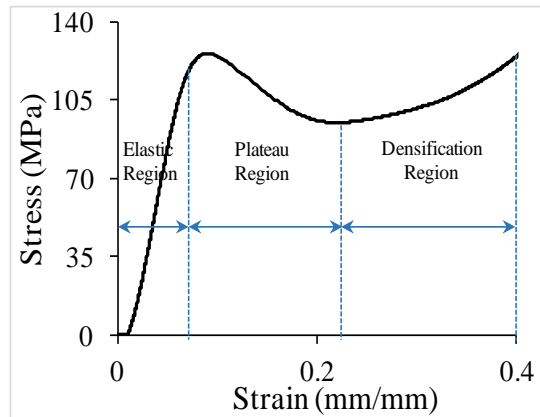
Figure 4.2 Representative stress-strain curves of syntactic foams.

4.2 Compressive modulus and strength in quasi-static mode

Mechanical properties of syntactic foams in quasi-static compression are presented in Table 4.1. Neat epoxy samples register lower elastic modulus as compared to both EXX-U and EXX-T foams. The average elastic modulus is observed to increase with increase in filler content and strain rate for syntactic foams (Figure 4.3a). Among all syntactic foams, E60-T foam shows the highest modulus for all compressive strain rates. However, poor interfacial bonding between the constituent compromise modulus values of untreated syntactic foams. Silane treated syntactic foams registered higher modulus.

Compared to the modulus of neat resin at 0.001, 0.01 and 0.1 s^{-1} strain rates, the modulus of EXX-U foams increased in the range of 0.9-27, 15-37, 29-106% while for EXX-T foams the increase in modulus is in the range of 25-79, 28-107, 76-203%, respectively with increasing filler content.

All the syntactic foams present higher specific modulus as compared to neat epoxy (Figure 4.3b). E60-T at 10^{-1} s^{-1} strain rate depicts the highest specific modulus as compared to all other compositions making the EXX-T foams very suitable for applications demanding light weight structures with enhanced modulus.

Table 4.1 Quasi-static compressive properties of neat epoxy and their foams.

Material	Strain rate (s^{-1})	Elastic Modulus (GPa)	Yield strength (MPa)	Yield strain (%)	Energy absorption (MJ/mm^3)	Densification stress (MPa)	Densification strain (%)
	10^{-1}	1.86±0.037	126.04±2.52	8.92±0.17	38.73±0.77	-	-
E0	10^{-2}	1.76±0.035	116.93±2.33	9.03±0.18	37.86±0.75	-	-
	10^{-3}	0.96±0.019	104.62±2.09	11.99±0.23	36.33±0.72	-	-
	10^{-1}	2.16±0.043	111.94±2.23	8.37±0.16	41.77±0.83	88.95±1.77	24.52±0.49
E20-U	10^{-2}	2.23±0.044	107.30±2.14	8.52±0.17	40.31±0.80	90.74±1.81	19.71±0.39
	10^{-3}	0.97±0.019	98.17±1.96	9.93±0.19	38.43±0.76	86.71±1.73	19.98±0.39
	10^{-1}	2.29±0.045	107.02±2.14	9.12±0.18	42.09±0.84	86.20±1.72	24.98±0.49
E40-U	10^{-2}	2.02±0.04	95.64±1.91	9.74±0.19	39.02±0.78	83.52±1.67	20.58±0.41
	10^{-3}	1.31±0.026	87.82±1.75	12.94±0.25	39.01±0.78	83.21±1.66	22.29±0.44
	10^{-1}	2.39±0.047	93.14±1.86	6.96±0.13	45.17±0.90	77.56±1.55	14.95±0.29
E60-U	10^{-2}	2.35±0.047	91.95±1.83	8.82±0.17	43.38±0.86	72.60±1.45	11.98±0.23
	10^{-3}	1.99±0.039	86.12±1.72	12.32±0.24	39.15±0.78	71.97±1.43	18.56±0.37
	10^{-1}	2.67±0.053	121.86±2.43	7.07±0.14	39.85±0.79	103.18±2.06	22.58±0.45
E20-T	10^{-2}	2.20±0.044	116.65±2.33	9.31±0.18	38.33±0.76	101.04±2.02	19.14±0.38
	10^{-3}	1.73±0.034	104.29±2.08	10.70±0.21	37.89±0.75	93.91±1.87	21.17±0.42
	10^{-1}	2.66±0.053	118.38±2.36	6.76±0.13	39.91±0.79	99.12±1.98	20.56±0.41
E40-T	10^{-2}	2.26±0.045	112.12±2.24	8.27±0.16	38.91±0.77	94.80±1.89	14.35±0.28
	10^{-3}	1.99±0.039	99.92±1.99	10.09±0.20	37.79±0.75	84.39±1.68	19.45±0.28
	10^{-1}	3.56±0.071	118.44±2.36	5.04±0.10	46.57±0.93	92.43±1.84	26.02±0.52
E60-T	10^{-2}	3.11±0.062	106.64±2.13	5.51±0.11	41.00±0.82	85.33±1.70	14.35±0.28
	10^{-3}	2.91±0.058	96.78±1.93	7.91±0.15	40.47±0.80	80.18±1.60	15.66±0.31

Neat epoxy samples registered higher strength values as compared to the syntactic foams (Figure 4.3c). Strength of neat epoxy sample for 0.001, 0.01 and 0.1 s^{-1} strain rates is 104.62, 116.93 and 126.04 MPa respectively. With increasing cenosphere content, strength of EXX-U and EXX-T foams decreases in the range of 18-26% and 6-9% respectively as compared to neat epoxy for different strain rates. Decrease in the load bearing matrix content with increase in content of hollow particles in the syntactic foam reduces the overall strength of the composites.

Further, it is clear that the compressive strength of EXX-T foams is more in contrast to EXX-U foams for same volume percentage of cenospheres. Considering the advantages of weight saving potential (Table 3.1) and higher modulus offered by EXX-T foams, decrease in strength can be considered as very marginal as compared to neat epoxy samples. Figure 4.3d presents the specific compressive strength of all the samples. Specific values of neat epoxy samples are higher as compared to EXX-U foams but lower as compared to EXX-T foams. Specific compressive strength values of EXX-U foams decreases in the range of 5-14, 3-9, 1-6% while it increases for EXX-T foams in the range of 2-6, 3-6, 4-6% at 0.001, 0.01 and 0.1 s^{-1} strain rates respectively as compared to neat epoxy. Densification point (Smith et al. 2012). And associated results are presented in Table 4.1. The densification stress decreases as strain rate is decreased from 0.1 to 0.001 s^{-1} for all syntactic foams.
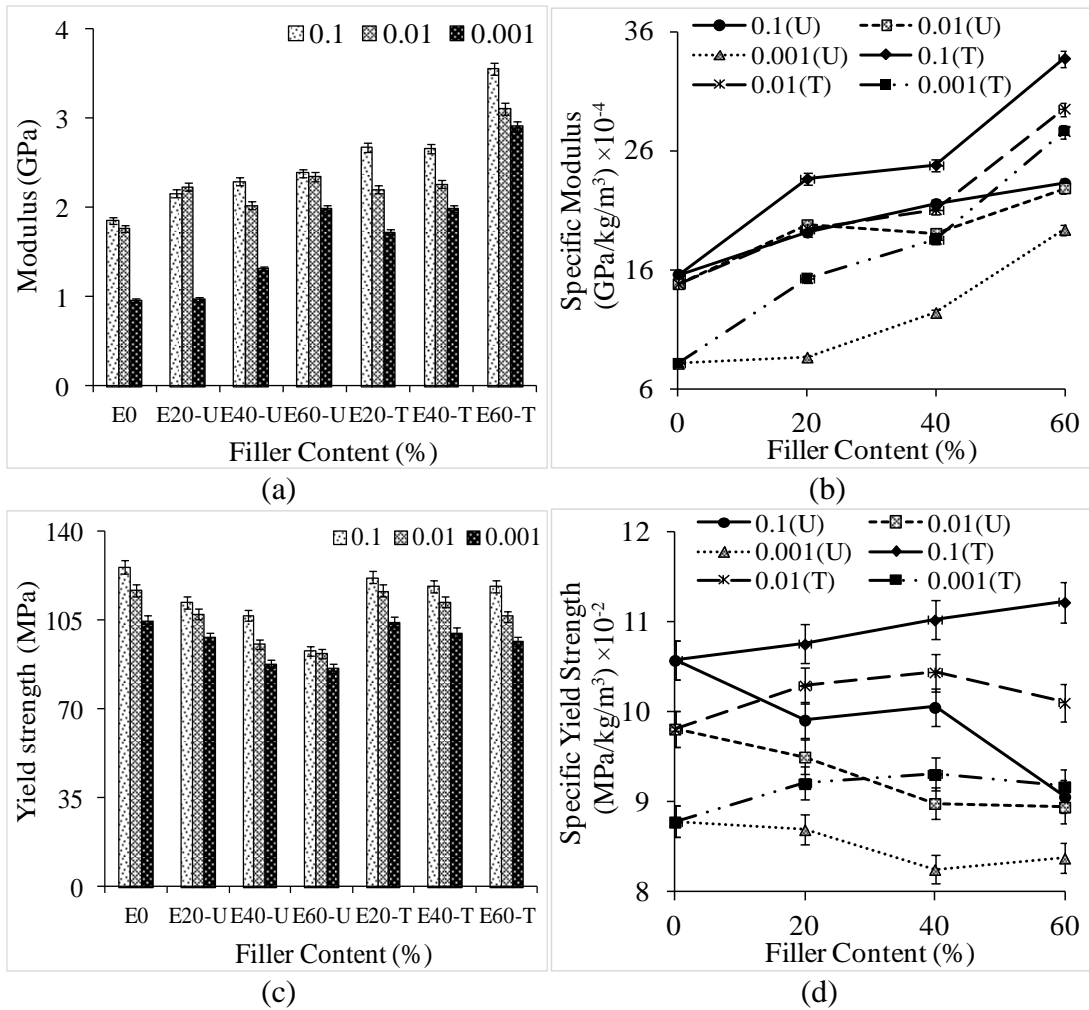
Figure 4.3 Experimental compressive (a) modulus (b) specific modulus (c) yield strength and (d) specific yield strength of samples in quasi-static mode.

4.3 Energy absorption

Syntactic foams are extensively used in packaging applications owing to their enhanced ability to energy absorption as compared to neat resin samples. Further, this attractive characteristic of syntactic foams to energy absorption makes them best suited as cores in sandwich structures. It is preferred to have an increased plateau region in the stress-strain curves in order to increase the stiffness of these foams. Increase in the content of hollow spheres increases the plastic strain in the matrix, thereby extending the plateau region (Swetha and Kumar 2011).

In the present study, the energy absorbed is calculated from the onset of crack initiation in the matrix till the end of plateau region wherein the stress value starts to increase again. Energy absorbed by the syntactic foams for varying filler contents including neat epoxy is represented in Table 4.1. Neat resin presents lower energy absorption for all the strain rates. However, the energy absorbed by the syntactic foams increases with increase in the filler content for both EXX-U and EXX-T foams. Further, silane treated syntactic foams show better energy absorption capacity compared to neat epoxy and EXX-U foams.

Surface modification of cenospheres enhances the bonding between the constituents and thereby helps matrix stiffening. Increase in cenosphere content further enhances the stiffness of the sample and helps to attain better energy absorption capacity.

4.4 Micrographic analysis of the samples

Micrographs of neat epoxy and syntactic foams with lower (E20) and higher (E60) filler content for 0.001, 0.01, 0.1 s^{-1} strain rates are presented in Figure 4.4, Figure 4.5, Figure 4.6, respectively. Even though the compressive strain rate is changed by two orders of magnitude, the difference in the failure mode of syntactic foams is not sufficient to depict any change as seen from these figures.

Extensive deformation of the neat matrix can be seen in Figure 4.4a. Similar features are previously observed in literature (Swetha and Kumar 2011). It can be observed that some cenospheres are intact in EXX-U foams even after densification strain is reached (Figure 4.4b). However, EXX-T foams with relatively thicker-walled cenospheres owing to silane treatment are noted to absorb more energy during the compression (Figure 4.4c).

Micrographs for E60-U and E60-T samples are depicted by Figure 4.4d and Figure 4.4e respectively. For E60-U foams more number of intact cenospheres is observed (Figure 4.4d). Further, it is revealed that even though there are intact cenospheres, poor bonding between the constituents restricts the ability of the foam to resist further compression.

Micrograph of E60-T foam reveals that strongly bonded and fragmented cenospheres are seen to be intact with the matrix (Figure 4.4e). Compressive loading appears to fragment the silane treated cenospheres in relatively easy manner as compared to EXX-U foams owing to relatively more brittleness owing to treated cenospheres presence.

However, strong bonding between the constituents tends to offer more resistance to compression, post cenospheres fragmentation. It is clearly evident from Figure 4.4e that the strongly bonded cenospheres have been compressed to the maximum extent before and after the fragmentation of cenospheres. Such events enhance the overall resistance to compression loading.
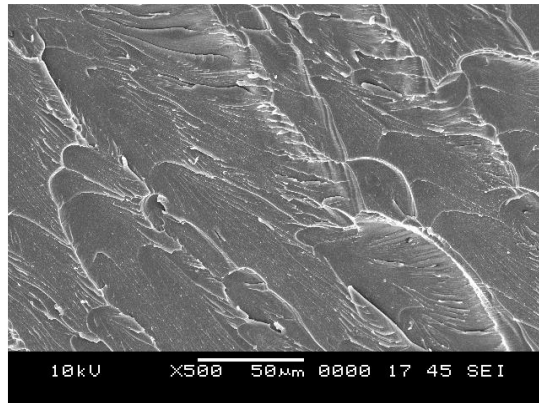
(a)
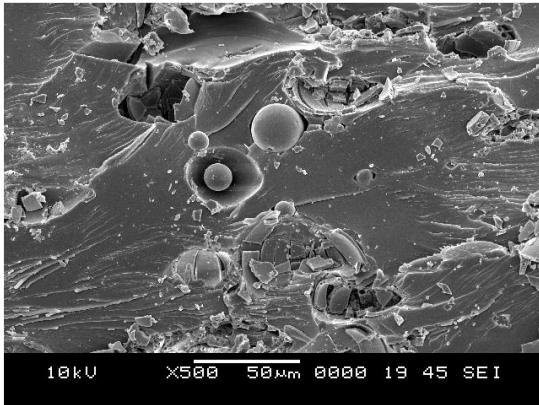
(b)
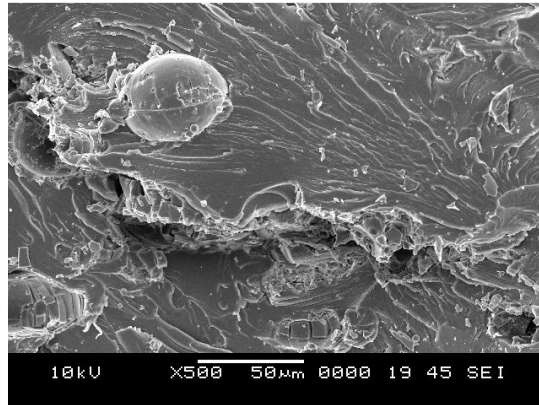
(c)
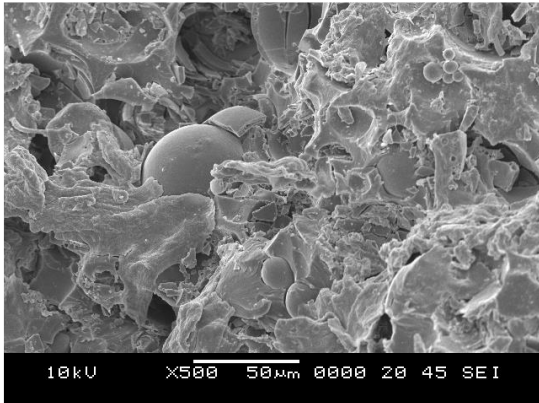
(d)

(e)

Figure 4.4 Micrographs of post compression samples at 0.001 s^{-1} (a) E0 (b) E20-U (c) E20-T (d) E60-U and (e) E60-T.
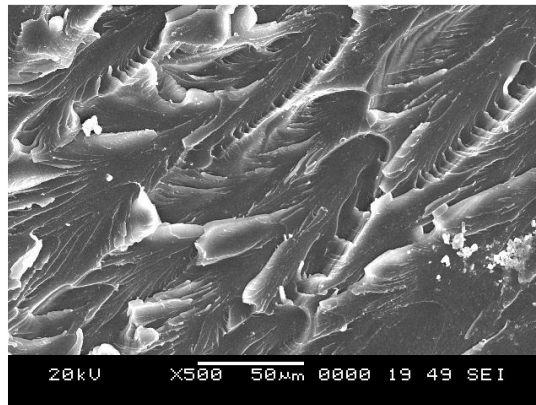
(a)
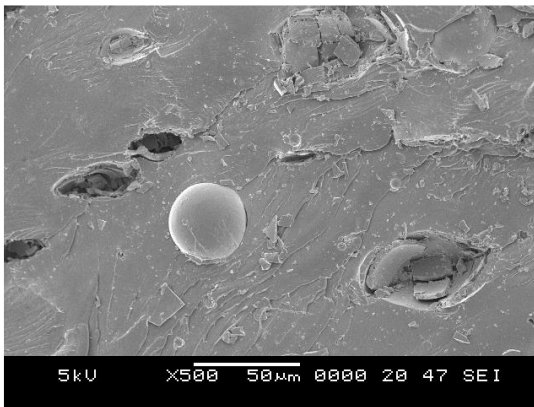
(b)
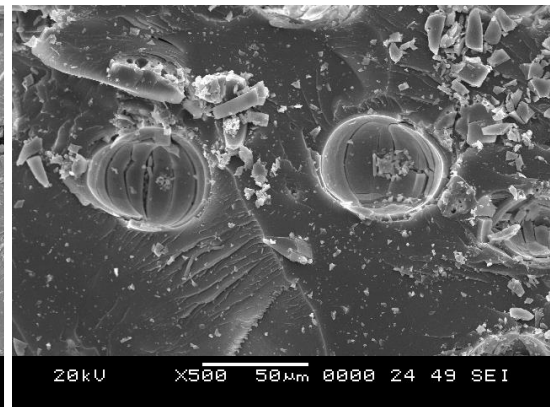
(c)
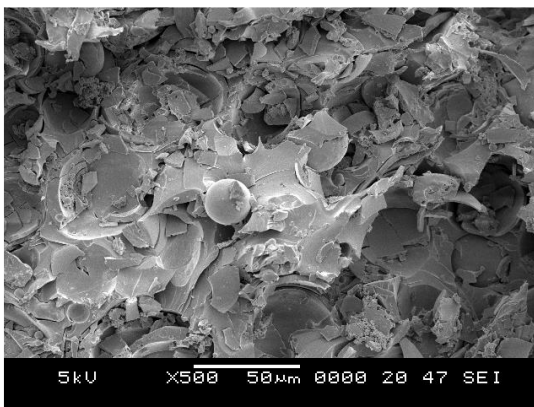
(d)
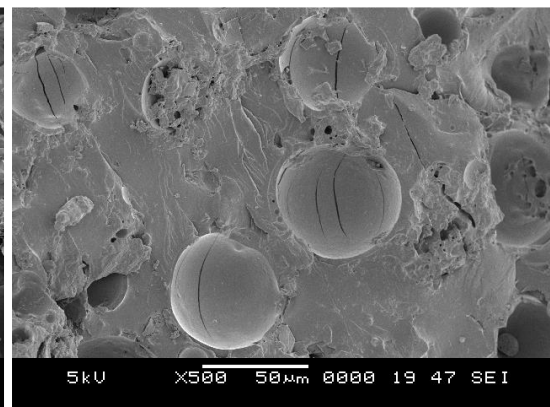
(e)

Figure 4.5 Micrographs of post compression samples at 0.01 s^{-1} (a) E0 (b) E20-U (c) E20-T (d) E60-U and (e) E60-T.
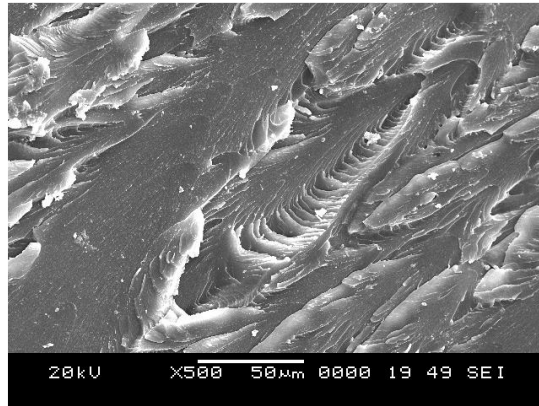
(a)
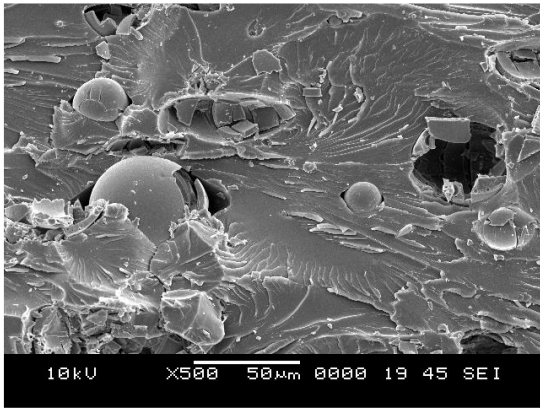
(b)
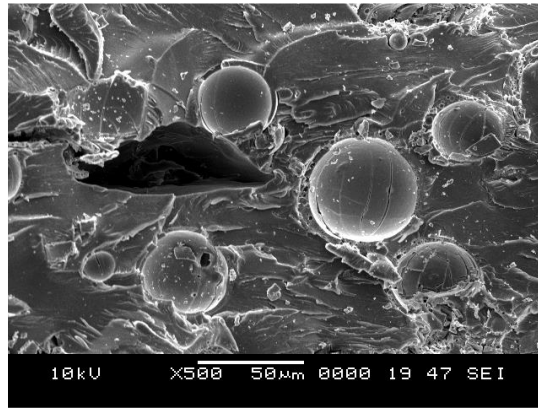
(c)

(d)
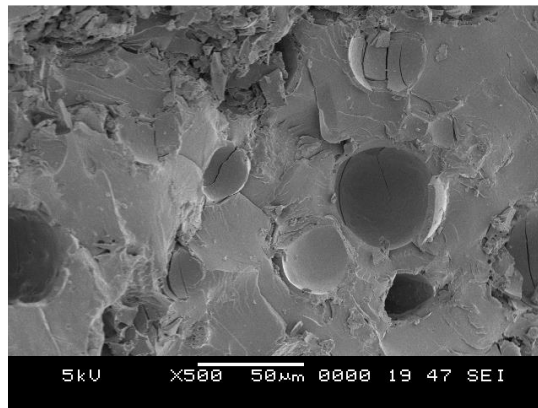
(e)

Figure 4.6 Micrographs of post compression samples at 0.1 s^{-1} (a) E0 (b) E20-U (c) E20-T (d) E60-U and (e) E60-T.

4.5 Property map

For selecting specific composition based on particular applications, property map is presented here which might act as a guideline for industrial practioners. Compressive modulus at a strain rate of 0.001 s^{-1} are plotted in Figure 4.7 as a function of density for composites having different reinforcements (Ahmadi et al. 2015, Swetha and Kumar 2011). Results from the present study and extracted data from the available literature are plotted with respect to density for comparative analysis.

It can be observed from the figure that composites with lower density exhibit lower compressive modulus. However, the advantage of naturally available and cost effective hollow fly ash cenospheres filled lightweight syntactic foams is clearly evident from Figure 4.7. Density of all the syntactic foams including neat epoxy is higher compared to other composites investigated in the literature. Hollow glass microballoons and ceramic microballoons are artificial manufactured. Therefore, the density associated with these foams is lower as compared to fly ash cenospheres. However, fly ash cenospheres are naturally available, thereby control over the density is difficult.

Syntactic foams tested in the present study outperform hollow glass microballoon/epoxy and ceramic microballoon/epoxy composites. Compressive modulus is significantly higher for higher filler contents of cenospheres (E60) as seen from Figure 4.7. E60-T foam reveals the highest modulus as compared to all other composites. Therefore, from the property map it can be concluded that cenosphere/epoxy syntactic foams with higher cenosphere contents provide higher modulus as compared to other composites signifying their aptness in weight sensitive applications demanding higher modulus.

Abundant availability of environment pollutant fly ash cenospheres can be effectively utilized to prepare foams for various applications based on the specific requirements.
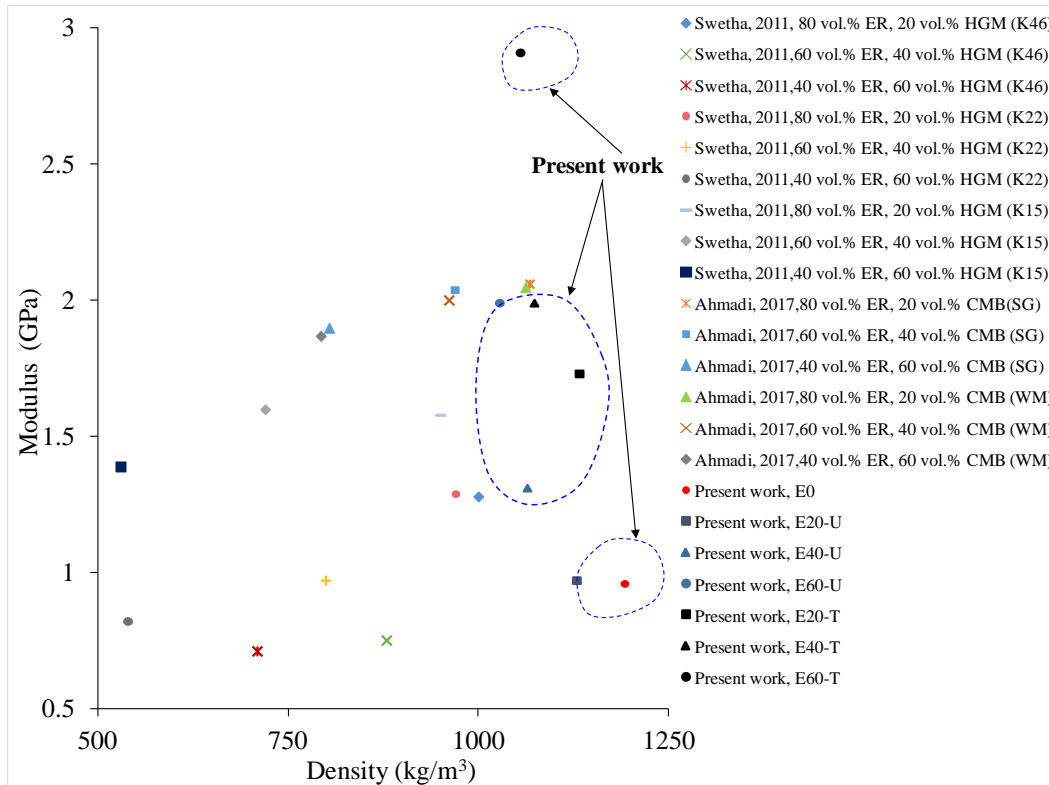
Figure 4.7 Compressive modulus plotted against density from available studies
(Ahmadi et al. 2015, Swetha and Kumar 2011).
Note: ER – Epoxy resin, HGM – Hollow glass microballoons, CMB – Ceramic
microballoons.

Conclusions

Quasi-static compressive response for varying filler contents of untreated and treated
syntactic foams reveals that,

- Neat epoxy sample has the lowest modulus among all the samples. With increase
  in volume fraction of the cenospheres modulus increases in the range of 0 to 48%
  for untreated syntactic foams and 3 to 44% for silane treated syntactic foams
  respectively.

- Strength of the syntactic foams decrease with increase in volume fraction of the
  cenospheres in EXX-U and EXX-T syntactic foams in the range of 11 to 28% and
  3 to 8% respectively as compared to neat epoxy.

- With increase in cenosphere content, energy absorption of the foam increases for
  all the syntactic foams. E60-T sample presents the highest energy absorption among
  all the samples.

80

5 FLEXURAL RESPONSE

5.1 Flexural modulus and strength

Figure 5.1 exhibits stress-strain response of representative samples. Irrespective of the testing environment, all types of syntactic foams fail in brittle mode post peak region. EXX-U foams exhibit non-linear behavior at room temperature (Figure 5.1a) as compared to EXX-T foams (Figure 5.1b). Poor adhesion between the constituents (Figure 3.4c) resulting in an unconstrained matrix flow around the cenosphere particles and relatively easier displacement of cenospheres within the matrix under applied load might be the reason for such an observation. Owing to enhanced interfacial bonding between the treated cenospheres and matrix, the response of EXX-T foams are dictated by the cenospheres, resulting in a linear stress-strain response in the pre peak region as observed in Figure 5.1b.

In case of the arctic conditioned specimens, the stress-strain response curves presented two linear regions. The second linear region is used for all calculations to determine the stiffness and strength properties. Failure response is found to be similar in both the arctic conditioned and unconditioned samples, which resembles brittle fracture as mentioned earlier. Similar response under flexural mode at -60°C is reported for carbon fiber reinforced composites (Jia et al. 2018).
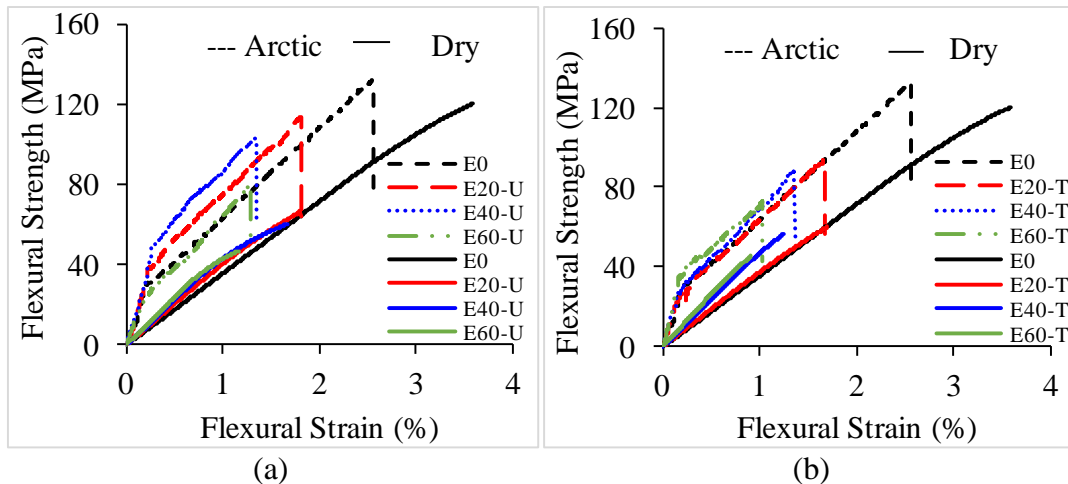
Figure 5.1 Flexural stress-strain of neat resin and their foams with (a) untreated and (b) treated cenospheres.

Table 5.1 Flexural modulus and strength properties of neat resin and their foams.

Material	30°C		-60°C	
	Modulus (MPa)	Strength (MPa)	Modulus (MPa)	Strength (MPa)
E0	3436.98±68.74	120.29±2.41	4078.49±101.96	124.12±3.72
E20-U	3729.55±74.59	60.09±1.20	4264.80±85.30	93.81±2.35
E40-U	4431.51±88.63	56.74±1.13	5082.54±152.48	102.26±3.07
E60-U	4755.30±95.11	45.23±0.90	5090.78±178.18	73.88±2.59
E20-T	3958.71±79.17	66.23±1.32	4522.59±90.45	87.02±2.18
E40-T	4746.83±94.94	59.82±1.19	4625.50±138.76	83.77±2.51
E60-T	5196.11±103.92	48.28±0.97	5041.52±176.45	75.50±2.64

Flexural modulus and strength values are computed for each case using the experimentally obtained load-displacement data. Figure 5.2a and Figure 5.2b displays the effect of filler loading and cenospheres treatment on modulus. With increasing filler content modulus for both foam types (EXX-U and EXX-T) increases (Table 5.1). EXX-T foams registered higher moduli at all the volume fractions as compared to EXX-U ones at room temperature. Further, all the foams out performed neat epoxy sample by registering higher flexure modulus (Figure 5.2b). This trend is in-line with the results presented in literature (Doddamani et al. 2015, Gupta and Nagorny 2006, Huang and Gibson 1993). In the case of the arctic conditioned samples also, untreated and treated cenospheres exhibit increase in modulus with increase in filler content. However, EXX-U foams register higher modulus values at all the volume fractions as compared to EXX-T foams. Neat resin registers lower elastic modulus as compared to EXX-U and EXX-T foams. Arctic conditioning increases the stiffness of the samples due to matrix hardening (Rivera and Karbhari 2002). Further, for every 1°C decrease in temperature, the modulus of the resin increases by 20 MPa (Dutta and Hui 1996, Hartwig 1979). In the present study, for every 1°C decrease in temperature, an increase of 7.12, 5.94, 7.23, 3.72, 6.26, -1.34, -1.71 MPa is observed for E0, E20-U, E40-U, E60-U, E20-T, E40-T, E60-T respectively. Increase in modulus with decrease in temperature is found to be reasonable with the available literature, except for E40-T and E60-T foams. Hence, 11-14% weight saving in structures can be obtained by using cenosphere/epoxy syntactic foams (Table 3.1) with superior specific properties making these foams suitable for naval applications where structural design is driven by higher buoyancy criteria (Gupta 2007).
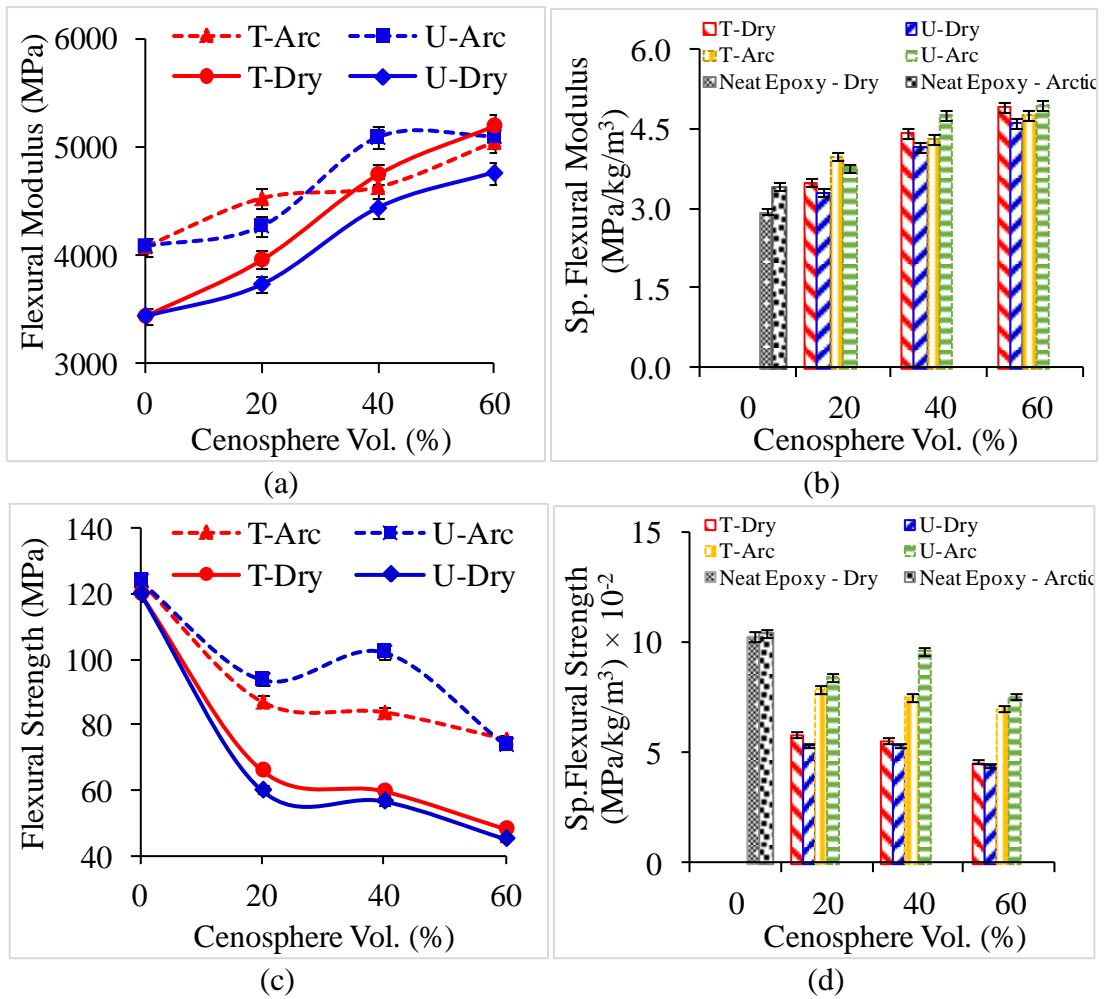
Figure 5.2 Experimentally measured flexural (a) modulus (b) specific modulus (c) strength and (d) specific strength of samples under investigation.

Flexural strength of cenosphere filled epoxy composites is exhibited by Figure 5.2c and Figure 5.2d, where the flexural strengths for both EXX-U and EXX-T is lower as compared to neat resins load bearing capability at room temperature and arctic conditions. Specific strength is shown in Figure 5.2d and fracture strain in Figure 5.1 exhibit similar trend. However, foams with treated fillers have registered better response under room temperature test conditions whereas opposite trend is noted for arctic conditioned samples. Foam with untreated filler registered better response in arctic environment. As these foams can be used as core in sandwiches, lower fracture strength and strains do not limit their applicability in marine vessels. Filler content influences flexural strength significantly while marginal effect is noted due to particle surface treatment. Higher brittleness at the cenosphere-epoxy interface and silane

modified particles might have played a significant role for such insensitivity pertaining to surface modification. Increasing filler content decreases strength implying reduction in foam strength owing to lower matrix content. Fracture features as presented in Figure 5.3 indicate, matrix cracking post particle-resin debonding in EXX-U foams. Whereas, particles cracking (Figure 5.3e) is the failure source for EXX-T foams.

Increase in flexural modulus of 7-15% for EXX-U foams is observed when arctic conditioned samples are compared to dry (unconditioned) samples. On the other hand, in case of treated samples it was observed that the modulus increased only for E20 samples by 14% while causing a reduction in its modulus by 3% as the filler content increased. In case of flexural strength, an increase between 56-80% and 31-56% was observed for EXX-U and EXX-T respectively in in-situ arctic samples. Arctic conditioned samples became more rigid causing increase in flexural modulus and strength. For arctic conditioned samples, increase in flexural strength of neat epoxy samples is less as compared to EXX-U and EXX-T foams. Due to arctic conditioning, the matrix shrinks around the cenosphere particles inducing residual tensile stresses in the matrix and compressive stresses on the cenosphere particles. Neat epoxy exhibits slight increase in strength as compared to room conditioned sample owing to matrix hardening. Further, arctic conditioned EXX-U and EXX-T foams exhibit higher strength compared to room conditioned samples due to better interlocking of the cenosphere particles with matrix resin.

Degradation caused by the environmental exposure is observed to be more predominant in E40 foams in arctic conditioned samples. A combined effect between the matrix and the cenospheres exists in the mechanical properties of the samples. Given that the interphase between matrix and cenospheres has a higher influence on the material properties for this configuration, a higher degradation of this region may lead to property decline. Treated cenosphere samples have better adhesion between matrix and cenospheres. Exposure to temperatures of -60 °C results in higher degradation of the interphase as compared to untreated samples leading to a higher difference as observed in Figure 5.2a and Figure 5.2c. On the other hand, 20 and 60 vol. % are matrix and

cenospheres dominated respectively and the interphase influence is insignificant at these filler loadings.

5.2   Micrographs analysis of fractured samples

The fracture features of E0, E20 and E60 untreated and treated cenosphere reinforced foams at room temperature tests are presented in Figure 5.3. The micrographs are taken post flexure test on the fractured surfaces. Absence of debris is observed in all these micrographs indicating tensile fracture (Tagliavia et al. 2010). Such a feature is also noted in syntactic foams with cenospheres in thermoplastic (HDPE) matrix (Bharath Kumar et al. 2016, Bharath Kumar et al. 2016) like in thermosetting (epoxy) ones. In flexural loading conditions, debris absence on the fracture surface is due to crack initiation from the tensile side of the sample which governs the brittle mode of fracture. Extensive plastic deformation marks are seen on neat epoxy samples without any debris as observed in Figure 5.3a. Interaction of the deformation waves as seen in Figure 5.3a with untreated and treated cenospheres are worthy of investigation. Figure 5.3b and Figure 5.3d shows debonding and displacements of cenospheres from the matrix (EXX-U) during the deformation and fracture as compared to EXX-T (Figure 5.3c and Figure 5.3e). This implies that most of the stress in the composite is withstood by the matrix material in foams with treated filler that determines the composite failure strength. This is obvious owing to good interfacial bonding between the constituents in EXX-T (Figure 3.4d) foams. Strength values of foams with treated particles are higher compared to untreated ones for all the compositions tested at room temperature. Constrained matrix movement around relatively tougher treated particles registered higher strength values. With increasing filler content variations in particle sphericity, wall thickness and built-in porosities (Figure 3.2c) induce additional stress concentration suppressing silane coating effect and thereby lowers flexure strength. Though these foams have limitations in strength, they are promising in terms of high stiffness if used in sandwich composites as core materials.
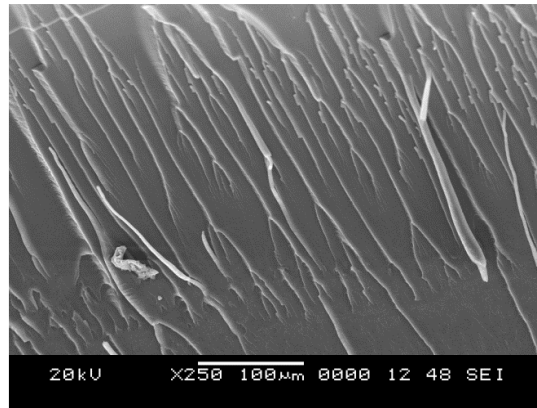
(a)
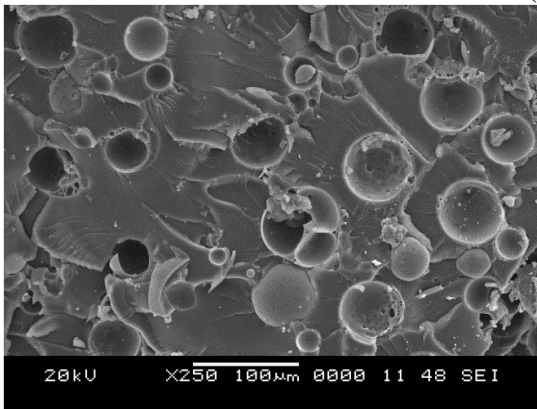
(b)
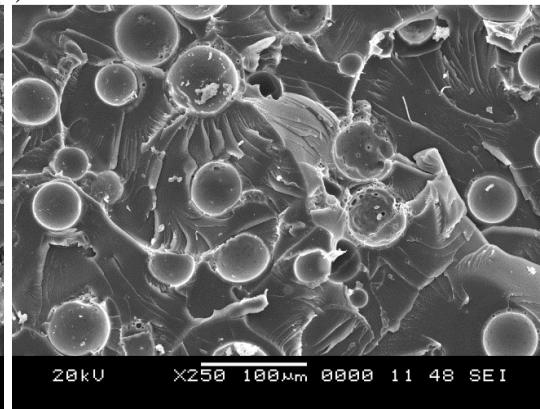
(c)
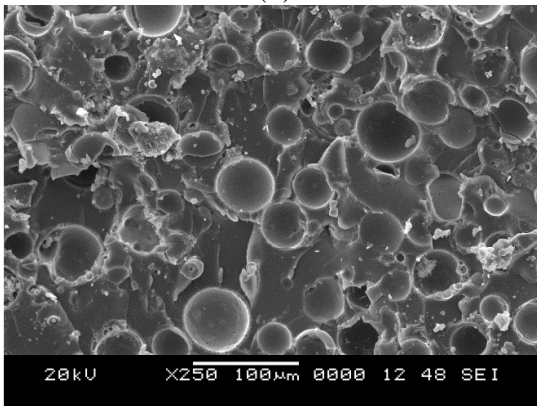
(d)
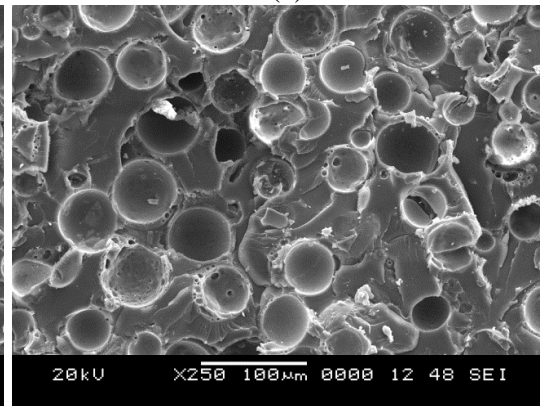
(e)

Figure 5.3 Micrographs of (a) Neat epoxy resin (b) E20-U (c) E20-T (d) E60-U and (e) E60-T post flexure room temperature tests.

Fracture features for representative syntactic foam containing 40 vol. % of untreated and treated cenospheres in arctic environment can be observed in Figure 5.4 and Figure 5.5 respectively. All micrographs are obtained across the fracture surfaces post flexural tests. Similar fracture features are observed for both treated and untreated samples. Like for unexposed samples, tensile fracture is also observed in arctic conditioned samples.

Tension Surface

Compression Surface

Cross-Section View of Damaged
Surface
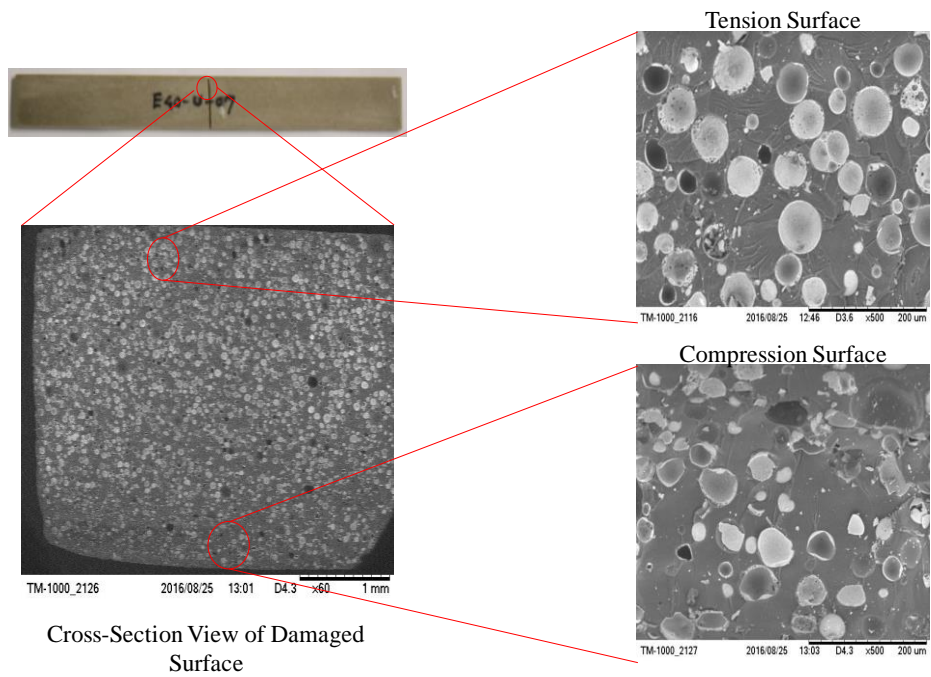
Figure 5.4 E40-U flexural specimen schematic post arctic condition tests.

Tension Surface

Compression Surface

Cross-Section View of Damaged
Surface
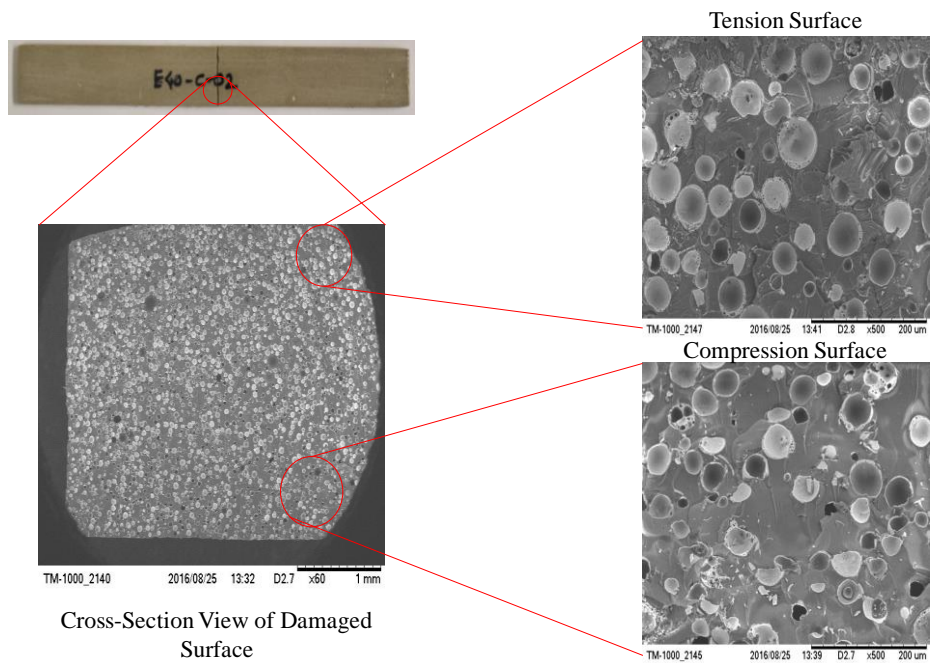
Figure 5.5 E40-T flexural specimen schematic post arctic condition tests.

Conclusions

Room and arctic temperature effect on EXX-U and EXX-T cenosphere/epoxy foams under flexure is presented in this section. Specific modulus in flexure is observed to be considerably higher than the neat epoxy resin. Flexural modulus of these foams can be effectively tailored by filler surface modification and varying filler volume fraction. Resin content governs the strength of these lightweight foams. It is observed that the flexural strength decreases as the filler content increases. Lack of interfacial bonding between the foam constituents limits the load transfer at the interface for composites with untreated cenospheres. Similar trend is observed for treated particle foams owing to geometrical imperfection with such naturally available fillers. Arctic environment is simulated by subjecting the foams to -60 °C. Lower failure strains in EXX-U and EXX-T foams compared to neat sample is also noted. Arctic exposed samples reported a slight increase in their modulus of elasticity as compared to room temperature samples. Key finding are as follows:

- Weight saving potential for EXX-U and EXX-T foams is 11-14% as compared to neat epoxy samples.

- An increase in flexural modulus is observed in syntactic foams at room and arctic temperature as compared to neat resin at room temperatures, whereas flexural strength is noted to be decreased.

- An increase in flexural modulus between 7-15% is recorded for syntactic foams with untreated cenospheres under arctic conditions as compared to the ones tested at room temperature.

- EXX-U and EXX-T foams exhibit higher specific modulus as compared to E0 samples for room temperature and arctic conditioned samples. Specific strength of arctic conditioned EXX-U and EXX-T foams is significantly higher compared to room conditioned samples.

Flexural strengths of arctic exposed EXX-U and EXX-T syntactic foams increased in the range of 56-80 and 31-56% respectively as compared to those at room temperature. This is accredited to matrix hardening experienced by the samples when exposed to arctic temperatures that facilitates the cenospheres to carry more load.

After examining the behavior of syntactic foams in arctic environment, it is concluded that the flexural modulus increases with arctic exposure and filler volume percentage. These materials systems have great potential to be used as core materials for sandwich construction in such extreme conditions, where a significant improvement in the flexural modulus can be achieved with better weight saving potential and specific values.

However, due to inferior flexural strengths, using only syntactic foams in primary load bearing structures without other high strength materials, like carbon or glass facings, is not suggested. The findings reported here offers a pathway to improve the structural integral design by taking advantage of the favorable results in terms of low density and better modulus of elasticity and avoiding the unfavorable ones.

6   TENSILE BEHAVIOR

6.1   Stress strain curves

Figure 6.1 presents representative tensile stress-strain curves of untreated and treated cenosphere/epoxy syntactic foams including neat sample. The stress-strain curves of all the syntactic foams exhibit similar stress-strain profiles until peak stress comprising of linear elastic region followed by brittle failure. Similar behavior is observed for glass microballoon/epoxy syntactic foams (Nikhil and Ruslan 2006). Reinforcing relatively brittle cenospheres into epoxy has decreased the ultimate stress value without any deformation till the final fracture. The curves obtained for tensile tests are different from compressive stress-strain curves, which show a small stress-plateau region (Shahapurkar et al. 2018).
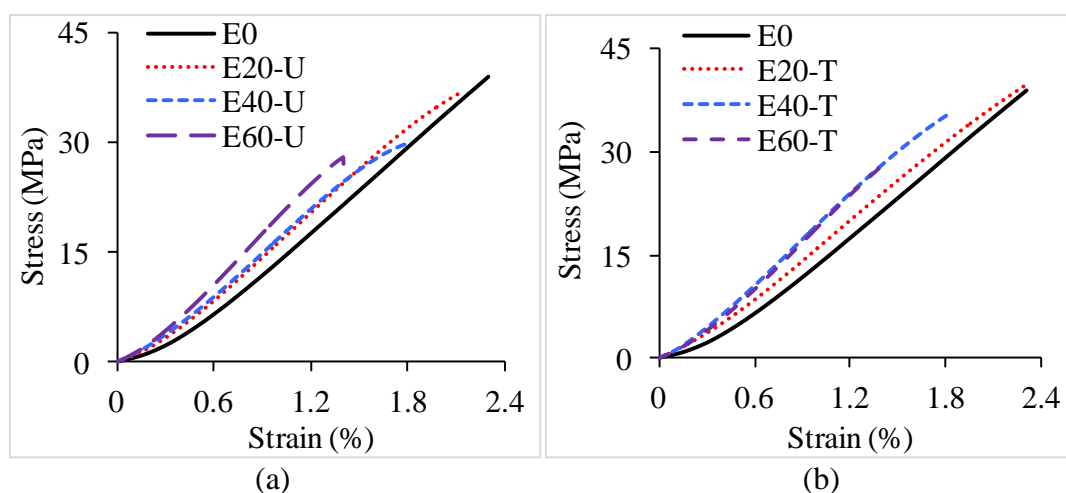
Figure 6.1 Representative tensile stress-strain curves of neat resin and their foams having (a) untreated and (b) treated cenospheres..

6.2   Tensile modulus and strength

Tensile modulus and strength values are depicted by Figure 6.2. Tensile modulus increases for both EXX-U and EXX-T foams as compared to neat epoxy for all the compositions. Modulus values increase in the range of 57-94% and 70-124% for EXX-U and EXX-T foams as compared to pure resin respectively (Figure 6.2a). Better interfacial bonding of matrix with cenospheres for EXX-T foams have led to significant rise in modulus as compared to neat epoxy and EXX-U foams. Similarly, specific modulus for EXX-U and EXX-T foams are 68-127% and 75-155% higher compared to neat sample (Figure 6.2b). Significant weight savings can be achieved over pure

resin if EXX-T foams are used in tensile conditions. Strength of untreated and treated syntactic foams decreases with increase in cenosphere volume fraction upto 28% and 25% respectively (Figure 6.2c) as compared to tensile strength of neat resin. Replacing load bearing matrix with cenospheres has decreased the strength of syntactic foams. Weak interface between matrix-filler appears to decrease strength for EXX-U foams. However, EXX-T foams have comparable or slightly better strength compared to pure resin attributing to superior bonding of the constituents due to silane treatment of cenospheres (Figure 6.2d). Further surface defects present on cenospheres might have resulted in such an observation.

(a)　　　　　　　　　　　　(b)

(c)　　　　　　　　　　　　(d)
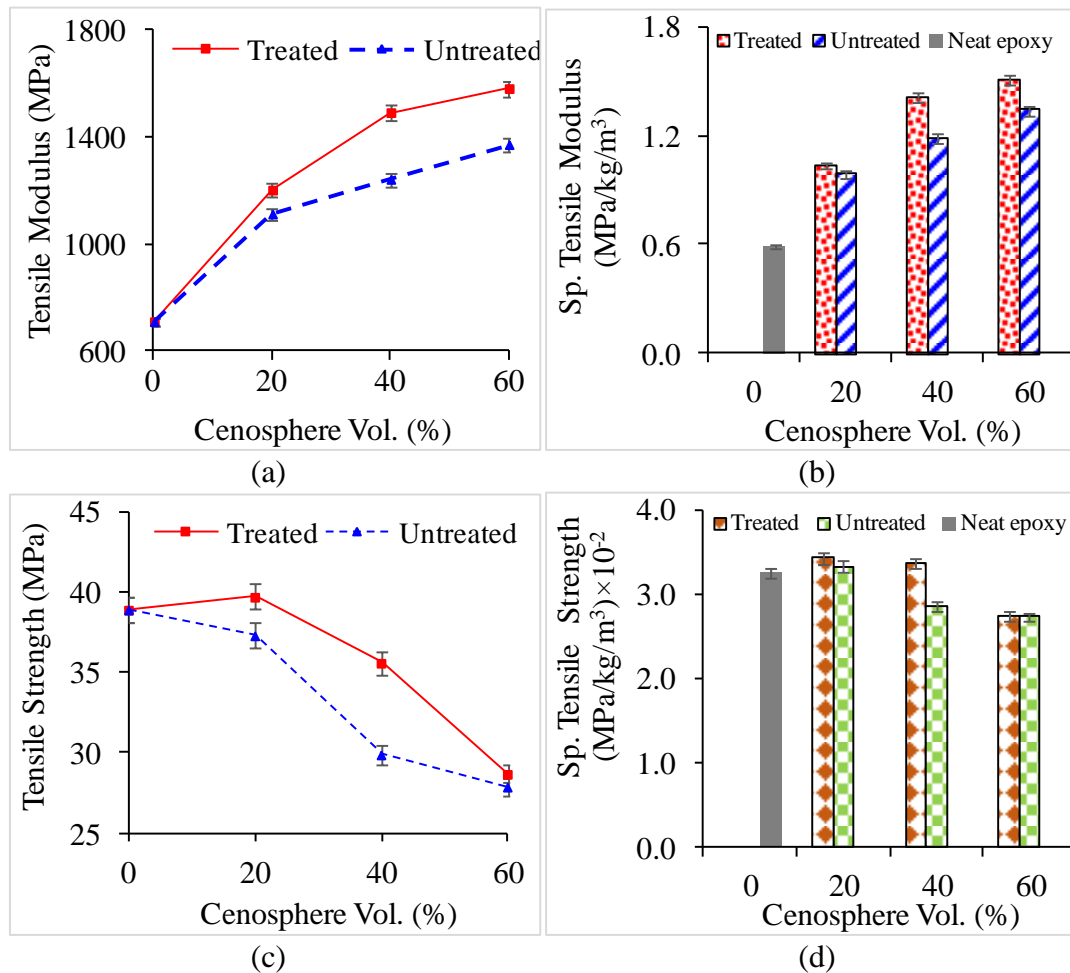
Figure 6.2 Experimentally measured tensile (a) modulus (b) specific modulus (c) strength and (d) specific strength of samples.

6.3   Micrographic analysis

Fracture surfaces of neat epoxy, EXX-U and EXX-T foams are presented in Figure 6.3. For neat epoxy, deformation and fracture features can be clearly observed (Figure 6.3a). From Figure 6.3b and Figure 6.3c it can be observed that EXX-T foams have deformed with less number of deformation marks as compared to EXX-U foams containing 20 vol.% of cenospheres. Good interfacial bonding of the constituents is observed for EXX-T foams compared to EXX-U foams. Micrographs with 60 vol.% of cenospheres are shown in Figure 6.3d and Figure 6.3e for EXX-T and EXX-U foams respectively. It is observed that with increase in filler content of cenospheres, particle debonding has increased for EXX-U foams compared to EXX-T.

Higher number of intact particles and overall increase in mean particle diameter of coated cenospheres has improved the stiffness of EXX-T foams at higher filler content. Nevertheless, from the study presented here, EXX-T foams show better results compared to neat resin and EXX-U foams. Specific modulus values of EXX-T foams are significantly higher than others samples.

Conclusions

Tensile properties of untreated and silane treated syntactic foams fabricated by manual stir casting route are presented in this chapter. All the syntactic foams fail at lower strains as compared with neat epoxy sample. Untreated and treated syntactic foams show an increase in modulus for all the filler contents compared to neat epoxy resin. Weight saving potential of 12% is achieved for untreated syntactic foams. Strength of untreated and treated syntactic foams is lower than neat epoxy sample.

Lower tensile properties of syntactic foams have been a challenge in developing new applications. Based on the modulus and strength values, these materials need to be chosen carefully. Significant increase in modulus and comparable strength to neat epoxy for surface modified syntactic foams make these foams viable for applications demanding better specific properties.
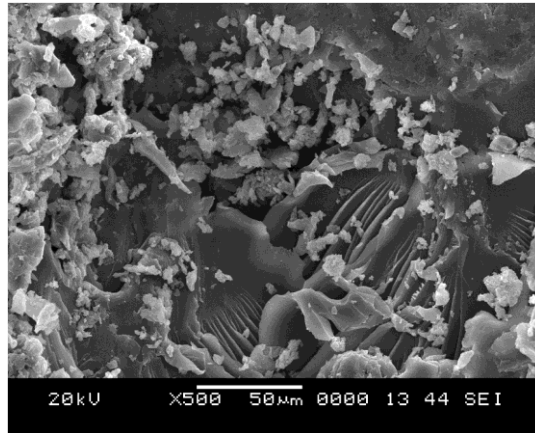
(a)
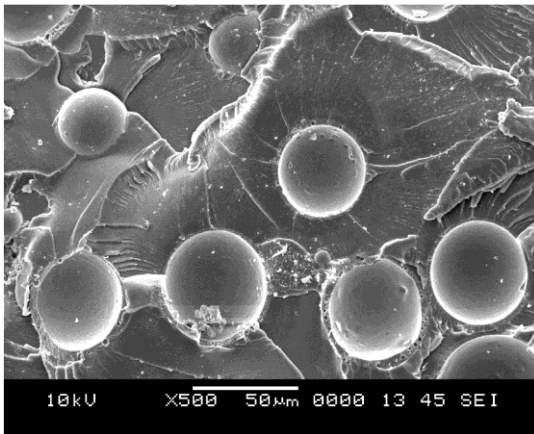
(b)
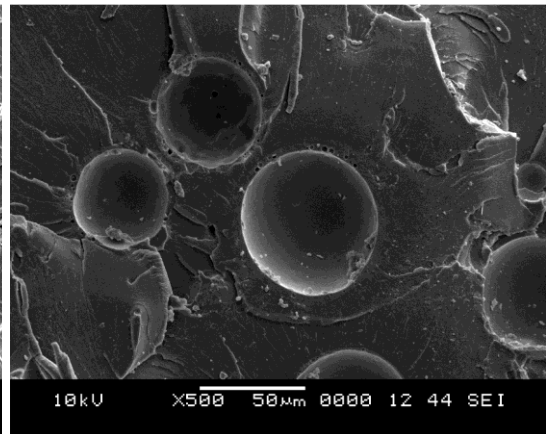
(c)
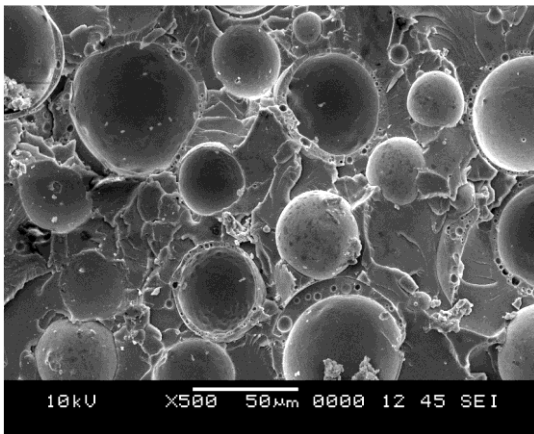
(d)
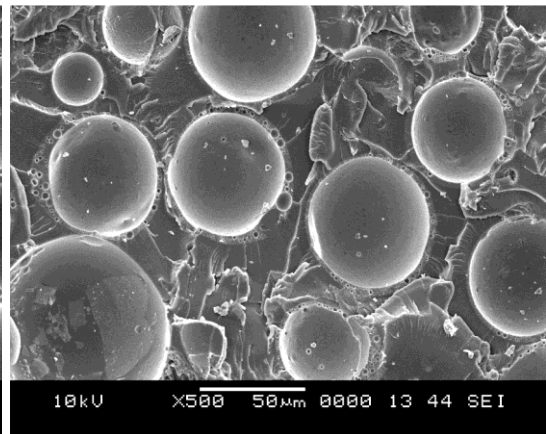
(e)

Figure 6.3 Micrographs of (a) E0 (b) E20-U (c) E20-T (d) E60-U and (e) E60-T syntactic foams.

7   DYNAMIC MECHANICAL ANALYSIS

7.1   DMA curves

Ability of the material to convert mechanical energy into heat energy subjected to an external loading is expressed by DMA ($Tan\ \delta$). As a general characteristic, the graphs have three distinct regions as presented in Figure 7.1. Region I depicts decrease in storage modulus with increase in temperature. In region II, storage modulus reduces significantly with increase in temperature. This is attributed to the sample reaching its glass transition temperature. In region III, storage modulus stabilizes to a very low value compared to that in region I. Region III defines the flow region wherein variation of storage modulus is negligible.

The storage modulus at four representative temperatures, 30, 60, 90 and 175°C (Figure 7.1), are presented in Table 7.1 to determine the extent of variation of storage modulus with respect to temperature. Selection of these representative temperatures is based on the observations that,

- 28°C is defined as the room temperature for this study and is important for a large number of applications.

- In region I, trend of storage modulus is linear and the graphs are well separated in the temperature range of 28-60°C, enabling selection of representative temperature of 60°C to demonstrate the dependence of storage modulus on cenosphere volume fraction.

- In region II around 90°C, the storage modulus decreases drastically after attaining glass transition temperature.

- In region III, 175°C is maximum temperature of the test. It is observed that no variation in storage modulus with respect to temperature is observed. Thereby, any temperature value can be selected for illustration of the trends.
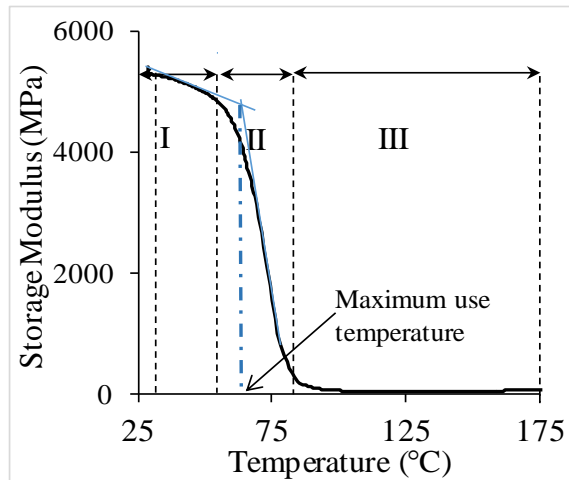
Figure 7.1 Schematic representation of variation of storage modulus against temperature for all the samples. Regions I, II, and III are identified by arrows. The dashed lines correspond to 30, 60, 90 and 175°C where storage modulus values are noted and presented in Table 7.1.

Table 7.1 Comparison of storage modulus values for syntactic foams at four representative temperatures.

Material	Storage Modulus (MPa)			
	30°C	60°C	90°C	175°C
E0	5275.62±105.51	4507.34±90.14	90.30±1.80	45.30±0.90
E20-U	5983.13±119.66	5513.82±110.27	110.30±2.20	92.77±1.85
E40-U	6908.12±138.16	6316.76±126.33	195.99±3.91	109.79±2.19
E60-U	7526.96±150.53	6962.18±139.24	309.52±6.19	192.32±3.84
E20-T	6759.16±135.18	6311.65±126.23	222.75±4.45	162.36±3.24
E40-T	7248.21±144.96	6711.07±134.22	251.41±5.02	193.21±3.86
E60-T	8275.87±165.51	7426.27±148.52	293.94±5.87	212.89±4.25

7.2 Storage modulus

Figure 7.2 presents the temperature dependence of storage modulus of all the syntactic foams including neat epoxy measured at 1 Hz. With increase in temperature the storage modulus decreases steadily in the temperature range from 28 to 60°C and drops sharply thereafter. Storage modulus for neat epoxy is lower than the foams in region I. E60-T syntactic foams presents highest storage modulus (Table 7.1). Increase in cenosphere volume fraction results in higher storage modulus (Gu et al. 2007). This can be attributed to less molecular motion of epoxy molecules due to addition of stiff cenosphere particles. However, silane treated foams present higher storage modulus as

compared to untreated ones owing to superior adhesion between the constituents resulting in higher stiffness of the foams (Gu et al. 2007). Comparing with neat epoxy, the storage modulus increases in the range of 13-43% and 28-57% for untreated and treated syntactic foams, respectively.

In region II, all the samples reach glass transition temperature, as a result, storage modulus decreases drastically attributing to change from glassy to rubbery state. Region III is characterized by lowest storage modulus for the neat resin and is measured to be in the range of 105-325% and 258-370% lower than untreated and treated syntactic foams respectively (Table 7.1). In this region, storage modulus increases with cenosphere volume fraction but does not show significant change with respect to silane treatment of cenospheres. However, the retention of properties at elevated temperatures in treated syntactic foams can be beneficial for large number of applications.
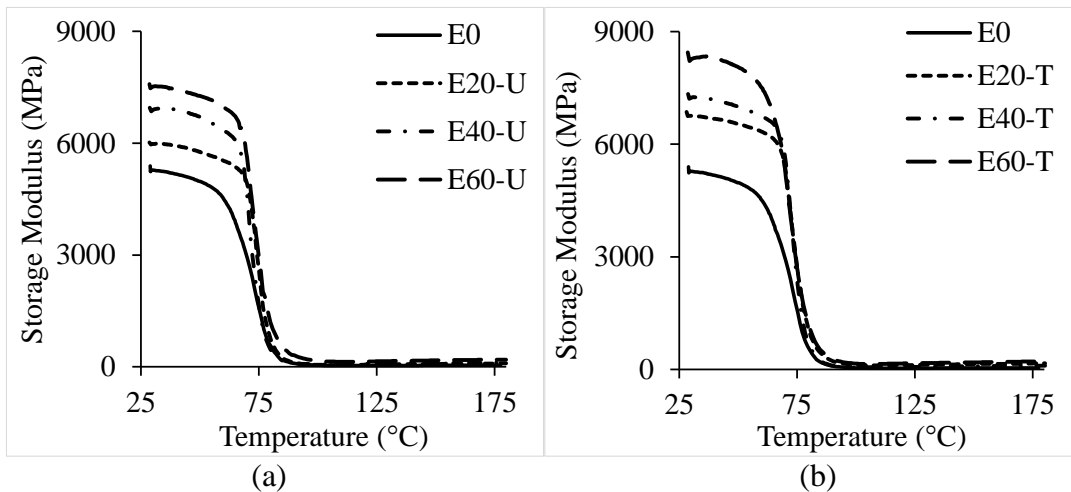
Figure 7.2 Experimental storage modulus of all samples having (a) as received and (b) treated cenospheres.

The maximum use temperature (T_{max}) is defined as the temperature at which the storage modulus starts to decrease drastically (Capela et al. 2010, Sankaran et al. 2006). The intersection point of the tangents drawn to the curve in regions I and II in Figure 7.1 is defined as T_{max}. The values of T_{max} and glass transition temperature are presented in Table 7.2. T_{max} is lower for neat resin as compared to all the samples. Compared to the T_{max} of neat epoxy (61°C), syntactic foams have T_{max} above 65°C. However, increase in T_{max} is observed for syntactic foams with increase in the cenosphere volume fraction.

96

Table 7.2 Maximum use and glass transition temperature for all the samples.

Material	Maximum use temperature T_{max} (°C)	Glass transition temperature T_g (°C)
E0	61.54±1.23	76.22±1.52
E20-U	67.20±1.34	75.95±1.51
E40-U	69.05±1.38	74.82±1.49
E60-U	71.24±1.42	74.15±1.48
E20-T	66.32±1.32	75.40±1.50
E40-T	68.52±1.37	74.33±1.48
E60-T	69.74±1.39	74.00±1.48

7.3 Loss modulus

Figure 7.3 shows the sets of graphs for loss modulus variation with respect to temperature for all the samples. Loss modulus reaches peak around 61°C and decreases thereafter. It might be due to non-crystalline phase in matrix for such transition in temperature. Glass transition temperature of the matrix is found to be around 76°C. Further, the values of loss modulus diminish to zero as temperature surges over 90°C. Glass transition temperature is defined as the corresponding temperature to the maximum loss modulus curve and is presented in Table 7.2 (Ray et al. 2002, Sankaran et al. 2006). T_g of the neat resin is higher than all the syntactic foams. T_g of syntactic foams decreases with volume fraction of cenospheres. Maximum loss modulus values are presented in Table 7.3. Some of the notable trends in the loss modulus behavior are:

- In region I, loss modulus is lower for syntactic foams when compared to the neat resin except for treated sample with 60 vol.% of cenospheres owing to less internal sliding between the molecules of epoxy and sliding between the particles and interface matrix. When the volume fraction is less the contribution of matrix viscoelasticity is higher while that of frictional energy dissipation is lower. At higher filler content the contribution of matrix viscoelasticity reduces attributing to intense dilution effect of the cenospheres to the matrix. Thereby, the internal molecular motion of the matrix becomes difficult, hindering the frictional energy dissipation of chain segments and consequently reducing the heating loss (Gu et al. 2007).

- With increase in temperature post 60°C and cenosphere volume fraction, increase in the intensity of peaks is observed.

(a)   (b)
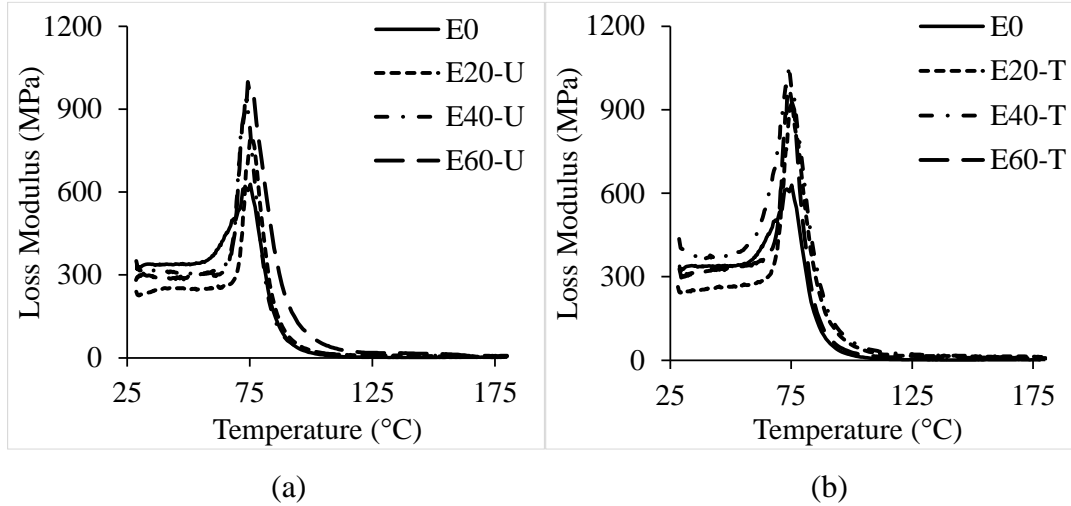
Figure 7.3 Experimentally measured loss modulus of samples with (a) untreated and (b) treated cenospheres.

Table 7.3 Maximum and room temperature loss modulus values of all the samples.

Material	Loss modulus at 30°C (MPa)	Maximum loss modulus (MPa)
E0	327.17±6.54	628.64±12.57
E20-U	229.23±4.58	798.48±15.96
E40-U	298.91±5.97	917.40±18.34
E60-U	316.43±6.32	999.25±19.98
E20-T	244.61±4.89	925.68±18.51
E40-T	302.56±6.05	978.14±19.56
E60-T	338.51±6.77	1060.46±21.20

7.4   Damping

Measure of the damping capability of the material is given by the ratio of loss modulus and storage modulus and is termed as $Tan\,\delta$ (Zhu et al. 2010).

$$Tan\,\delta = \frac{E''}{E'}$$
(7.1)

$Tan\,\delta$ is an important parameter to characterize viscoelasticity. Figure 7.4 shows the representative sets of plots for variation of $Tan\,\delta$ with respect to temperature for various syntactic foams and neat epoxy. Increase in volume fraction results in increasing $Tan\,\delta$ as observed from Figure 7.4 Neat resin and all syntactic foams exhibit maximum $Tan\,\delta$ at approximately the same value implying matrix properties

98

determine damping. Increase in cenosphere volume fraction reduces area under $Tan\,\delta$ curve Figure 7.4. Increase in stability of the polymer materials is attributed with decrease in the area under the $Tan\,\delta$ curve (Shunmugasamy et al. 2013). This implies that with increasing volume fraction of cenospheres, stability of syntactic foams at higher temperatures increases. Properties of the syntactic foams are significantly affected by the operating temperature, volume fraction and surface modification of cenospheres. Initially $Tan\,\delta$ increases and later noted to be decreasing with increasing temperature. Neat epoxy reveals lower $Tan\,\delta$ values as compared to all the syntactic foams, demonstrating that addition of cenospheres improves the damping capability. However, syntactic foams with treated cenospheres reveal higher values of $Tan\,\delta$ for all the volume fractions. Peak $Tan\,\delta$ value of 0.914 appears at 87°C for E60-T foam which is higher as compared to all other foams and neat epoxy. Furthermore, comparing the $Tan\,\delta$ value of the matrix with those of the syntactic foams, it is observed that the addition of fly ash cenospheres enhances the damping capacity. This is attributed to contributions of in-built porous structure in cenospheres and frictional damping. Increase in filler content further lead to incremental energy loss leading to increasing damping loss factor (Gupta and Woldesenbet 2004, Shunmugasamy et al. 2012). Surface treatment of cenospheres enhances the bonding of the constituents enhancing stability further.
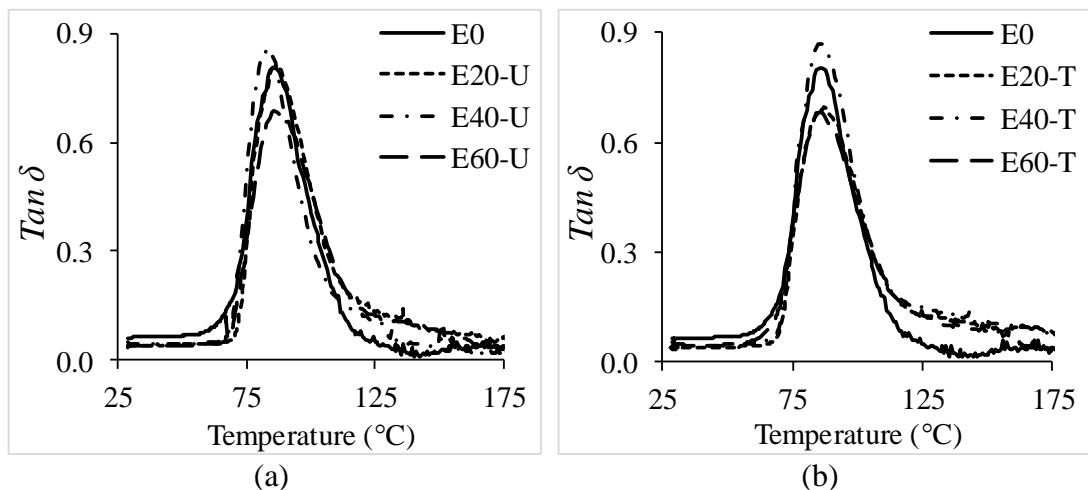
Figure 7.4 Experimentally measured $Tan\,\delta$ of all samples.

7.5 Morphology

Freeze fracture features of all the samples are presented in Figure 7.5. The micrographs are taken post temperature sweep on the samples. Deformation marks are observed on the surface of neat epoxy indicating plastic deformation (Figure 7.5a). At elevated temperature, neat epoxy undergoes more deformation owing to more induced viscoelasticity. As a result, neat samples undergo more plastic deformation. Such an observation is not observed for E20 samples (Figure 7.5b and Figure 7.5c). Reinforcing hard shelled cenospheres into the matrix reduces deformation of the foams considerably. Cenospheres absorb the deformation transferred from the matrix effectively. Increasing the cenosphere content in the system reduces the matrix deformation further (Figure 7.5 d and Figure 7.5e). As a result, material tends to absorb more energy at elevated temperatures resulting in enhanced stiffness as compared to foams with lower cenosphere content and neat epoxy samples. Treated syntactic foams exhibited higher stiffness and damping as compared to untreated syntactic foams and neat epoxy owing to better bonding between the constituents (Figure 3.4d).

Conclusions

Effect of temperature on the dynamic mechanical properties of syntactic foams is presented. Combination of cenosphere volume fraction and surface treatment on the storage modulus, loss modulus and damping parameter are analyzed. The following conclusions are drawn from the analysis of experimental results:

- Neat epoxy sample presents lowest storage modulus as compared with tested syntactic foams. Increase in cenosphere volume fraction results in increase of storage modulus for both untreated and treated cenosphere syntactic foams.
- Storage modulus of neat resin is lower by 105-325% and 258-370% as compared to untreated and treated syntactic foams respectively.
- Loss modulus of syntactic foams is lower than neat epoxy owing to reduced molecular motion of epoxy matrix due to the presence of cenosphere particles.
- Presence of cenospheres helps in increasing the retention of mechanical properties of syntactic foams at temperatures beyond T_g.

- Addition of fly ash cenospheres enhances the damping capacity of the foams. Peak $Tan\ \delta$ value of 0.914 appears at 87°C for E60-T foam which is higher as compared to all other foams and neat epoxy.
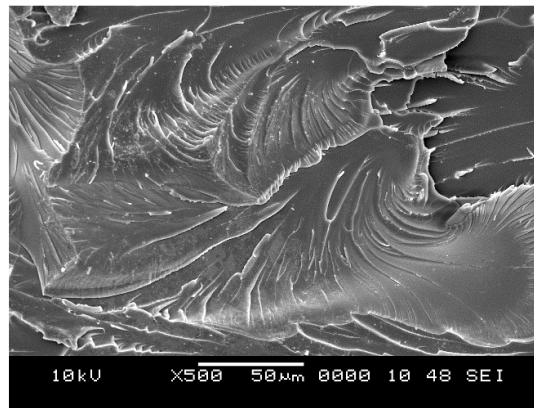
(a)
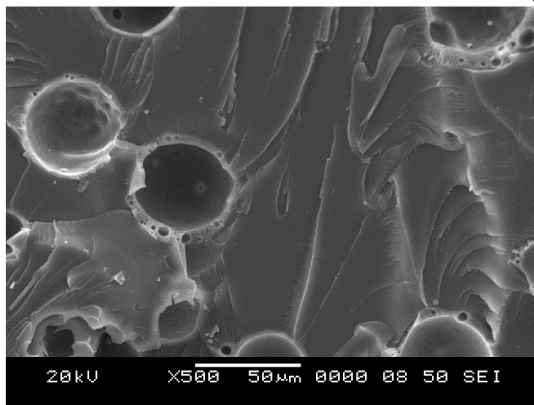
(b)
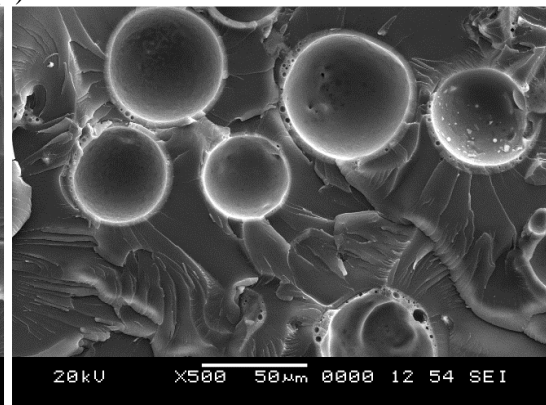
(c)
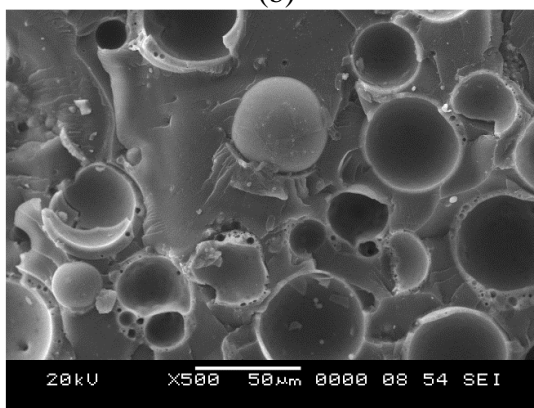
(d)
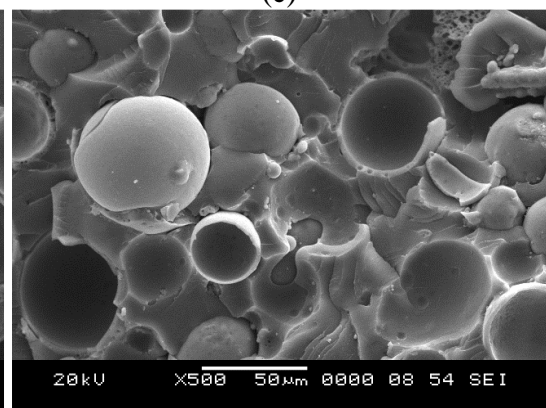
(e)

Figure 7.5 Micrographs of (a) E0 (b) E20-U (c) E20-T (d) E60-U and (e) E60-T.

Syntactic foam density changes with a number of parameters, which include densities of resin, hollow particle material, volume fraction of constituents and surface modification of cenospheres. Each of these parameters may have a different effect on the viscoelastic properties. Clear trend is observed for loss modulus and maximum glass transition temperature in the presented work. These results are useful in selecting suitable parameters for designing syntactic foam microstructure based on the conditions demanded by envisaged applications.

8   DRY SLIDING WEAR RESPONSE

8.1   Height loss and frictional force

Figure 8.1 presents a typical set of dry sliding wear test results. Height loss (Figure 8.1a) and frictional force (Figure 8.1b) are graphed with time of wear. These representative results are obtained on E0, E60-U and E60-T samples for $V_2F_{50}D_3$ conditions. For neat epoxy samples, the wear attains a steady state after an initial transition period as observed from Figure 8.1a. A similar trend is demonstrated by E60-U and E60-T foams as seen from this figure, although the transient region is less pronounced.

Further, height loss in neat epoxy specimens is twice as that of syntactic foam specimens at 1500 seconds as observed in Figure 8.1a. This observation implies that the cenospheres in epoxy resin enhances wear resistance. Further, frictional force of syntactic foams show decreasing trend with increasing time as compared to the neat epoxy samples. All the samples attain a steady state frictional force as time progresses. For the same time interval, the frictional force in E60-U and E60-T syntactic foam specimen reduces by 55 and 71 % respectively compared to the neat epoxy samples highlighting the effectiveness of syntactic foams for wear resistive applications.

The fluctuations observed in Figure 8.1b are more for neat epoxy samples as compared to the syntactic foam samples. For neat epoxy samples, the generated wear debris come in contact with the sliding surface and disc, resulting in more undulations leading to higher frictional force. In the case of syntactic foams, some cenospheres are partially cut on the initial wear surface, which tend to fill with the wear debris (Figure 8.1b). Over a period of time, the rate of new cenospheres opening up for filling with debris and the older cenospheres wearing out and releasing the accumulated debris on the wear surface balance each other, resulting in reduced frictional force as compared with neat epoxy sample.
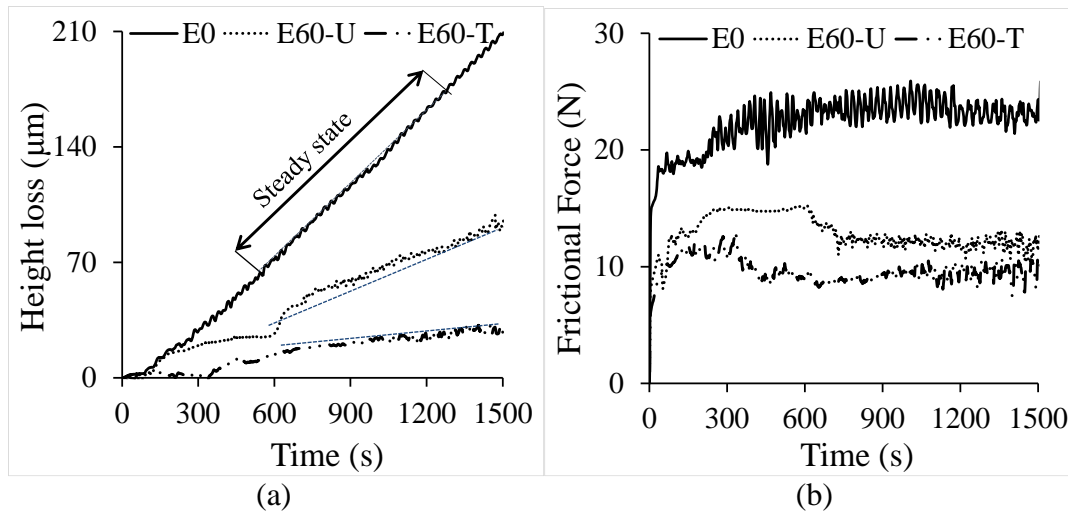
Figure 8.1 Typical graphs of the wear test (a) height loss and (b) frictional force with respect to time of wear.

8.2 Wear rate

The experimental values of w_t, w_s and μ for sliding velocity of 2 and 5 m/s are presented in Table 8.1 and Table 8.2 respectively. Wear rate is found to decrease with increase in sliding velocity for 30N load whereas an increase is noted for 50N load (Figure 8.2). Further, it is noted that w_t shows declining trend with increasing filler loading and sliding distances. Neat epoxy reveals the highest w_t as compared to EXX-U and EXX-T foams for all the tested conditions. Increase in the applied load increases w_t for neat epoxy samples and foams with lower filler contents (E20) whereas decrease with increasing cenospheres signify the advantage of having higher filler contents in epoxy matrix. w_t for treated syntactic foams is better as compared to EXX-U and E0 under all the tested conditions. Maximum w_t of 21.9, 18.9 and 15.5 mm^3/km for neat epoxy, E20-U and E20-T foams respectively is observed at $V_5F_{50}D_3$.

In case of V_2F_{30} test condition, w_t is maximum for neat epoxy samples. Further, it is observed that cenosphere presence decreases w_t (Figure 8.2a). Primary constituents of cenospheres are aluminium and silica. These cenosphere particles are broken into fine fragments and get mixed with the matrix resin constituting debris (Mondal et al. 2009). Combination of brittle aluminium and silica particles with epoxy matrix resists the wear in case of syntactic foams. Increasing the filler content further ensures better wear resistance. Figure 8.2a reveals that w_t decreases with increasing sliding distance for all

104

the samples. Lower sliding distance (D_3) provide high w_t as compared to D_7. Surface of both epoxy and cenospheres gets smoothened as the wear progresses reducing it further. Deviation in w_t with increase in D is attributed to changes in the surface roughness, surface chemistry and effective contact area (Rao and Das 2011). Abrasive mode of wear mechanism is observed for these conditions.

At V_5F_{30} condition, w_t decreases with increase in sliding velocity for all the samples (Figure 8.2b). Frictional heating is very low at an applied load of 30N. As a result, w_t of neat epoxy sample decreases slightly. On the other hand, nominal contact surface between syntactic foams and the disc reduces owing to opening of void space within the microballoons, post fracture. Under lower applied load (F_{30}), wear debris does not get compacted in the void spaces effectively resulting in marginal variation of wear rate with increase in velocity.

For V_2F_{50} condition, w_t decreases with increasing load from 30 to 50 N for syntactic foam samples (Figure 8.2c) whereas w_t increases for neat epoxy. Volume loss of epoxy based composites generally increases with the rise in sliding speed and applied force (Kanchanomai et al. 2011). For neat epoxy samples at F_{50}, load distribution across the overall asperities increases. These asperities pierce deeper in the matrix surface registering higher w_t (Siddhartha and Gupta 2012). However, syntactic foams show decrease in w_t owing to the presence of higher cenosphere content (Figure 8.2c). These hard shell particles of cenospheres are effective in reducing w_t by preventing matrix damage over a greater scale. Lower contents of matrix in E40 and E60 samples reduce wear rate considerably as compared to E20. Higher load reduces surface asperities effectively. Transition from abrasive to adhesive mode of wear mechanism is observed for V_2F_{50}.

At V_5F_{50} condition, w_t increases significantly for neat epoxy samples owing to high frictional forces generated at the interface whereas w_t decreases for EXX-U and EXX-T foams due to better resistance offered by the cenosphere particles (Figure 8.2d). For neat epoxy samples, the surface is severely strained and wear debris tend to adhere to

the disc. The size of this neat epoxy debris is larger, exhibiting undulations in w_t. On the contrary, for EXX-U and EXX-T foams, the debris generated is smaller in size and gets accumulated at the craters of broken cenosphere sites. Small amounts of wear debris that lie on the surface facilitate better plastic flow making the surface relatively smoother. Increase in filler loading provides more void spaces for debris accumulation reducing w_t further. Increase in applied load creates localized fusion of broken cenosphere fragments leading to a high degree of adhesive wear. As a result, adhesive mode of wear mechanism is prominent for V_5F_{50} condition. These events lower w_t in syntactic foams.

For EXX-U and EXX-T foams, w_t decreases in the range of 8-94% and 21-98% respectively, compared to neat epoxy for all the tested conditions. E20 poses less void spaces for wear debris accumulation as compared to E40 and E60. Further, behavior of E20 is matrix dominated. Therefore, E20 samples register higher w_t. Significant reduction in w_t is achieved with increase in the cenosphere content (E60) owing to higher space availability for accommodating wear debris. Epoxy matrix being the softer phase compared to cenospheres, the wear resistance of the matrix is very low.

Embedding more number of cenospheres in matrix considerably enhances overall wear resistance of the syntactic foam. However, for all the filler contents, EXX-T foams show lower w_t compared to EXX-U. As compared to EXX-U foams, wear rate in EXX-T foams decreases in the range of 2-92%. Lower resistance of EXX-U foams is due to poor interfacial adhesion between the constituents (Figure 3.4b). While in case of EXX-T, good interfacial bonding (Figure 3.4d) resists the material removal over longer period of contact time before finally getting worn out resulting in reduced w_t. Weaker interfacial adhesion between cenospheres and epoxy resin in EXX-U easily initiates cracks at the interfacial region under the applied load. As a result, the matrix resin is easy to rub-off without the effective reinforcement of cenosphere in friction leading to the rough worn surface, higher friction coefficient and wear rate.

Table 8.1 Experimentally measured w_t, w_s and μ for D at $V = 2$ m/s, $F = 30$ and 50 N.

Input parameters				Output		
V (m/s)	F (N)	D (km)	Material	w_t (mm³/km)	w_s (mm³/N-km)	μ
2	30	3	E0	16.5	0.5607	0.5545
			E20-U	13.2	0.4485	0.4441
			E40-U	12.8	0.4349	0.4156
			E60-U	9.6	0.3262	0.3378
			E20-T	10.7	0.3636	0.3397
			E40-T	10.4	0.3534	0.3281
			E60-T	9.3	0.3160	0.2035
		5	E0	12.2	0.4145	0.5263
			E20-U	9.8	0.3330	0.4656
			E40-U	9.2	0.3126	0.4128
			E60-U	7.3	0.2480	0.3573
			E20-T	9.6	0.3262	0.4547
			E40-T	7.2	0.2446	0.3585
			E60-T	6.9	0.2345	0.2764
		7	E0	10.9	0.3704	0.5121
			E20-U	10	0.3398	0.4642
			E40-U	4.5	0.1529	0.4046
			E60-U	3.6	0.1223	0.357
			E20-T	6.8	0.2311	0.4295
			E40-T	4.1	0.1393	0.3468
			E60-T	1.4	0.0476	0.3247
	50	3	E0	18	0.3670	0.5954
			E20-U	13	0.2650	0.4228
			E40-U	8.5	0.1733	0.4131
			E60-U	7.9	0.1611	0.2975
			E20-T	8.5	0.1733	0.3524
			E40-T	4.5	0.0917	0.3479
			E60-T	4.1	0.0836	0.1894
		5	E0	14.4	0.2936	0.5642
			E20-U	11.8	0.2406	0.4016
			E40-U	7.1	0.1448	0.3877
			E60-U	7.3	0.1488	0.3279
			E20-T	5.3	0.1081	0.4011
			E40-T	2.8	0.0571	0.3818
			E60-T	0.6	0.0122	0.3494
		7	E0	12.8	0.2610	0.5332
			E20-U	10.6	0.2161	0.402
			E40-U	3.7	0.0754	0.3877
			E60-U	2	0.0408	0.3181
			E20-T	4.1	0.0836	0.4379
			E40-T	2.1	0.0428	0.4254
			E60-T	0.5	0.0102	0.3466

Table 8.2 Experimentally measured w_t, w_t and μ for D at $V = 5$ m/s, $F = 30$ and 50 N.

Input parameters				Output		
V (m/s)	F (N)	D (km)	Material	w_t (mm³/km)	w_s (mm³/N-km)	μ
			E0	14.1	0.4791	0.5856
			E20-U	12.1	0.4111	0.451
			E40-U	9.5	0.3228	0.4312
		3	E60-U	4.4	0.1495	0.379
			E20-T	9.7	0.3296	0.4678
			E40-T	6.4	0.2175	0.464
			E60-T	3.1	0.1053	0.4158
			E0	13.1	0.4451	0.5772
			E20-U	9.3	0.3160	0.4686
			E40-U	7.4	0.2514	0.4593
	30	5	E60-U	4.3	0.1461	0.395
			E20-T	7.2	0.2446	0.464
			E40-T	5.1	0.1733	0.4618
			E60-T	1.9	0.0646	0.4158
			E0	10.6	0.3602	0.5236
			E20-U	7.6	0.2582	0.4509
			E40-U	4	0.1359	0.4312
		7	E60-U	3.2	0.1087	0.4003
			E20-T	5.9	0.2005	0.4666
			E40-T	2.6	0.0883	0.4562
			E60-T	1.2	0.0408	0.3864
5			E0	21.9	0.4465	0.6345
			E20-U	18.9	0.3853	0.4951
			E40-U	9.6	0.1957	0.3878
		3	E60-U	10	0.2039	0.3038
			E20-T	15.5	0.3160	0.5225
			E40-T	7.1	0.1448	0.4103
			E60-T	3.9	0.0795	0.3961
			E0	21.4	0.4363	0.6223
			E20-U	16.4	0.3344	0.5389
			E40-U	7.6	0.1549	0.4391
	50	5	E60-U	1.5	0.0306	0.3877
			E20-T	11.2	0.2283	0.4381
			E40-T	5.8	0.1182	0.3991
			E60-T	0.9	0.0183	0.3859
			E0	19.5	0.3976	0.6061
			E20-U	12.5	0.2548	0. 4951
			E40-U	5	0.1019	0.4641
		7	E60-U	1.2	0.0245	0. 402
			E20-T	10.9	0.2222	0. 4715
			E40-T	3.1	0.0632	0.41
			E60-T	0.4	0.0082	0. 4085

Figure 8.2 Plots of w_t for different filler contents (a) V_2F_{30} (b) V_5F_{30} (c) V_2F_{50} and (d) V_5F_{50}.

Poor interfacial bonding between the constituents in EXX-U results in cenospheres getting dislodged easily with scuffing of the counterpart surface leading to higher wear. For EXX-T foams, due to enhancement in constituent materials bonding, cenospheres are strongly adhered to the matrix. During the wear test, surface modified cenospheres carry most of the load. Thereby, direct contact and adhesion between the matrix and the counterpart are reduced leading to lower friction coefficient and smoother worn surface. With the strong bonding between cenosphere and the matrix, the fillers cannot be easily dislodged from the matrix under the applied load. The load-carrying ability of the foam is thus improved restraining large-scale shedding and rubbing-off of epoxy matrix reducing w_t.

Figure 8.3 present micrographs of post wear test of E20-U and E20-T foams. Void spaces are seen to be completely filled for both E20-U and E20-T foams as seen from Figure 8.3. Further, it's clearly evident that effective compaction of wear debris is seen in E20-T (Figure 8.3b) as compared to untreated filler (Figure 8.3a). Additionally worn out surface is observed to be smoother (Figure 8.3b) in surface modified filler reinforced epoxy matrix. Such occurrences enhance the wear resistance of EXX-T foams as compared to EXX-U foams.

| (a) | (b) |
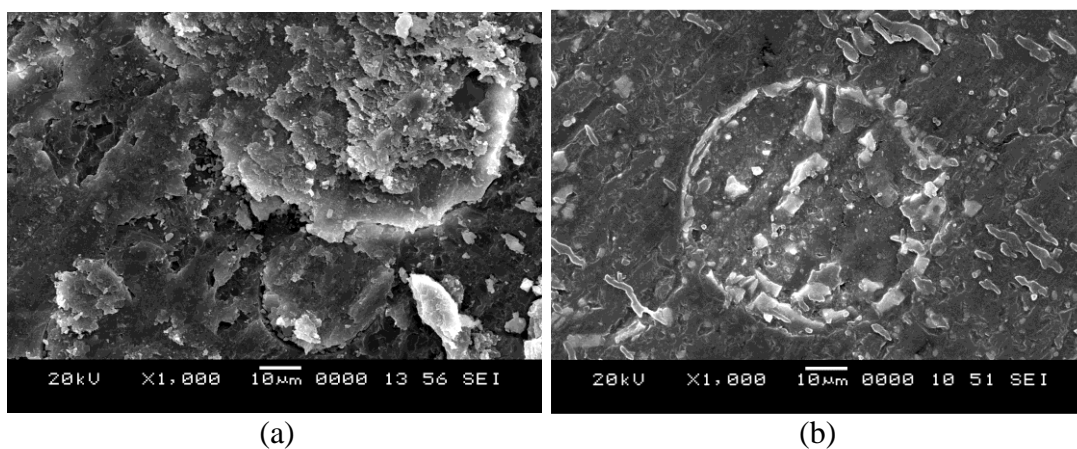
Figure 8.3 Micrograph of post wear test of (a) E20-U and (b) E20-T foams.

8.3   Specific wear rate

Specific wear rate of neat epoxy and their syntactic foams are presented in Figure 8.4. Effect of D and filler loading on the w_s at V_2F_{30} condition is presented in Figure 8.4a. In line with w_t, w_s of all the syntactic foam decreases with increase in D and cenosphere content (Figure 8.4). It is further observed from Figure 8.4b that as the applied load is increased to 50 N, w_s decreases substantially for all the compositions demonstrating enhanced wear resistance at higher loads (Ghazali et al. 2005, Kumar and Hiremath 2014, Shalwan and Yousif 2014). EXX-T foams reveal the highest resistance among all the compositions. Higher resistance offered by treated syntactic foams to wear can be solely due to the strong bonding exhibited between the constituents making them suitable potential candidate materials in dry sliding wear environments. Further, similar trends are observed with increase in sliding velocity (Figure 8.4c and Figure 8.4d).

Figure 8.4 reveal that E60 exhibited minimum w_s from all the test conditions. Combined effect of higher sliding velocity and applied load is beneficial in reducing the specific wear rate (Manakari et al. 2015). At higher sliding velocity and applied load, the transfer film is formed easily which is difficult to rupture for EXX-U and EXX-T foams due to the adhesive mechanism, resulting in better wear resistance as compared to neat epoxy. In E60, cenospheres are available in higher numbers as compared to E20. Higher particles on worn surface result in higher contact area. As a result, the resistance offered with higher filler content is much better. EXX-T foam with E60 has minimum w_s among all the sample compositions. E60-T foam has minimum w_s of 0.0082 mm³/N-km and maximum w_s of 0.5607 mm³/N-km is observed for neat epoxy samples.
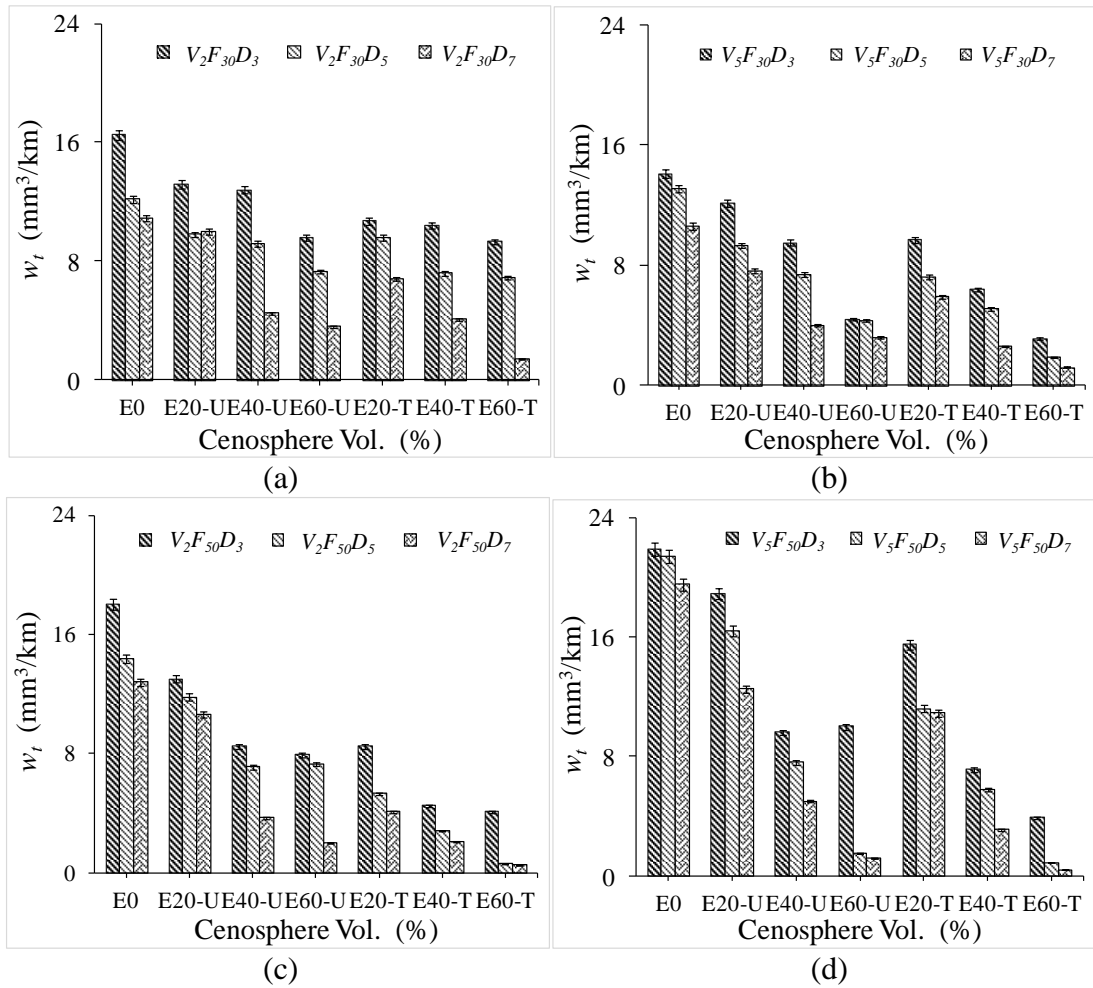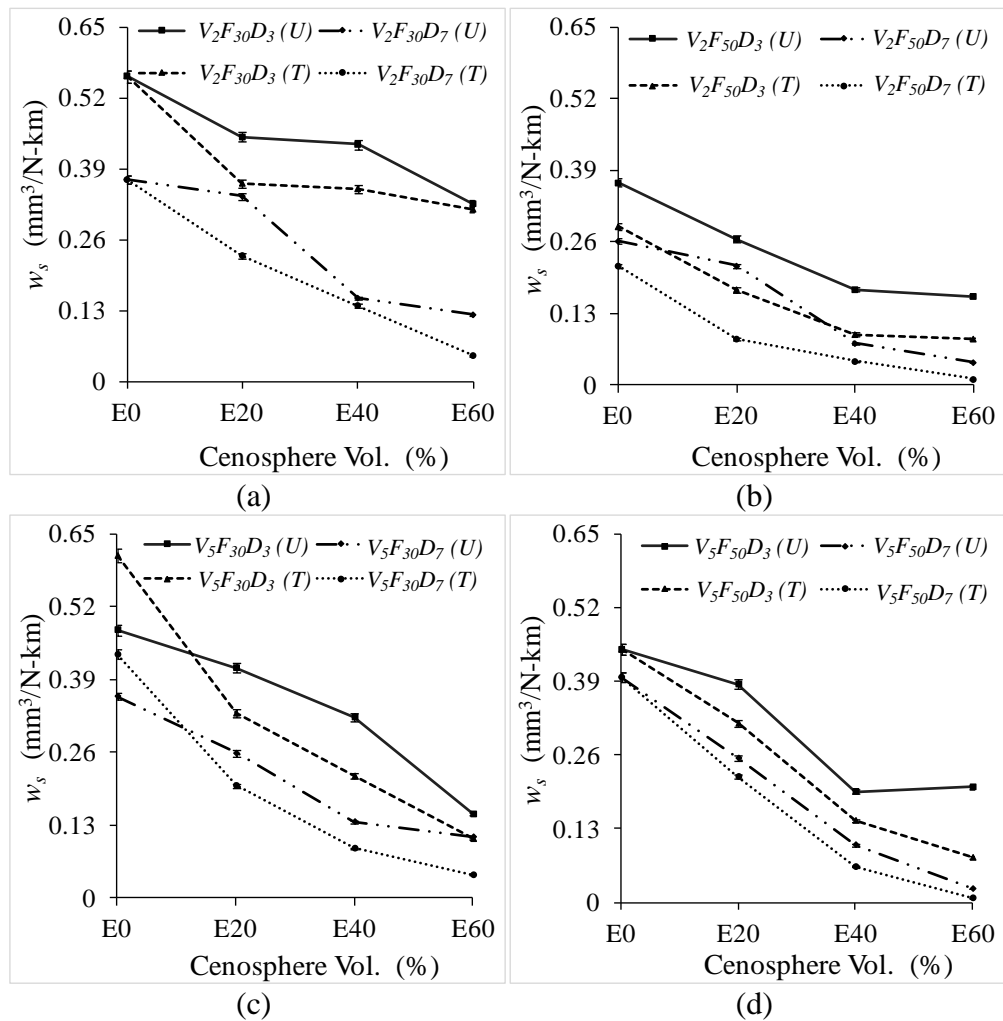

Figure 8.4 Plots of w_s for different filler contents at (a) V_2F_{30} (b) V_2F_{50} (c) V_5F_{30} and (d) V_5F_{50}.

111

8.4 Coefficient of friction

Variation of μ for different study parameters are presented in Figure 8.5. Neat epoxy presents the highest μ compared to EXX-U and EXX-T foams. It is seen from Figure 8.5a, that with V_2F_{30}, μ decreases with increase in cenosphere content. As filler loading increases, fragmented cenospheres coming into contact with counter surface are more, resulting in lower data fluctuations leading to lower values of surface roughness and μ. The values of μ vary in the range of 0.20-0.55.

It is noted from Figure 8.5b that, μ values are significantly reduced at F_{50} as compared to F_{30} (Jia et al. 2007). It is attributed to the increase in frictional heat at the interface which leads to lubricating film formation on the worn surface. Thereby, the flowability of the syntactic foam sample increases and causes slip phenomena. In addition to this, wear debris get easily accumulated within the void space of broken cenospheres making the surface still smoother.

The values of μ vary in the range of 0.19-0.6 for testing condition of V_2F_{50}. With increase in sliding velocity, μ increases (Figure 8.5c) owing to higher shear force. These shear forces leads to temperature rise at the interface of sample and disc resulting in increased thermal penetration from disc towards test samples. As a result, the bond across filler-matrix interface weakens. Consequently, cenosphere particles get dislodged easily and shear away owing to axial thrust, increasing μ.

The values of μ are seen to be varying in the range of 0.38-0.59 for V_5F_{30}. Similar to Figure 8.5b, with increase in F and V, μ decreases as observed from Figure 8.5d. As mentioned earlier, the combination of increase in temperature and shearing forces at the interface results in marginal decrease of μ. The values of μ vary in the range of 0.30-0.63 for V_5F_{50} condition.

Further, it is observed that μ increases with increase in D for all the tested conditions. Therefore, it can be concluded that μ is a strong function of V and D. With increase in

V and *D*, μ for syntactic foams increases while it decreases with increasing cenosphere content and *F*.
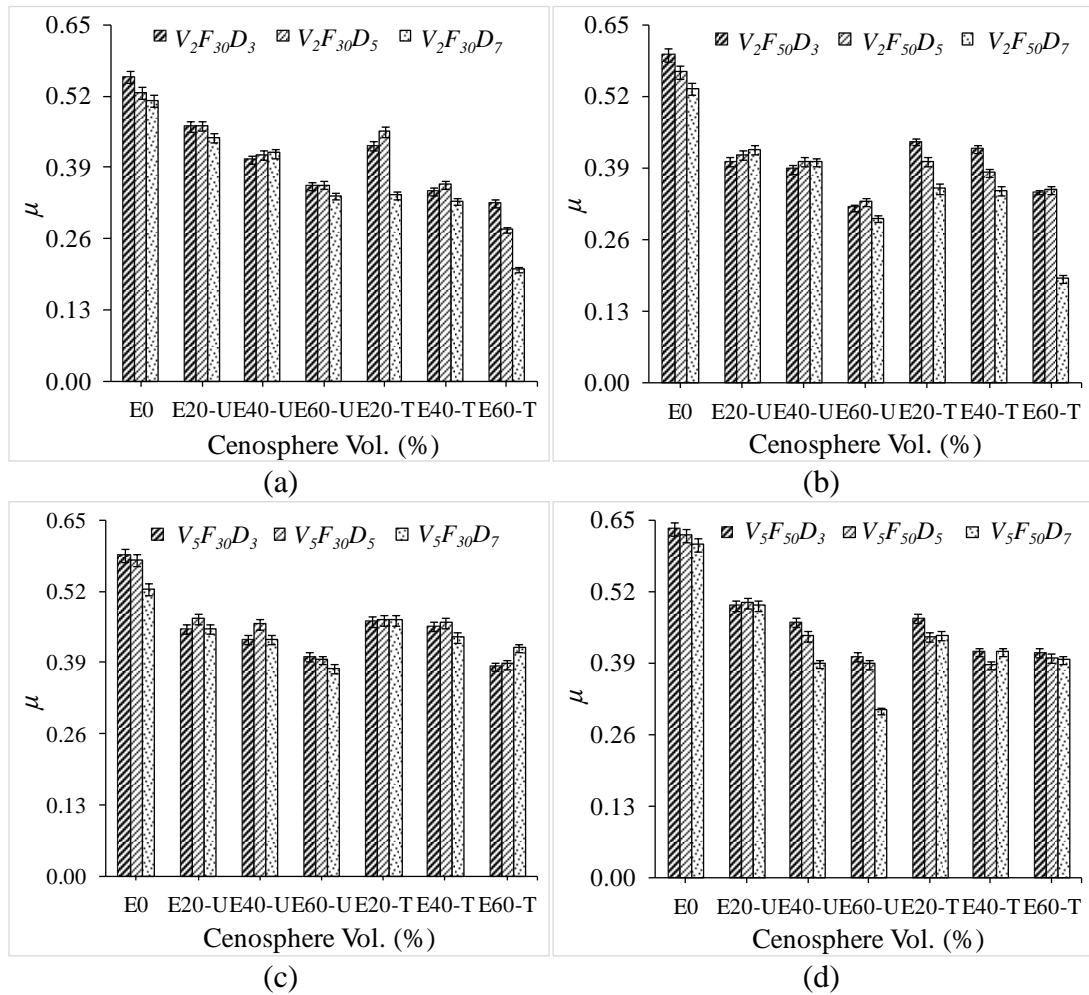
Figure 8.5 Plots of μ for different filler contents at (a) V_2F_{30} (b) V_2F_{50} (c) V_5F_{30} and (d) V_5F_{50}.

8.5 Temperature rise

The variation of disc temperature for minimum and maximum conditions of sliding velocity and applied load are presented in Figure 8.6. At V_2F_{30} condition, the temperature increases with increase in *D* wherein low adiabatic heating takes place (Figure 8.6a). It is further noted that the temperature decreases with increase in filler loading. It is attributed to reduced undulations of samples owing to the presence of cenosphere particles. Further, increase in interconnected spaces between the cenosphere particles results in a higher effective surface area. Absence of such hollow

cenospheres in neat epoxy samples registers highest temperature. EXX-T foams registered lowest disc temperature as compared to EXX-U foams. Rise in temperature is significant for V_5F_{50} conditions (Figure 8.6b). This is due to the combination of high frictional forces and increased adiabatic heating at the interface. Temperature rise is seen to be a strong function of V, F and D. Irrespective of V and F, the temperature decreases with increase in cenosphere content.
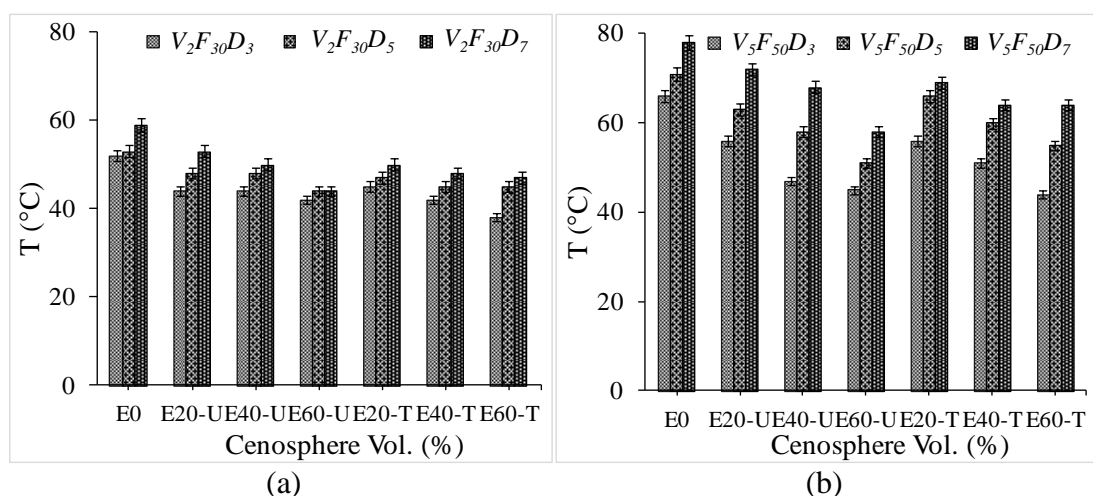
Figure 8.6 Plots of temperature with respect to filler content for (a) V_2F_{30} and (b) V_5F_{50}.

8.6   Wear debris analysis

Elemental composition of debris analysed by EDS is presented in Table 8.3. The elements found in wear debris are aluminium, silica, iron, carbon and oxygen. Aluminium and silica present in the debris are the primary constituents of cenospheres. These hard elements are effective in minimizing wear. Significant wear resistance is achieved with increase in cenosphere content (presence of aluminium and silica). Presence of iron in the wear debris is mainly from the disc counterpart (EN 31 steel) and is observed to be highest in E0 due to absence of transfer film formation on the disc counter face. For E20, the rough worn surfaces of the foams and discontinuous transfer films on counter faces result in large amount of iron particles transferred from EN 31 steel disc to the worn surfaces compared to other foams. In E60, the amount of iron content in the wear debris decreases due to the presence of transfer film. For EXX-T foams, smooth worn surface and uniform transfer film on counter face effectively

114

reduces the wear of the counterpart further. Thereby, small traces of iron are observed as compared to EXX-U foams (Table 8.3). Content of carbon and oxygen in the debris being high implies that the debris is constituted primarily of epoxy resin.

Table 8.3 Elemental composition of the wear debris for representative samples.

Composition (wt.%)	E0	E20-U	E20-T	E60-U	E60-T
Carbon	64.65	59.95	68.63	64.57	62.82
Oxygen	22.78	22.51	21.56	21.28	23.23
Silicon	-----	4.81	1.78	5.20	6.22
Aluminium	-----	2.97	0.47	3.35	2.82
Iron	12.57	9.76	7.56	5.60	4.91

Micrographs of wear debris post wear test for all the samples are presented in Figure 8.7. The wear debris chunks are seen to be much larger for neat epoxy (Figure 8.7a) as compared to syntactic foams (Figure 8.7b-e). During the wear test, material removal for neat epoxy is in the form of large chunks owing to the brittle behavior of matrix and high frictional force caused therein (Figure 8.7a).

With higher filler loading, wear debris chunk size decreases and smaller size cenosphere fragments combine with matrix to form wear debris. Lower amount of filler content provides limited source of broken cenosphere fragments to be part of wear debris. As a result, the size and shape of the debris at E20 is governed by the epoxy matrix (Figure 8.7b and Figure 8.7c).

At E60, large amount of fragmented cenosphere particles availability and lower matrix content decreases the wear debris size further (Figure 8.7d and Figure 8.7e) as compared to neat epoxy and foams with lower filler contents. However, it is observed from Figure 8.7c and Figure 8.7e (EXX-T) that the size of the wear debris is considerably smaller as compared to neat epoxy and EXX-U foams. This is attributed to the constrained source of finely fragmented cenospheres particles and matrix from the wear surface owing to better bonding between the constituents.
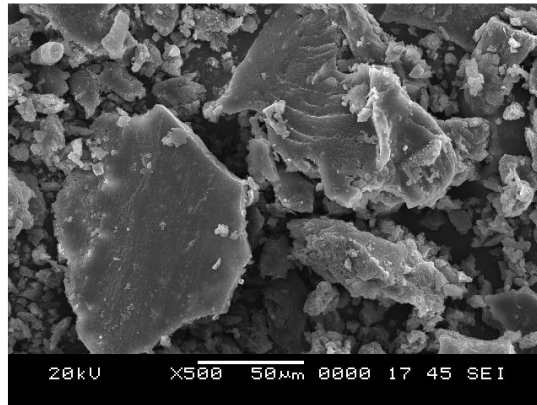
(a)
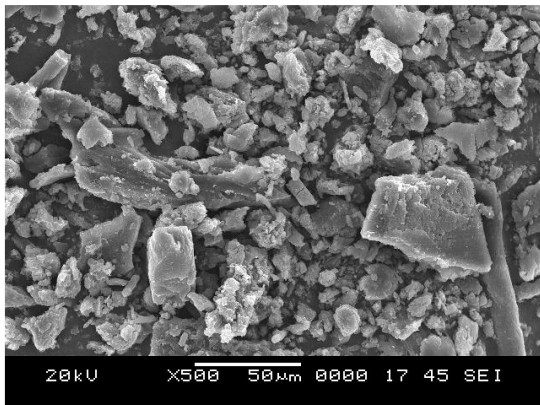
(b)
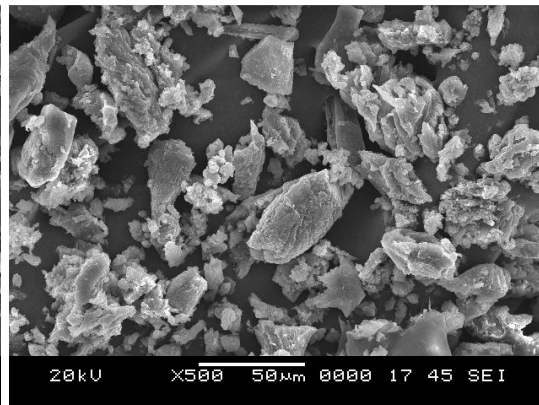
(c)
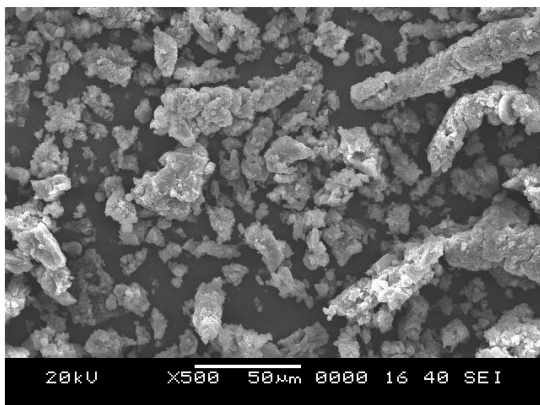
(d)
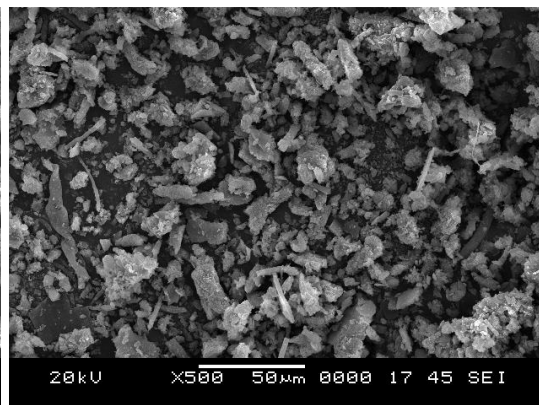
(e)

Figure 8.7 Wear debris micrographs of (a) E0 (b) E20-U (c) E20-T (d) E60-U (e) E60-T samples.

8.7 Wear surface analysis

Micrographs of worn-out samples under lower operating conditions (V_2F_{30}) are presented in Figure 8.8. On the surface of neat epoxy sample, grooves having larger width are visible in the sliding direction. These grooves increase wear rate owing to material removal (wear debris). For E20, matrix dominates the wear behaviour. A closer observation of worn out surface in Figure 8.8c reveals fine grooves on the EXX-T foam surface and material flow along the sliding direction. These grooves are primarily due to the discontinuity created at the cenosphere-epoxy interface due to presence of cenosphere wall in the sliding direction. Similar observations are observed for EXX-U foam (Figure 8.8b).

As the wear debris approaches the craters of partially broken cenosphere sites, they tend to fill the void space. At the same time, inadequate compaction of wear debris at the surface of the broken cenosphere due to lower applied load leads to initiation of small grooves, post cenosphere wall in the sliding direction. Due to series of such events, w_t increases at lower filler contents, primarily indicating dominance of abrasive wear mechanism at lower cenosphere content.

Similar type of worn surface is also noted for E60-U and E60-T samples (Figure 8.8d and Figure 8.8e). The discontinuities in the form of grooves are observed again at the cenospheres location having lower scale as compared to E20 syntactic foam. Matrix being relatively softer phase tends to deteriorate far more easily as compared to filler. Addition of higher filler in matrix effectively reduces wear of the syntactic foams (Manakari et al. 2015).

As a result, the discontinuities at the cenosphere locations decrease for E60 samples owing to the fact that with increase in filler loading matrix content reduces. Thereby, w_t decreases at higher filler contents. It is clearly evident from these observations that wear behavior is greatly influenced by the filler content in the syntactic foam. It can be observed from Figure 8.8e that silane treatment of cenospheres shows better

117

compaction of wear debris as compared to untreated foams (Figure 8.8d) leading to enhanced wear resistance for surface modified foams.
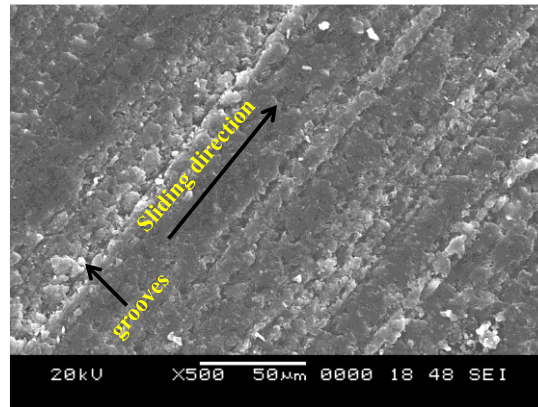
(a)
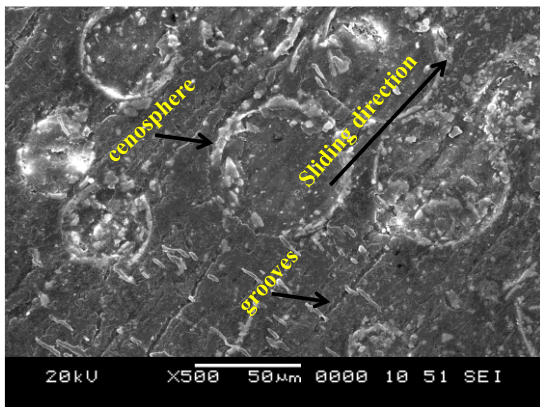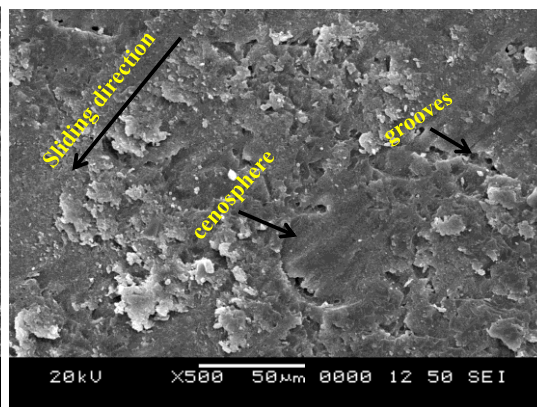
(b)   (c)
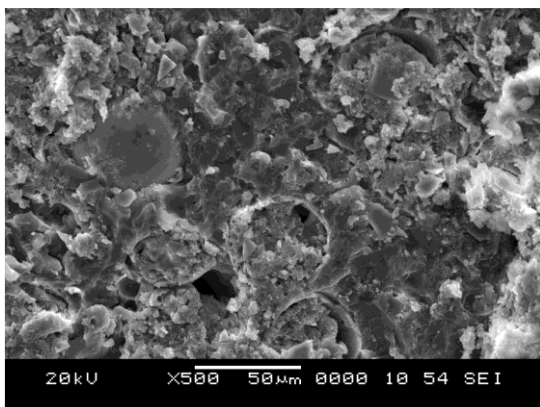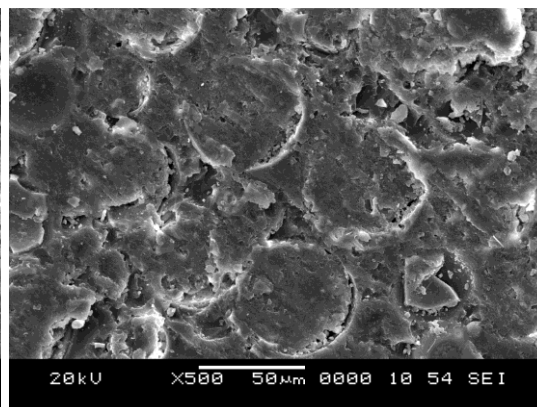
(d)   (e)

Figure 8.8 Micrographs of worn-out surface of (a) E0 (b) E20-U (c) E20-T (d) E60-U (e) E60-T at V_2F_{30}.

Post wear test, micrographs of worn-out surface of samples at V_5F_{50} conditions are presented in Figure 8.9. Increasing load increases possibility of wear debris being smeared along the sliding direction with greater extent of material flow for neat epoxy samples (Figure 8.9a). Plucking and ploughed marks appear all along the sliding direction of the neat sample confirming higher wear rate.

Wear response of E20-U and E20-T foams are presented in Figure 8.9b and Figure 8.9c respectively. A closer observation reveals that the debris is slithered at the disc-sample interface and gets entrapped in void space of the partially broken cenosphere. Further, higher amount of compacted wear debris gets detached (combined action of localized fusion and weak bonding between constituents) from the cenosphere craters in EXX-U is clearly visible (Figure 8.9b). These observations indicate that combo effect of high velocity and applied load increases the shearing force and softens wear debris substantially by plastic deformation (Mondal et al. 2009). As a result wear rate is higher for E20.

Wear rate reduces significantly for E60 as compared to E0. This is due to the presence of more cenosphere particles in the matrix. Formation of wear debris and transfer film is very high owing to more fragmented particles of cenospheres at higher filler loadings (Kato 2000). At higher sliding velocity and applied load, possibility of transfer film formation from wear debris is higher leading to reduced wear as compared to lower filler contents. Moreover, higher loads normalizes the surface asperities and thereby exhibit more stable w_t (Manakari et al. 2015).

The distance to reach steady state decreases with increasing load. In addition to this, the resistance offered by the hard shells of cenospheres that are primarily made up of alumina silicates also help in reducing w_t further. Debris accumulated in the broken cenospheres is very well compacted at higher sliding velocity and applied load as seen from Figure 8.9e. Such an effective compaction leads to reduced fluctuations lowering w_t significantly.
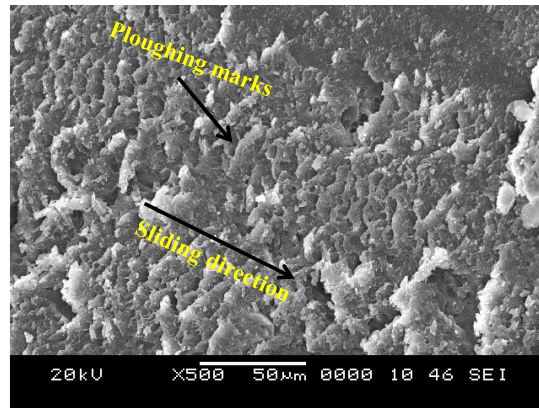
(a)
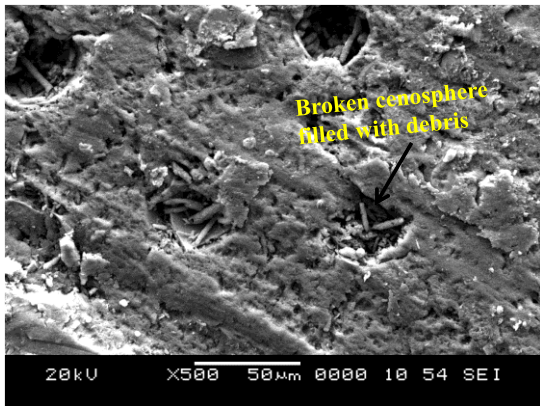
(b)
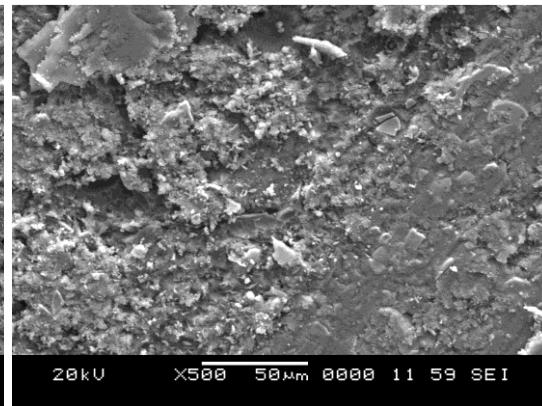
(c)
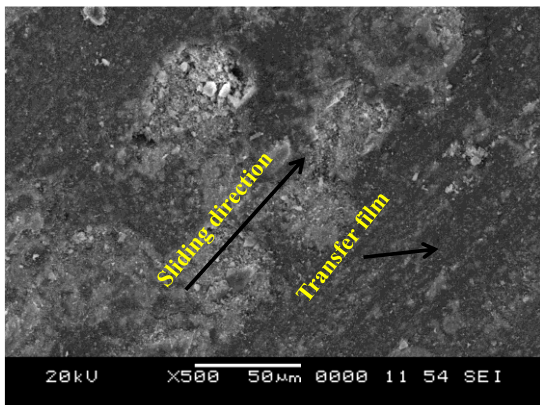
(d)
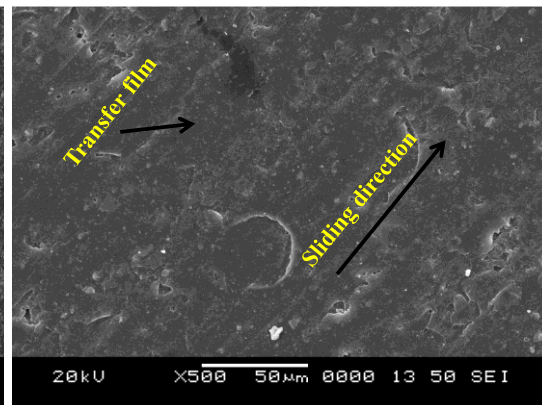
(e)

Figure 8.9 Post wear test micrographs of (a) E0 (b) E20-U (c) E20-T (d) E60-U (e) E60-T samples at V_5F_{50}.

From the micrographs presented in Figure 8.8, it is clearly evident that at lower operating conditions, w_t is higher due to initiation of fine grooves along the sliding direction. As filler loading increases, w_t decreases due to reduction in the magnitude

120

and number of grooves because of lower matrix content. Abrasive or ploughing mode of wear mechanism is observed from these micrographs.

At higher operating conditions (Figure 8.9), w_t decreases with increase in cenosphere content due to the increase in frictional heat which helps in thin film formation. Surface modification of cenospheres has effectively reduced the wear rate by providing effective transfer film and better compaction of wear debris. E60-T is best suited for dry sliding wear applications with weight saving potential of around 12% as presented through this study.

8.8   Property map

Property map is presented in this section which comes handy and acts as an industrial guideline for choosing the specific composition based on the envisaged application. Results presented in this work and the data extracted from the available literature are graphed as a function of density for comparative analysis (Chauhan and Thakur 2013, Rashid et al. 2017) (Figure 8.10). It is clearly evident from the figure that composites with higher density exhibit higher wear rates. However, the advantage of hollow cenospheres filled lightweight syntactic foams is clearly evident from Figure 8.10. In the present study, density of all the syntactic foams including neat epoxy is lower than the other composites investigated in the literature.

Syntactic foams outperform alkali treated, sea water treated, sugar palm fiber reinforced phenolic resin composites and vinylester/cenosphere composites. Wear rates are lower at higher filler contents of cenospheres (E60) as seen from Figure 8.10. E60-T foam reveals the lowest wear rate whereas E60-U foam presents the lowest density. Therefore, from the property map it can be concluded that cenosphere/epoxy syntactic foams with higher cenosphere contents provide lower wear rates and density as compared to other composites signifying their suitability in weight sensitive applications and wear environments. Abundant availability of environment pollutant fly ash cenospheres can be thus effectively utilized to prepare foams for various applications demanding lightweight and wear resistance properties.

121
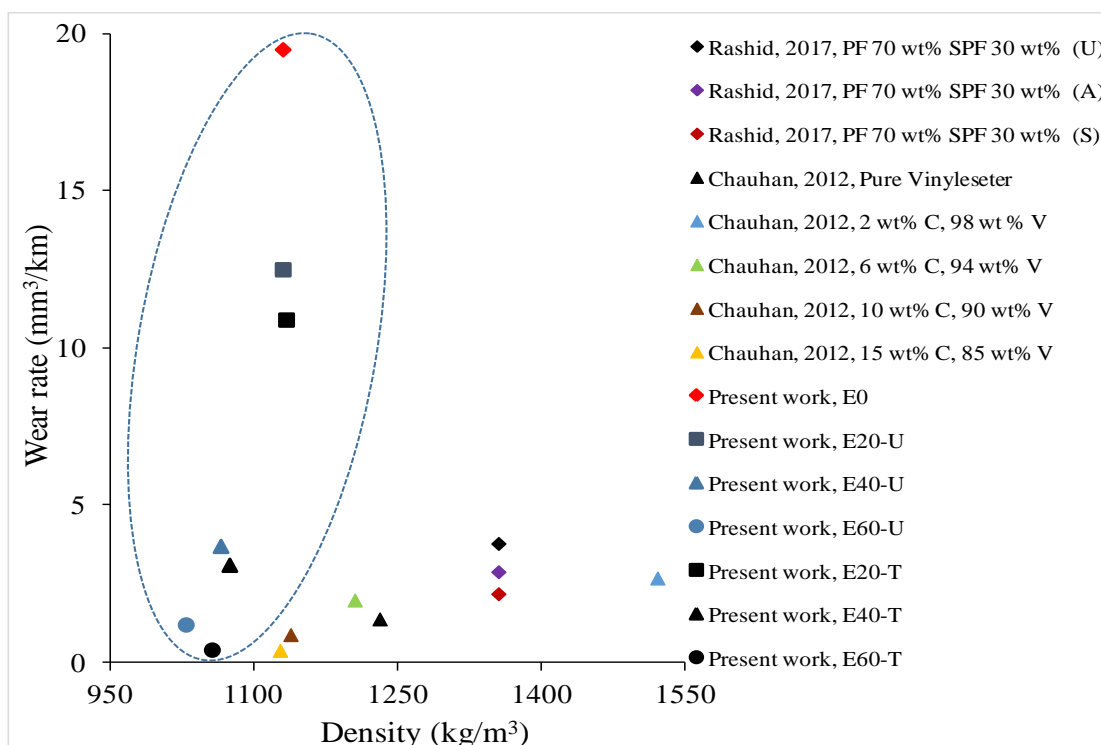
Figure 8.10 Wear rate plotted against density from available studies (Chauhan and Thakur 2013, Rashid et al. 2017).

Note: PF – Phenolic resin, SPF – Sugar Palm Fiber, U – Untreated, A – Alkali treated, S – Seawater treated, C - Cenosphere, V - Vinylester.

Conclusions

Dry sliding wear of cenosphere/epoxy syntactic foams is investigated for varying velocity, applied load and sliding distance. Effect of filler loading and surface treatment as a function of wear test parameters are presented in this work. Following conclusions are drawn:

- Maximum wear takes place for neat epoxy samples. Wear rate decreases with increasing filler content of cenospheres for EXX-U and EXX-T foams.

- Compared to neat epoxy, wear resistance of EXX-U and EXX-T foams increases in the range of 8-94% and 21-98% respectively.

- Silane treatment of cenospheres has increased the wear resistance of EXX-T foams and is in the range of 2-92% as compared to EXX-U foams. E60-T foams exhibit highest dry sliding wear resistance among all the samples.

122

- Specific wear rate of syntactic foams decreases significantly at higher applied loads. EXX-T foams are best suited for wear environments owing to good bonding between the constituents.

- Coefficient of friction decreases with increase in cenosphere content and sliding distance. Wear debris of neat epoxy samples is larger in size as compared to EXX-U and EXX-T foams.

- Micrographs of worn out surface reveal that for lower operating conditions, w_t is higher due to initiation of fine grooves along the sliding direction. As cenosphere content increases, w_t decreases.

- Abrasive mode of wear mechanism is observed in V_2F_{30}. At higher operating conditions, w_t decreases with increase in filler loading. Higher frictional heat in formation of thin films and better compaction of wear debris within the cenospheres contribute in reducing the wear for E60-T foams.

- Transition from abrasive to adhesive mode of wear mechanism is observed for V_5F_{50} for all the samples under investigation.

- Property map reveal cenosphere/epoxy syntactic foams exhibit lowest wear rates at higher cenosphere contents as compared to other composites signifying their suitability in weight sensitive applications subjected to dry sliding wear scenario.

9   SOLID PARTICLE EROSION BEHAVIOR

9.1   Particle size analysis of erodent

The shape of the erodent SiC particles is irregular (Figure 9.1a). The angularity in the SiC particles may assist in fracturing the thin walled hollow cenospheres, particularly at lower impact angles. Figure 9.1b shows size analysis of SiC particles. Weighted mean particle size is observed to be 249.1 μm.

(a)   (b)
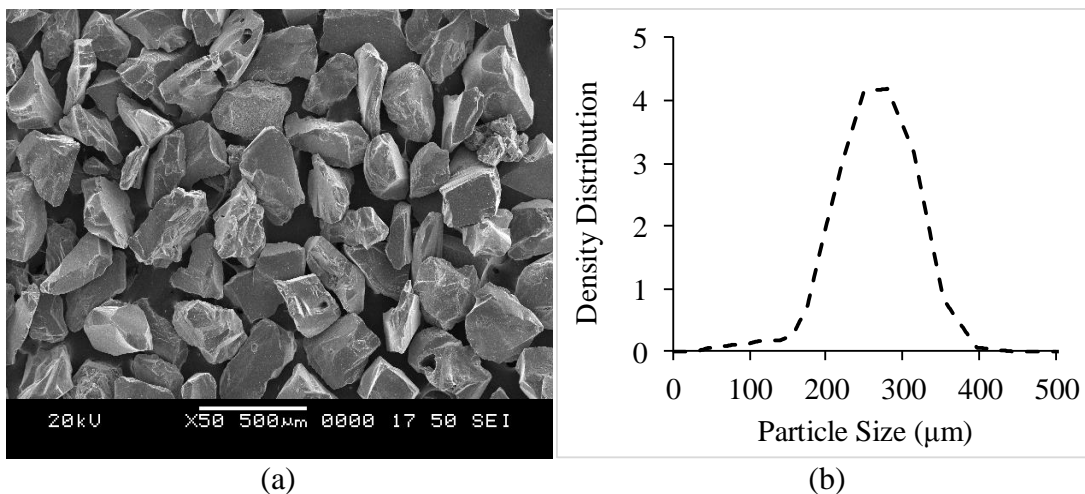
Figure 9.1 (a) Micrograph of SiC erodent particles before test and (b) particle size analysis of erodent particles.

9.2   Steady state erosion

Steady state of erosion needs to be attained to understand type and erosion mechanism. Table 9.1 presents the total mass of the erodent particles experimentally estimated to attain steady state erosion for all the materials at different velocities and impingement angles. For brevity, the standard deviations are not presented in the table but all the standard deviation values are within ±5% range.

Table 9.1 Erodent mass (g) for steady state erosion rate.

Material	$v = 30$ m/s				$v = 45$ m/s				$v = 60$ m/s			
	30°	45°	60°	90°	30°	45°	60°	90°	30°	45°	60°	90°
E0	115	105	105	95	145	125	115	115	175	155	155	145
E20-U	95	95	95	85	125	115	115	105	155	135	125	125
E40-U	95	85	85	75	115	115	105	95	135	115	115	115
E60-U	85	85	85	75	105	95	85	85	125	105	105	105
E20-T	95	95	95	95	115	105	105	95	135	125	125	115
E40-T	85	85	85	85	105	105	95	85	125	115	115	105
E60-T	85	85	75	75	95	95	85	75	115	105	105	95

The erosion angle of the specimen surface is measured with respect to the direction of the particle impingement. The total particle mass required to attain steady state decreases with (a) increasing impingement angle (b) decreasing velocity (c) increasing filler content and (d) silane coating. In all the cases, neat epoxy specimens require greater erodent particle mass to attain steady state compared to syntactic foams. Erodent mass required to attain the steady state is in the range of 75-175 g for all material types and test conditions.

Figure 9.2 shows a representative set of erosion rate plots for all material types at lower (Figure 9.2a) and higher impact angles (Figure 9.2b) at intermediate velocity of 45 m/s. The first mass measurement is obtained after an initial testing period of 5 minutes, corresponding to 25 g of erodent. Cumulative erodent particle mass is observed to decrease drastically as the test progresses for the next 2 minutes. Repeated impact of erodent particles breaks the hard cenosphere particles in the matrix resulting in debris. The particle fracture is among the main energy absorption mechanisms; therefore, all syntactic foams offer higher erosion resistance than the neat epoxy. With higher impact angles, erodent impingement is confined to smaller and more focused area resulting in attaining steady state much earlier (Figure 9.2b) as compared to lower impact angles (Figure 9.2a).
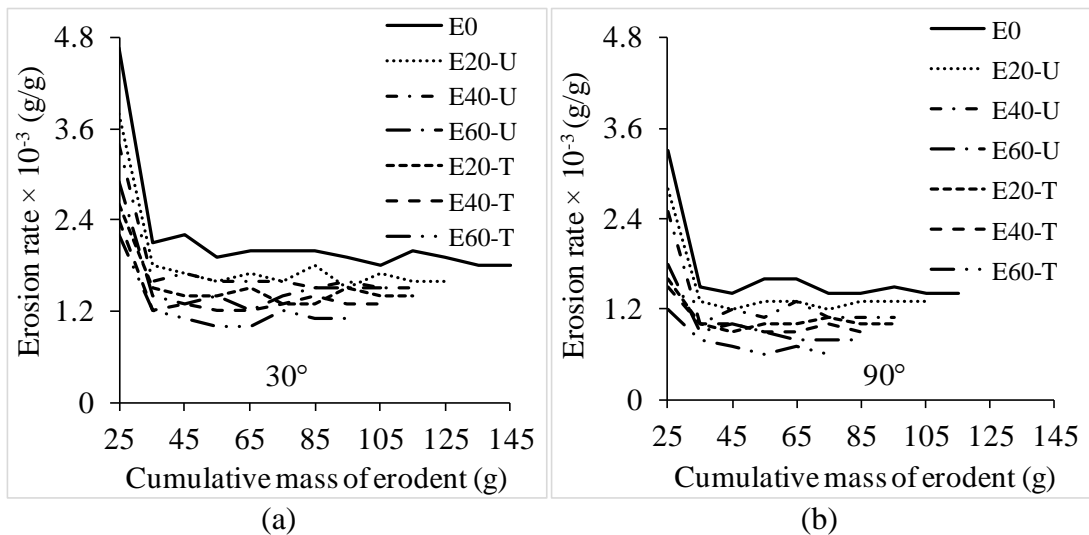
Figure 9.2 Steady state erosion rate of all samples at $v = 45$ m/s for (a) 30° and (b) 90° impingement angles.

125

Figure 9.3 schematically represents erosion mechanism in syntactic foams. Removal of erodent particles occurs easily over the surface at low angles 30° (Figure 9.3a). Erodent particles impacting at lower angles impart sliding action on the specimen surface leading to easy removal of debris and higher erosion rate. Further, erodent particles are in contact with target surface for longer time resulting in higher material removal rate. Retention time of erodent on the sample surface decreases with increasing impingement angle (Figure 9.3b-d) leading to lower erosion rates. Erosion rate decreases further at 90° (Figure 9.3d) owing to higher energy absorbing capabilities in foams under compression(Shahapurkar et al. 2018). Neat epoxy specimens tend to exhibit higher erosion rates as compared to syntactic foams due to absence of cenospheres, which are made of ceramics and resist erosion better than the matrix resin.
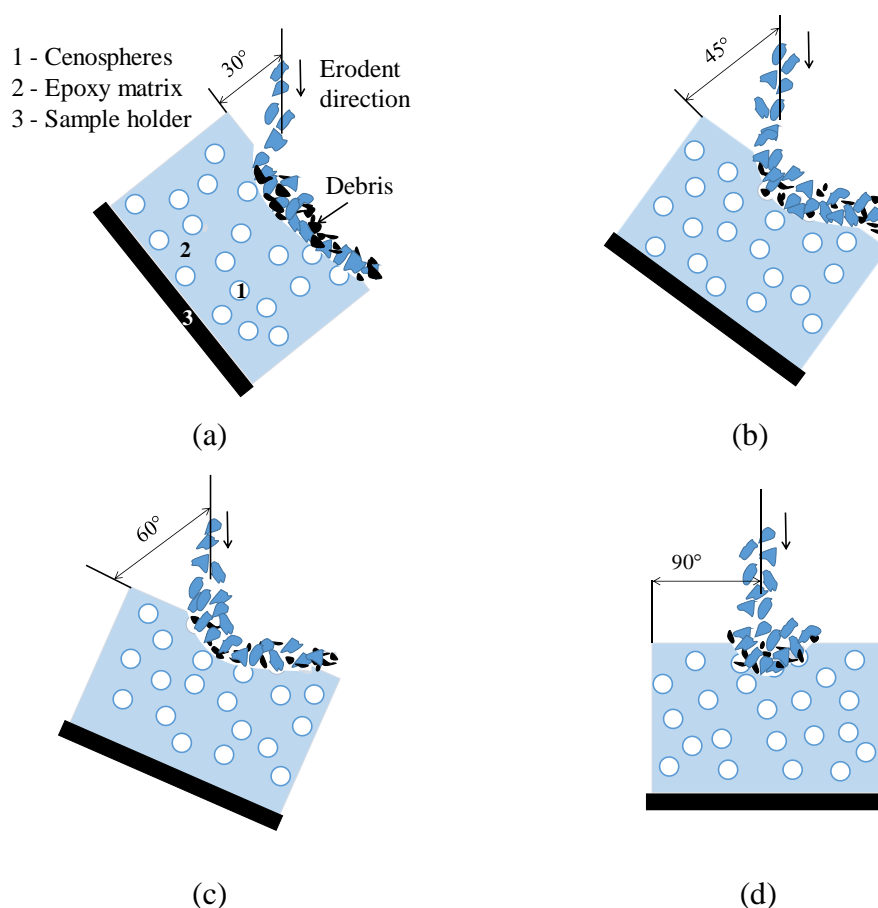
Figure 9.3 Representative erosion mechanism in syntactic foams for (a) 30° (b) 45° (c) 60° and (d) 90° impingement angles.

9.3 Influence of impingement angle on erosion

Erosion behavior strongly depends upon the experimental conditions and composition of target material (Hutchings 1992). Erosion rate of all the materials for different impingement angles are presented in Figure 9.4. It is observed that the maximum erosion occurs at 30° for neat epoxy and decreases further with increasing impingement angle (Bagci and Imrek 2011, 2013, Miyazaki and Takeda 1993, Patnaik et al. 2010).

Erosion rate recorded at 90° is at a relatively lower level as compared to that at 30° (Table 9.1). Impacting force resolves into normal and tangential components (Goretta et al. 2004), which results in larger erosion area at low angles with deeper erosion pit at higher angles. With increase in angle of impact, the reduction in the tangential force reduces erosion rate. In all cases, syntactic foams have lower erosion rate than the neat resin because of the presence of ceramic cenospheres.

9.4 Influence of filler content on erosion

Erosion resistance of syntactic foams containing untreated and silane treated cenospheres is higher by 12-42% and 22-60%, respectively, compared to neat epoxy. Presence of ceramic particles increases the erosion resistance of syntactic foams compared to matrix resin. Silane treatment increases the particle-matrix interfacial strength in syntactic foams, which increases their erosion resistance by 7-38% compared to syntactic foams containing untreated cenospheres.

In the absence of strong interfacial bonding, cenospheres can be dislodged easily by the impinging erodent particles. In comparison, additional energy is required to break strongly bonded cenospheres and dislodge the debris from the matrix. Figure 9.5 presents micrographs of representative specimens after erosion test at lower (20 vol.%) and higher (60 vol.%) filler contents for foams containing surface treated cenospheres. Extensive erosion damage to the matrix is evident in the specimen containing higher volume fraction of matrix (Figure 9.5a).
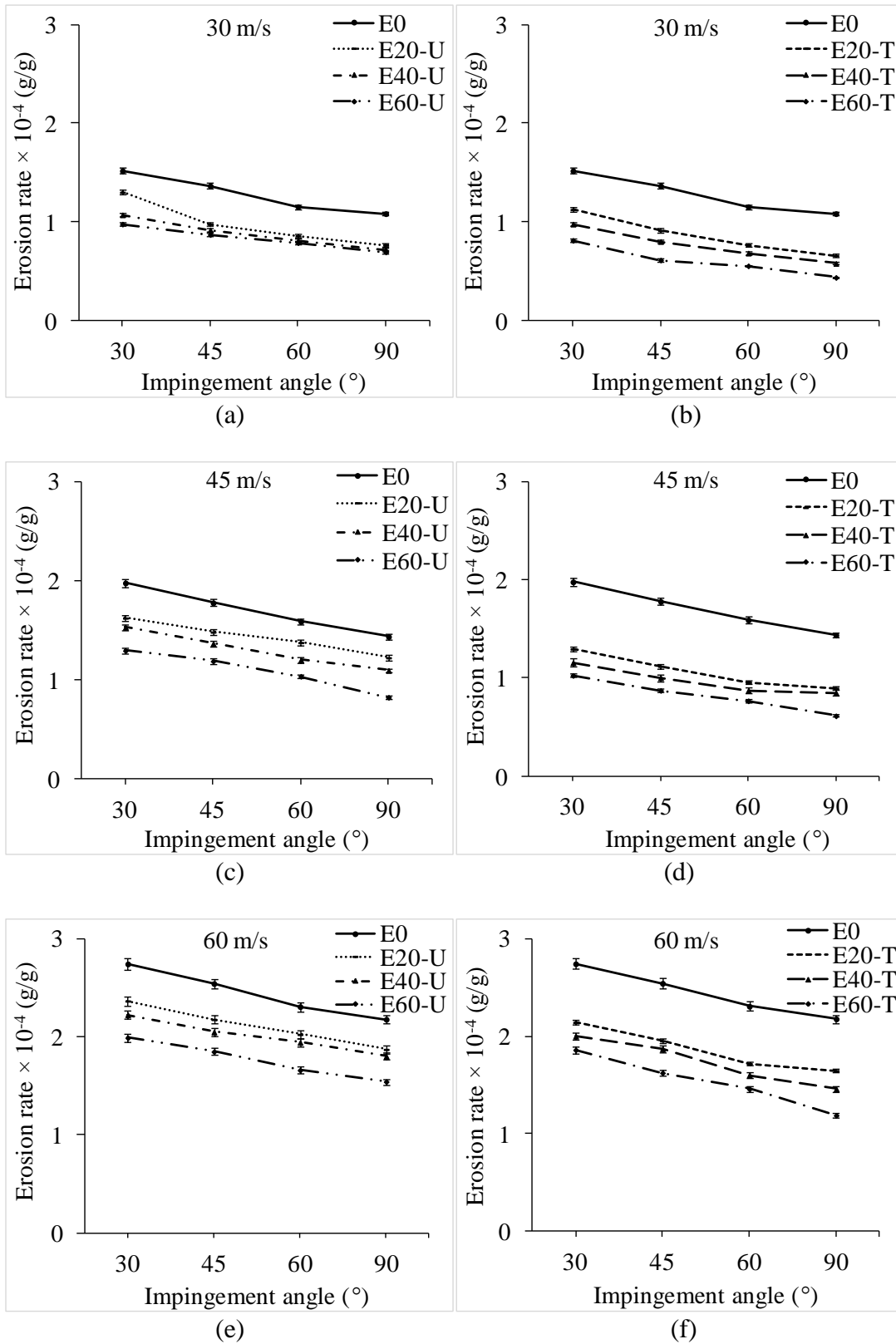
Figure 9.4 Erosion rate of all samples at different velocities and impingement angles.

<center>(a)   (b)</center>
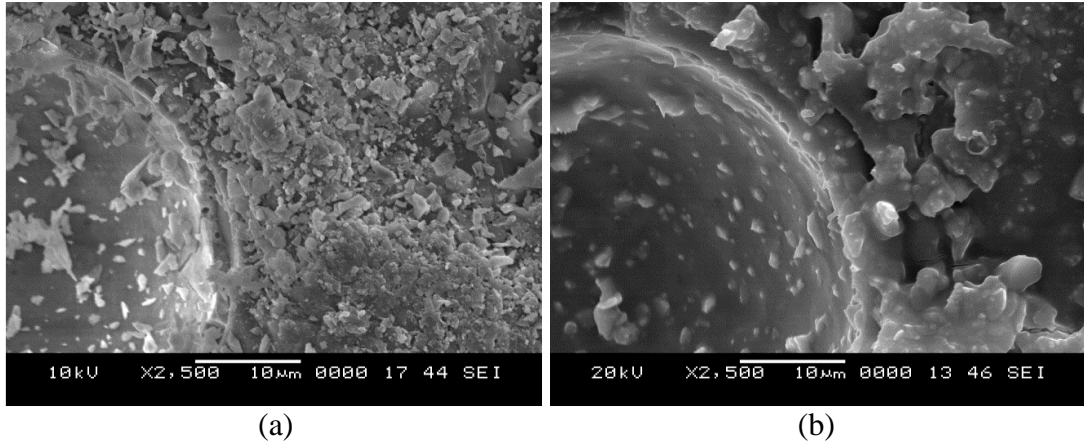
Figure 9.5 Micrographs of representative (a) E20-T and (b) E60-T syntactic foams.

9.1 Velocity exponent and erosion efficiency

Velocity of the erodent particles influences material removal from the target surface as observed in Figure 9.6a for lower and in Figure 9.6b for higher impingement angles. Increase in erodent velocity increases the erodent flow per unit time impacting on the specimens, which in turn increases erosion. Erosion rate is observed to be up to 1.5 times higher as the velocity increases. Erosion rate (E_r) of polymer composites is characterized by velocity exponent 'k', and is given by (Pool et al. 1986),

$$E_r \propto v^k \tag{9.1}$$

where v is impact velocity expressed in m/s. Equation 9.1 is used to estimate k for all the materials using E_r and v values presented in Table 9.1 and Table 2.4 respectively. Previous studies have established that materials are considered ductile or brittle based on the ranges $1 < k < 3$ or $3 < k < 5$, respectively (Goretta et al. 2004). In the present study, k values are in the range of 2.06-2.95, 2.03-2.81 and 2.0-2.68 for neat epoxy, EXX-U and EXX-T, respectively, which indicates ductile behavior.

Erosion efficiency (ε) is also a parameter used for identifying brittle and ductile erosion response of materials subjected to solid particle erosion. The erosion efficiency (ε) is given by (Sundararajan et al. 1990),

$$\varepsilon = \frac{2E_r H}{\rho v^2} \tag{9.2}$$

<center>129</center>
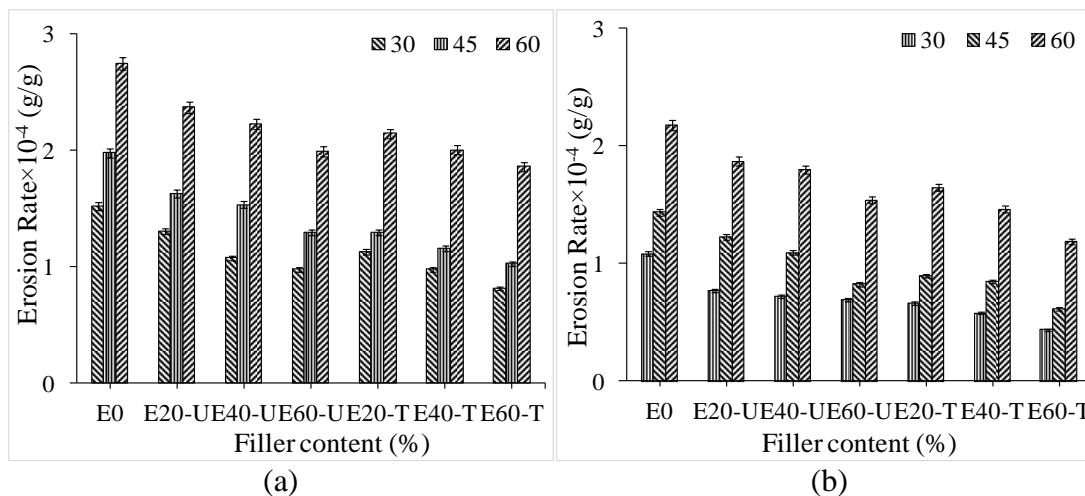
Figure 9.6 Erosion rate as a function of erodent velocity at (a) 30° and (b) 90° impingement angles.

Values of v, H, ρ and E_r are used from Table 2.4, Table 3.1 and Table 9.1, respectively. Shore hardness values are converted to Pascal and used in equation (9.2). Ductile materials possess very low erosion efficiencies (ε<10%) while for brittle materials its more than 100% (Sundararajan et al. 1990). For all the samples in the present case, ε varies in the range of 0.046-0.177% for different impact velocities and impingement angles implying ductile erosive behavior. Higher erosion efficiency represents lower erosion resistance. Erosion efficiency of neat epoxy, EXX-U and EXX-T vary between 0.063-0.177, 0.060-0.171 and 0.046-0.138%, respectively. From these observations it is clear that surface treated syntactic foams are suitable in erosive environment.

9.2   Surface morphology of eroded surfaces

Figure 9.7 presents erosion surface profiles of a representative set of specimens of all the material types. An elliptical shape of the damage zone is observed at 30°, whereas a circular shape is observed at 90°, which is consistent with the mechanism shown in Figure 9.3. It is observed in Figure 9.7 that, the use of surface treated cenospheres in the highest volume fraction provides the smallest erosion profile on the material surface, indicating the benefit of cenosphere surface treatment under erosion conditions.
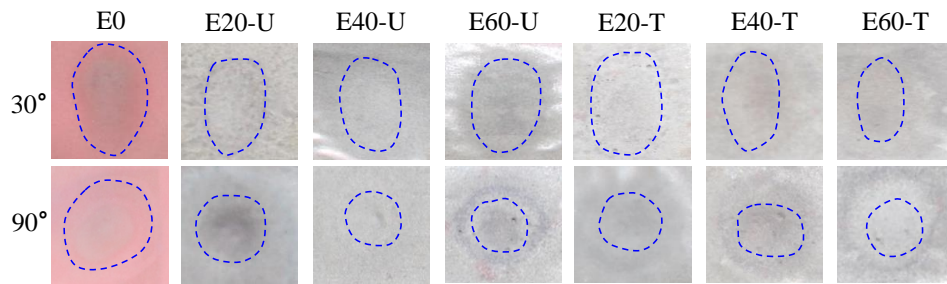
Figure 9.7 Erosion scars in representative samples.

Further observations of erosion profiles in 3-dimensions (3D) are presented in Figure 9.8. It is observed that at 30° the eroded area is comparatively larger than that observed at normal angle of impact. At lower impact angles, the erodent particle removal from the surface is easier because of tangential velocity component of the material. In comparison, the normal impact results in erodent particles impinging on the existing erodent particles, which results in slow expansion of the erosion zone. Syntactic foams have lower erosion damage zone compared to the neat resin.

Micrographs of the representative samples eroded at 30 and 90° for an erodent velocity of 60 m/s are presented in Figure 9.9. Removal of matrix material from the surface of neat epoxy sample due to the impact of erodent particles is clearly visible in Figure 9.9a and Figure 9.9b. At 30°, matrix eroded in the form of small chunks as seen from Figure 9.9a due to glazing effect. Debris is seen to be spread all over the surface. At 90° compressive stresses developed due to repeated impact of erodent on relatively smaller area reduces debris (Figure 9.9b).

The observations from micrographs reveal that the decrease in erosion rate with increase in angle of impact can be attributed to the change in material removal mechanism. Lower angle of impact induces swift material removal, whereas higher angle of impacts induce restricted material removal (Mohan et al. 2012). Figure 9.9c and Figure 9.9d show the micrographs of E20-U syntactic foams. At 30°, broken cenosphere particle with noticeable amount of debris is visible (Figure 9.9c). These cenosphere particles help in reducing erosion by absorbing the impact of erodent particles as the test progresses.

131
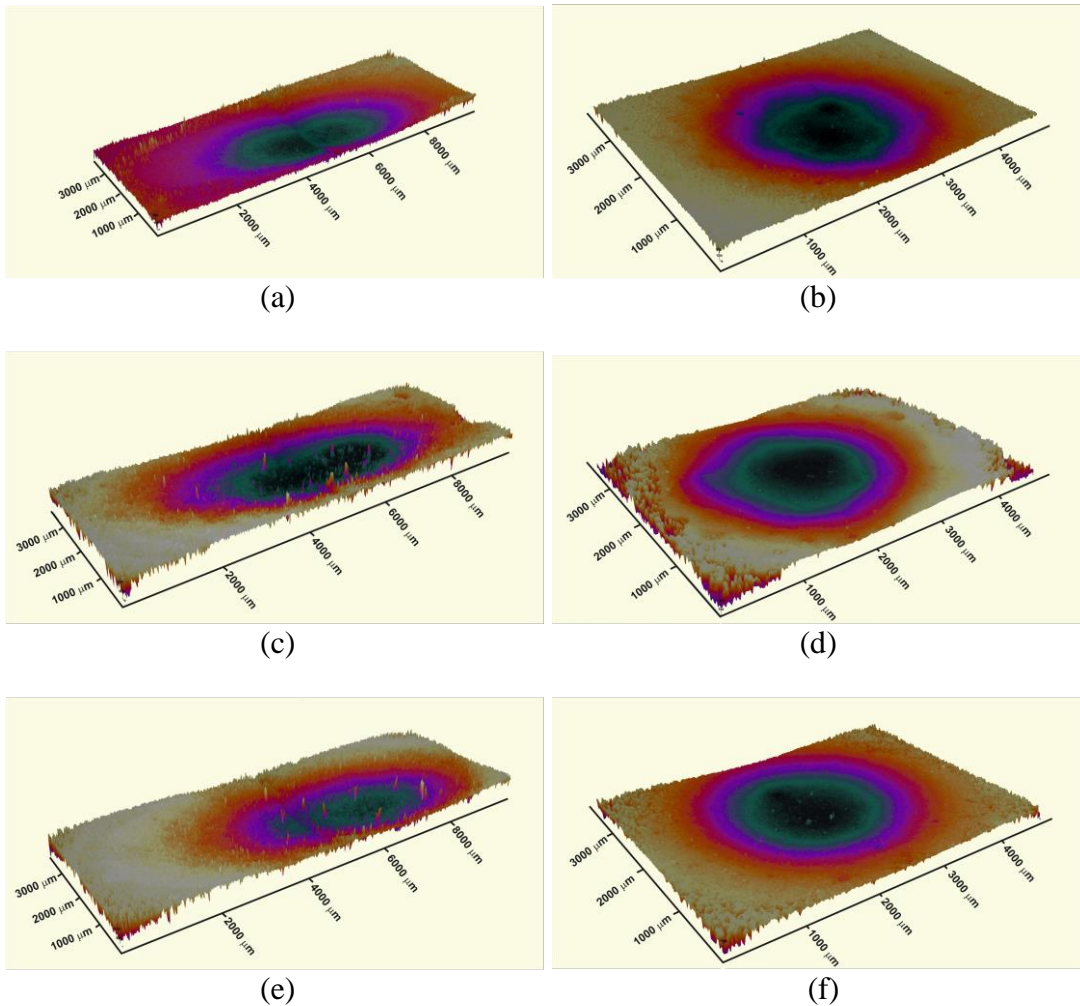
Figure 9.8 Eroded profile of syntactic foams at 60 m/s for Neat epoxy (a) 30° and (b) 90°; E20-U at (c) 30° and (d) 90° and E20-T at (e) 30° and (f) 90°.

At 90°, it is seen that a broken cenosphere particle at erosion site is filled with debris (Figure 9.9d). Closer observation reveals that the cenosphere particle has absorbed the erodent energy and resisted erosion. Figure 9.9e and Figure 9.9f shows the micrographs of E20-T syntactic foam. Similar observations are noted as untreated configuration in E20-T for both the impact angles. Cenosphere particles are seen to broken with half of the shell still in the matrix (Figure 9.9e and Figure 9.9f). More resistance offered by treated syntactic foams to erosion can be solely attributed to the strong bonding exhibited between the constituents making them suitable potential candidate materials in erosive environments.

(a)   (b)

(c)   (d)

(e)   (f)
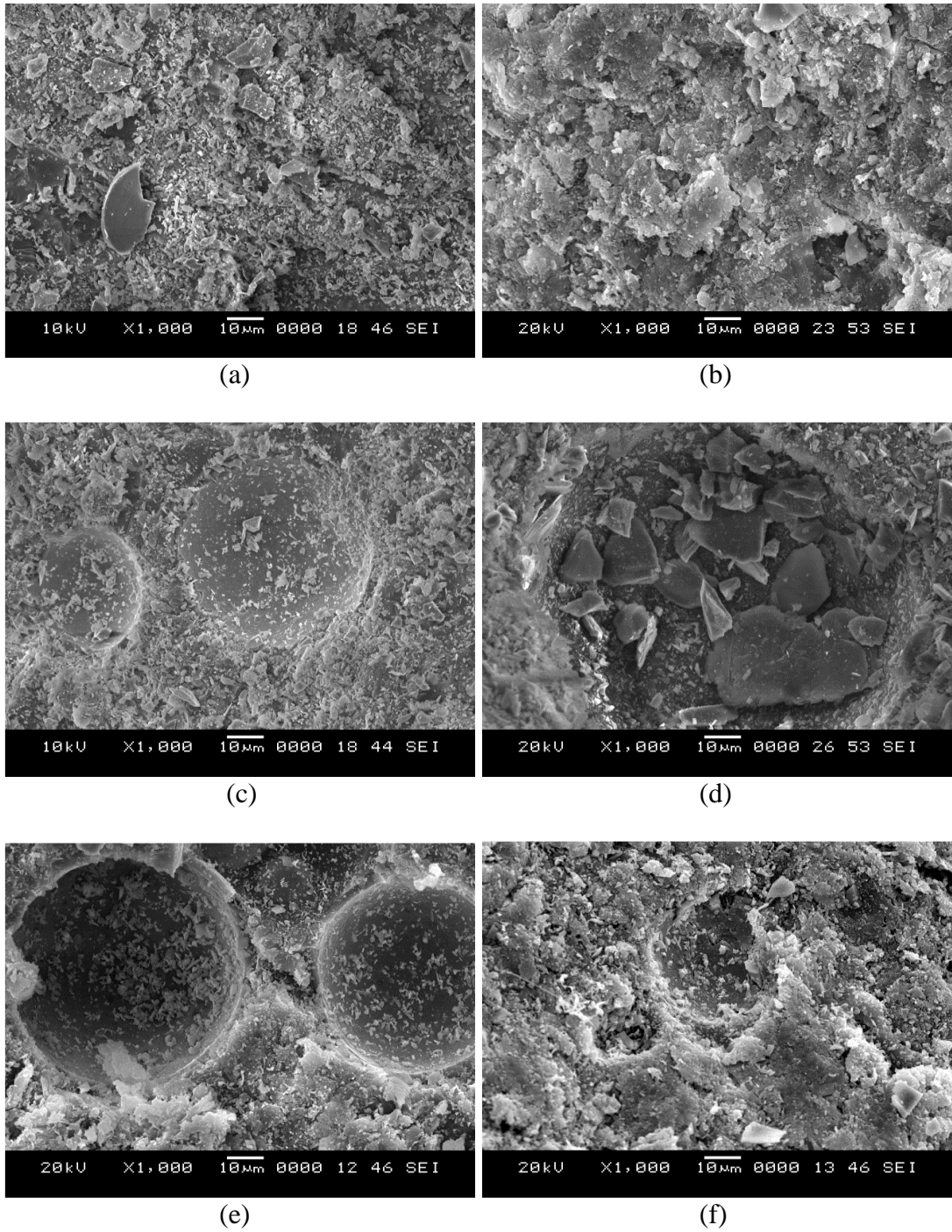
Figure 9.9 Micrographs of samples eroded at 60 m/s for Neat epoxy at (a) 30° and (b) 90°; E20-U at (c) 30° and (d) 90°; E20-T at (e) 30° and (f) 90°.

133

9.3 Property map

Erosion values obtained for 30 and 90° are plotted with respect to density for composites containing different reinforcements in Figure 9.10a and Figure 9.10b, respectively (Biswas and Satapathy 2010, Dalbehera and Acharya 2016, Hemalata et al. 2016, Srivastava and Pawar 2006). Results obtained in the present study and the data extracted from the published literature are plotted with respect to density for comparative analysis.

It can be observed from these figures that composites with higher density exhibit higher erosion rates. However, the advantage of hollow cenospheres filled syntactic foams is evident from Figure 9.10. Except for bamboo-epoxy/cenosphere composites, density of syntactic foams in the present study is lower than other composites. Syntactic foams outperform red mud, fly ash and cenosphere reinforced glass fiber composites whereas results are comparable to bamboo-epoxy/cenosphere composites for both the erodent impingement angles.

Erosion rates are lower at higher impact angles for all the composites as seen from Figure 9.10b. Therefore, from the property map it can be concluded that cenosphere/epoxy syntactic foams provide lower erosion rates at much lower density as compared to fiber reinforced composites signifying their suitability in weight sensitive applications. These foams can be utilized in a number of applications demanding light weightness with comparable erosion rates to thermosetting composites.

Conclusions

Solid particle erosion of cenosphere/epoxy syntactic foams is studied for variables such as impingement angle and velocity, and cenosphere content. Following conclusions are drawn:

- Lower impingement angles lead to higher erosion rate due to easy removal of material from the surface and continuous exposure of fresh surface of the specimen. The observations of erosion rate are supported by surface and volume

profiles of the erosion area, where lower angles show larger damage zone.

- Compared to neat epoxy, erosion resistance of syntactic foams is higher due to the presence of ceramic reinforcement. It is also noted that the surface treatment of cenospheres improves particle-matrix interfacial bonding and reduces erosion rate.

- Maximum erosion takes place at 30° for all the samples and decreases further with increasing impingement angle.

- Compared to neat epoxy, erosion resistance of EXX-U and EXX-T foams increases in the range of 12-42% and 22-60% respectively.

- Silane treatment of cenospheres has increased the erosion resistance of EXX-T foams and is in the range of 7-38% as compared to EXX-U foams. E60-T foams exhibit highest erosion resistance among all the samples.

- The velocity exponent and erosion efficiency confirm the ductile behavior of syntactic foams.

- 3D profiles reveal the extent of erosion for all the samples under the study. EXX-T foams reveal lowest material removal due to strong interfacial bonding between the constituents.

- From micrographs, it is observed that the overall erosion of syntactic foams consists of matrix material removal, cenosphere breakage and formation of cavities due to impact velocity. However, the presence of cenospheres restricts the erosion and the removal of matrix material, which in turn enhances the resistance of syntactic foams.

- Property maps reveal cenosphere/epoxy syntactic foams exhibit lower erosion rates as compared to fiber reinforced composites signifying their suitability in weight sensitive applications.
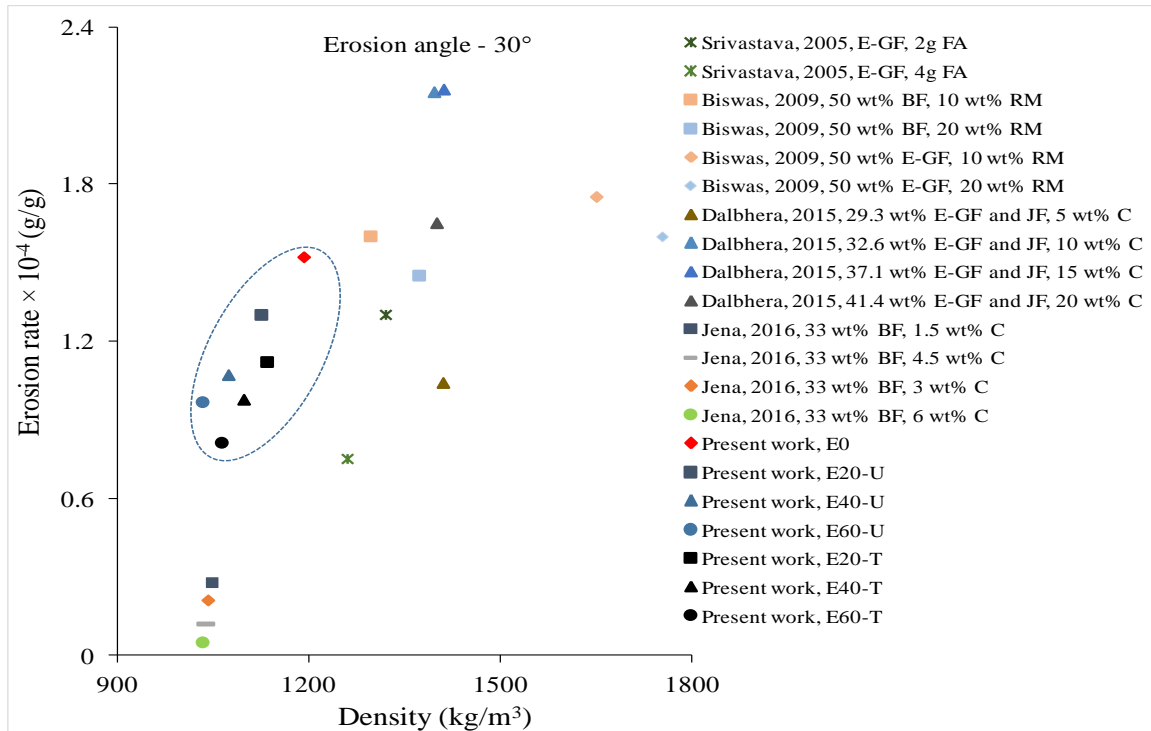
(a)
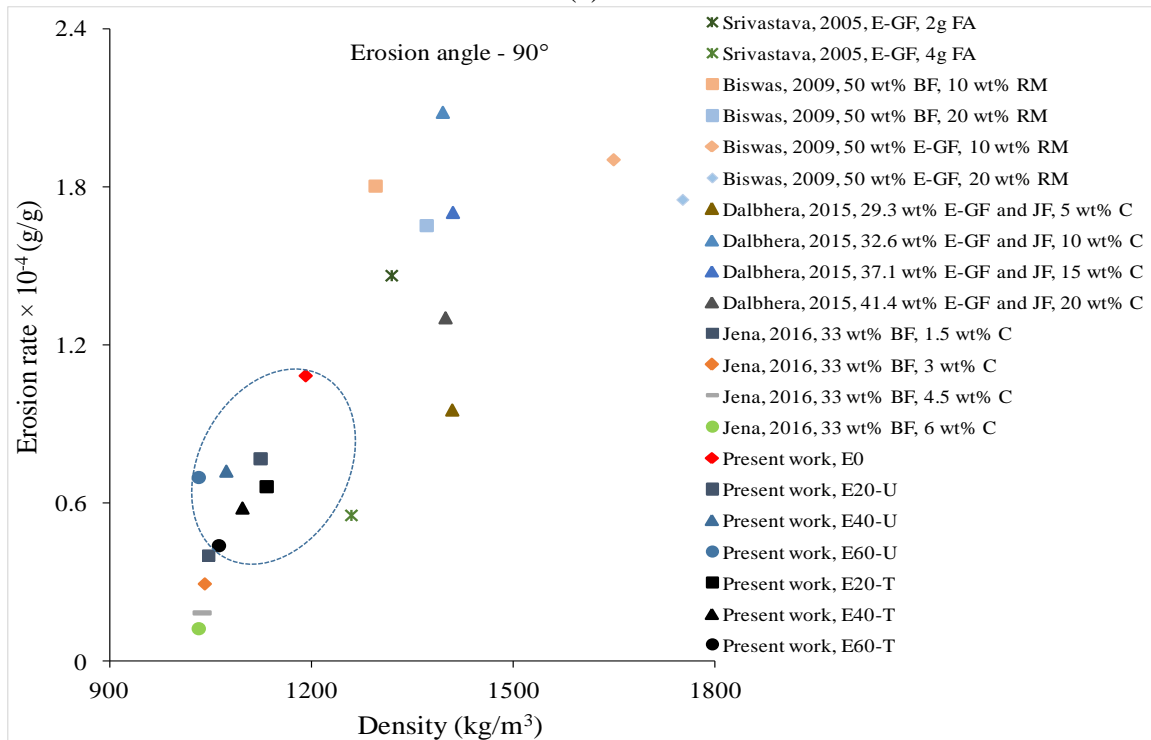
(b)

Figure 9.10 Erosion rate at (a) 30° and (b) 90° plotted against density from available studies (Biswas and Satapathy 2010, Dalbehera and Acharya 2016, Hemalata et al. 2016, Srivastava and Pawar 2006). Note: FA – Fly ash, RM – Red mud, C – Cenosphere, E-GF – E-Glass fiber, BF – Bamboo fiber, JF – Jute fiber.

136

SUMMARY AND CONCLUSIONS

Summary

A comprehensive investigation is conducted to prepare and characterize fly ash cenosphere/epoxy syntactic foams. Use of cenospheres in structural applications can reduce the landfill burden and help in effectively addressing the environmental concern of fly ash disposal. In the present study, manual stir casting method is used to develop the cenosphere/epoxy syntactic foam specimens and are characterized for mechanical and tribological properties. Syntactic foams are fabricated with 20, 40 and 60 vol.% of cenospheres in epoxy matrix. The effect of filler volume fraction and surface treatment of cenospheres are investigated.

Experiments are conducted for the properties of cenospheres/epoxy syntactic foams and evaluate the effectiveness of reinforcing cenospheres in epoxy matrix. Cenosphere/epoxy foams are characterized for temperature starting from -60°C to 175°C to study the behavior of samples at extreme conditions. Compressive and flexural characterization under room and arctic conditions are investigated. Further, compressive properties at quasi-static strain rate are dealt with. Tensile properties are also studied under room conditions.

Dynamic mechanical analysis is performed on the samples to analyse the behavior of samples at elevated temperatures. Finally, dry sliding wear and solid particle erosion of samples are studied to characterize these foams for their tribological response. Extensive scanning electron microscopy is performed to study the structure-property correlations and investigate the failure mechanisms.

Conclusions

The main conclusions are summarized as:

Density

- Reduction in the density of composites is observed as compared to the theoretical ones and is attributed to the air entrapment in matrix during the process of mechanical mixing of cenospheres in the resin.

- Syntactic foams with untreated cenospheres are noted to have better weight saving potential as compared to treated cenospheres. Silane coating on as received cenospheres increases the effective mean diameter, thereby increasing their density.

- The void content increases with increase in filler content except at highest filler loading.

Compressive behavior

- All the syntactic foam compositions show an increase in compressive modulus compared to that of the neat epoxy specimens.

- Significantly higher specific compressive moduli and marginally higher specific strength make treated cenosphere/epoxy (EXX-T) foams a viable material for marine applications and has potential for structural application at room temperatures.

- Arctic conditioning (-60°C) of foams to explore the feasibility of using them in arctic environment demonstrated lower failure strains compared to neat epoxy.

- Modulus decreased for arctic specimens compared to the unconditioned (dry) specimens. However, an overall increase in compressive strength is observed when tested under in-situ arctic condition. Conditioning of specimens under extreme low temperatures caused the material to reduce their compressive modulus.

Quasi-static compression

- Increase in the volume fraction of cenospheres increases modulus by upto 48% and 44% for untreated and silane treated syntactic foams respectively with respect to neat epoxy.

- Compared to neat epoxy, strength of untreated and treated syntactic foams decreases with increase in the volume fraction of cenospheres by 11-28% and 3-8% respectively.

- Energy absorption increases for all the syntactic foams. E60-T sample presents the highest energy absorption among all the samples.

Flexural behavior

- Slight increase in modulus is observed for arctic exposed samples as compared to samples at room temperature.

- An increase in flexural modulus is observed with syntactic foams at room and arctic temperature as compared to neat epoxy sample at room temperature, whereas flexural strength decreased.

- An increase in flexural modulus between 7-15% was observed for syntactic foams with untreated cenospheres under arctic conditions as compared to the ones tested at room temperature.

- Untreated and treated foams exhibit higher specific modulus as compared to neat samples for room temperature and arctic conditioned samples. Specific strength of arctic conditioned untreated and treated foams is significantly higher compared to room conditioned samples.

- Flexural strengths of arctic exposed untreated and treated syntactic foams increased in the range of 56-80 and 31-56% respectively as compared to those at room temperature accredited to matrix hardening due to exposure to arctic temperatures.

Tensile behavior

- All the syntactic foams fail at lower strains in tensile loading. Untreated and treated foams display an increase in modulus with increase in cenosphere content as compared to neat epoxy.

- Strength of untreated and treated syntactic foams is lower than neat epoxy.

- Surface modified syntactic foams show significant increase in modulus and comparable strength to neat epoxy making these foams viable for applications demanding better specific properties and weight savings.

Dynamic Mechanical Analysis

- Neat epoxy sample presents lowest storage modulus. Increase in cenosphere volume fraction results in increase of storage modulus for both untreated and treated cenosphere syntactic foams.

- Room temperature loss modulus value of neat epoxy is higher as compared with untreated and treated syntactic foams, except for treated sample at 60 vol.% of cenospheres.

- Glass transition of the neat epoxy is higher as compared to all the syntactic foams.

- Presence of cenospheres helps in increasing the retention of mechanical properties of syntactic foams at temperatures beyond glass transition temperature.

Dry sliding wear behavior

- Wear rate is maximum for neat epoxy samples whereas it decreases with increasing filler content of cenospheres for untreated and treated foams. Compared to neat epoxy, wear resistance of untreated and treated foams increases in the range of 8-94% and 21-98% respectively.

- Silane treated cenospheres has increased the wear resistance and is in the range of 2-92% as compared to untreated foams. E60-T foams exhibit highest dry sliding wear resistance among all the samples.

- Specific wear rate of syntactic foams decreases significantly at higher applied loads. Silane treated foams are best suited for wear environments owing to good bonding between the constituents.

- Coefficient of friction decreases with increase in cenosphere content and sliding distance. Wear debris of neat epoxy samples is larger in size as compared to syntactic foams.

- Abrasive mode of wear mechanism is observed at lower operating conditions. Whereas transition from abrasive to adhesive mode of wear mechanism is observed for higher operating conditions.

- Property map reveals cenosphere/epoxy syntactic foams exhibit lowest wear rates at higher cenosphere contents as compared to other composites signifying their suitability in weight sensitive applications subjected to dry sliding wear scenario.

Solid particle erosive response

- Lower impingement angles lead to higher erosion rate due to easy removal of material from the surface and continuous exposure of fresh surface of the specimen. The observations of erosion rate are supported by surface and volume profiles of the erosion area, where lower angles show larger damage zone.

- Compared to neat epoxy, erosion resistance of syntactic foams is higher due to the presence of ceramic reinforcement. It is also noted that the surface treatment of cenospheres improves particle-matrix interfacial bonding and reduces erosion rate.

- Silane treatment of cenospheres has increased the erosion resistance in the range of 7-38% as compared to EXX-U foams. E60-T foams exhibit highest erosion resistance among all the samples.

- The velocity exponent and erosion efficiency confirm the ductile behavior of syntactic foams.

- Property maps reveal cenosphere/epoxy syntactic foams exhibit lower erosion rates as compared to fiber reinforced composites signifying their suitability in weight sensitive applications.

Present work successfully demonstrates feasibility of manual stirring method for developing thermosetting syntactic foam composites based on fly ash cenospheres. Composites are eco-friendly, lightweight and more importantly provides 13% weight savings potential. Further, usage of fly ash cenospheres reduces landfill burden and environmental linked issues. Experiments are conducted to evaluate the effect of filler content and surface modification of cenospheres over a wide range of mechanical properties and temperature profiles. The experimental results presented as part of this work can be used by industry professionals for development of syntactic foams for specific applications. E60-T is the best choice based on the work presented here.

SCOPE OF FUTURE WORK

Present work demonstrates feasibility of manual stirring method in developing thermosetting syntactic foams. Geometrical imperfections and irregular wall thickness of fly ash cenospheres needs to be addressed for structure-property correlations. Further, considering the interaction between the hollow particles and epoxy matrix theoretical models can be adopted for comparing the experimental data. Further, most of the experiments are conducted at room temperature conditions. Studies on wear and erosion at elevated temperature profiles and sub-zero conditions can be worth investigating.

REFERENCES

Ahmadi, H, Liaghat, GH, Shokrieh, MM, Hadavinia, H, Ordys, A and Aboutorabi, A. (2015). "Quasi-static and dynamic compressive properties of ceramic microballoon filled syntactic foam." *Journal of Composite Materials,* 49(10), 1255-1266.

ASTM C272-01, *Standard Test Method for Water Absorption of Core Materials for Sandwich Constructions*, ASTM International PA, USA.

ASTM D638-14, *Standard Test Method for Tensile Properties of Plastics*, ASTM, International PA, USA.

ASTM D695-15, *Standard Test Method for Compressive Properties of Rigid Plastics*, ASTM International PA, USA.

ASTM D790-17, *Standard Test Methods for Flexural Properties of Unreinforced and Reinforced Plastics and Electrical Insulating Materials*, ASTM International PA, USA.

ASTM D792-13, *Standard Test Methods for Density and Specific Gravity (Relative Density) of Plastics by Displacement*, ASTM International PA, USA.

ASTM D5229-15, *Standard Test Method for Moisture Absorption Properties and Equilibrium Conditioning of Polymer Matrix Composite Materials*, ASTM International PA, USA.

ASTM G76-13, *Standard Test Method for Conducting Erosion Tests by Solid Particle Impingement Using Gas Jets*, ASTM International PA, USA.

ASTM G99-05, *Standard Test Method for Wear Testing with a Pin-on-Disk Apparatus*, ASTM International PA, USA.

Atikler, U., D., Basalp and F., Tihminlioğlu. (2006). "Mechanical and morphological properties of recycled high- density polyethylene, filled with calcium carbonate and fly ash." *Journal of Applied Polymer Science,* 102(5), 4460-4467.

143

Aureli, M., Porfiri, M. and Gupta, N. (2010). "Effect of polydispersivity and porosity on the elastic properties of hollow particle filled composites." *Mechanics of Materials,* 42(7), 726-739.

Bagci, Mehmet and Imrek, Huseyin. (2011). "Solid particle erosion behaviour of glass fibre reinforced boric acid filled epoxy resin composites." *Tribology International,* 44(12), 1704-1710.

Bagci, Mehmet and Imrek, Huseyin. (2013). "Application of Taguchi method on optimization of testing parameters for erosion of glass fiber reinforced epoxy composite materials." *Materials & Design,* 46, 706-712.

Bajaj, P., K., Jha N. and Ananda, Kumar R. (1992). "Effect of coupling agents on the mechanical properties of mica/epoxy and glass fiber/mica/epoxy composites." *Journal of Applied Polymer Science,* 44(11), 1921-1930.

Balch, Dorian K. and Dunand, David C. (2006). "Load partitioning in aluminum syntactic foams containing ceramic microspheres." *Acta Materialia,* 54(6), 1501-1511.

Bardella, Lorenzo. (2001). "A phenomenological constitutive law for the nonlinear viscoelastic behaviour of epoxy resins in the glassy state." *European Journal of Mechanics - A/Solids,* 20(6), 907-924.

Bardella, Lorenzo and Genna, Francesco. (2001). "On the elastic behavior of syntactic foams." *International Journal of Solids and Structures,* 38(40), 7235-7260.

Barpanda, P and Kulkarni, SM. (2009). "Sliding wear behavior of an epoxy system reinforced with particulate fly ash filler." *Advanced Composites Letters,* 18(6), 199-205.

Bharath Kumar, B. R., Doddamani, Mrityunjay, Zeltmann, StevenE, Gupta, Nikhil, Uzma, Gurupadu, S. and Sailaja, R. R. N. (2016). "Effect of particle surface treatment and blending method on flexural properties of injection-molded cenosphere/HDPE syntactic foams." *Journal of Materials Science*, 1-13.

144

Bharath Kumar, B. R., Singh, Ashish Kumar, Doddamani, Mrityunjay, Luong, Dung D. and Gupta, Nikhil. (2016). "Quasi-Static and High Strain Rate Compressive Response of Injection-Molded Cenosphere/HDPE Syntactic Foam." *JOM,* 68(7), 1861-1871.

Bharath Kumar, B. R., Zeltmann, Steven Eric, Doddamani, Mrityunjay, Gupta, Nikhil, Uzma, Gurupadu, S. and Sailaja, R. R. N. (2016). "Effect of cenosphere surface treatment and blending method on the tensile properties of thermoplastic matrix syntactic foams." *Journal of Applied Polymer Science*, 43881.

Biswas, Sandhyarani and Satapathy, Alok. (2010). "A comparative study on erosion characteristics of red mud filled bamboo–epoxy and glass–epoxy composites." *Materials & Design,* 31(4), 1752-1767.

Boyce, Mary C., Parks, David M. and Argon, Ali S. (1988). "Large inelastic deformation of glassy polymers. part I: rate dependent constitutive model." *Mechanics of Materials,* 7(1), 15-33.

Capela, Carlos, Ferreira, Jose A. Martins and Costa, Jose Domingos M. (2010). "Viscoelastic Properties Assessment of Syntactic Foams by Dynamic Mechanical Analysis." *Materials Science Forum,* 636-637, 280-286.

Chand, Navin, Sharma, Prabhat and Fahim, M. (2011). "Abrasive Wear Behavior of LDPE Filled with Silane Treated Flyash Cenospheres." *Composite Interfaces,* 18(7), 575-586.

Chauhan, S. R. and Thakur, Sunil. (2013). "Effects of particle size, particle loading and sliding distance on the friction and wear properties of cenosphere particulate filled vinylester composites." *Materials & Design,* 51, 398-408.

Dalbehera, Soma and Acharya, S. K. (2015). "Effect of Cenosphere Addition on Erosive Wear Behaviour of Jute-glass Reinforced Composite Using Taguchi Experimental Design." *Materials Today: Proceedings,* 2(4), 2389-2398.

Dalbehera, Soma and Acharya, S. K. (2016). "Impact of Cenosphere on the Erosion Wear Response of Woven Hybrid Jute–Glass Epoxy Composites." *Advances in Polymer Technology,* 37(1), 240-246.

Das, Arijit and Satapathy, Bhabani K. (2011). "Structural, thermal, mechanical and dynamic mechanical properties of cenosphere filled polypropylene composites." *Materials & Design,* 32(3), 1477-1484.

Dimchev, Momchil, Caeti, Ryan and Gupta, Nikhil. (2010). "Effect of carbon nanofibers on tensile and compressive characteristics of hollow particle filled composites." *Materials & Design,* 31(3), 1332-1337.

Doddamani, M., Parande, G., Manakari, V., Siddhalingeshwar, I., Gaitonde, V. and Gupta, N. (2017). "Wear Response of Walnut-Shell-Reinforced Epoxy Composites." *Materials Performance and Characterization,* 6(1), 55-79.

Doddamani, Mrityunjay, Kishore, Shunmugasamy, Vasanth Chakravarthy, Gupta, Nikhil and Vijayakumar, H. B. (2015). "Compressive and flexural properties of functionally graded fly ash cenosphere–epoxy resin syntactic foams." *Polymer Composites,* 36(4), 685-693.

Dutta, P. K. (1994). "Low-Temperature Compressive Strength of Glass-Fiber-Reinforced Polymer Composites." *Journal of Offshore Mechanics and Arctic Engineering,* 116(3), 167-172.

Dutta, Piyush K. (1988). "Structural Fiber Composite Materials for Cold Regions." *Journal of Cold Regions Engineering,* 2(3), 124-134.

Dutta, Piyush K. and Hui, David. (1996). "Low-temperature and freeze-thaw durability of thick composites." *Composites Part B: Engineering,* 27(3), 371-379.

Farinha, J. P. S., Winnik, M. A. and Hahn, K. G. (2000). "Characterization of Oil Droplets under a Polymer Film by Laser Scanning Confocal Fluorescence Microscopy." *Langmuir,* 16(7), 3391-3400.

Feldman, D. (1993). "Handbook of polymeric foams and foam technology, by D. Klepner and K. C. Frisch (editors), hanser publishers, Munich, 442 pp. D. M. 228.00." *Journal of Polymer Science Part B: Polymer Physics,* 31(7), 899-899.

Ferreira, J. A. M., Capela, C. and Costa, J. D. (2010). "A study of the mechanical behaviour on fibre reinforced hollow microspheres hybrid composites." *Composites Part A: Applied Science and Manufacturing,* 41(3), 345-352.

Garcia, R, Castellanos, AG and Prabhakar, P. (2017). "Influence of Arctic seawater exposure on the flexural behavior of woven carbon/vinyl ester composites." *Journal of Sandwich Structures & Materials,* 0(0), 1-19.

Gaurav, Gupta and Alok, Satapathy. (2015). "Processing, characterization, and erosion wear characteristics of borosilicate glass microspheres filled epoxy composites." *Polymer Composites,* 36(9), 1685-1692.

Gauthier, M.M. (1995), *Engineered Materials Handbook, Desk Edition*. Taylor & Francis.

Ghazali, M. J., Rainforth, W. M. and Jones, H. (2005). "Dry sliding wear behaviour of some wrought, rapidly solidified powder metallurgy aluminium alloys." *Wear,* 259(1– 6), 490-500.

Gokhale, Amol, Kumar, N. V., Sudhakar, B., Sahu, Shiba, Basumatary, Himalay and Dhara, S. (2011). "Cellular Metals and Ceramics for Defence Applications." *Defence Science,* 61(6), 567-575.

Goretta, K. C., Chen, Nan, Gutierrez-Mora, F., Routbort, J. L., Lukey, G. C. and van Deventer, J. S. J. (2004). "Solid-particle erosion of a geopolymer containing fly ash and blast-furnace slag." *Wear,* 256(7), 714-719.

Gu, Jian, Wu, Gaohui and Zhang, Qiang. (2007). "Effect of porosity on the damping properties of modified epoxy composites filled with fly ash." *Scripta Materialia,* 57(6), 529-532.

Gu, Jian, Wu, Gaohui and Zhang, Qiang. (2007). "Preparation and damping properties of fly ash filled epoxy composites." *Materials Science and Engineering: A,* 452-453, 614-618.

Guhanathan, S., Saroja, Devi M. and V., Murugesan. (2001). "Effect of coupling agents on the mechanical properties of fly ash/polyester particulate composites." *Journal of Applied Polymer Science,* 82(7), 1755-1760.

Gupta, N., Kishore, Woldesenbet, E. and Sankaran, S. (2001). "Studies on compressive failure features in syntactic foam material." *Journal of Materials Science,* 36(18), 4485-4491.

Gupta, N., Woldesenbet, E. and Kishore. (2002). "Compressive fracture features of syntactic foams-microscopic examination." *Journal of Materials Science,* 37(15), 3199-3209.

Gupta, Nikhil. (2007). "A functionally graded syntactic foam material for high energy absorption under compression." *Materials Letters,* 61(4), 979-982.

Gupta, Nikhil, Gupta, Sandeep Kumar and Mueller, Benjamin J. (2008). "Analysis of a functionally graded particulate composite under flexural loading conditions." *Materials Science and Engineering: A,* 485(1), 439-447.

Gupta, Nikhil, Karthikeyan, C. S., Sankaran, S. and Kishore. (1999). "Correlation of Processing Methodology to the Physical and Mechanical Properties of Syntactic Foams With and Without Fibers." *Materials Characterization,* 43(4), 271-277.

Gupta, Nikhil and Nagorny, Ruslan. (2006). "Tensile properties of glass microballoon-epoxy resin syntactic foams." *Journal of Applied Polymer Science,* 102(2), 1254-1261.

Gupta, Nikhil, Pinisetty, Dinesh and Shunmugasamy, Vasanth Chakravarthy. (2013). Processing and Microstructure of Syntactic Foams *Reinforced Polymer Matrix Syntactic Foams: Effect of Nano and Micro-Scale Reinforcement* (pp. 19-24). Cham: Springer International Publishing.

Gupta, Nikhil, Priya, Shashank, Islam, Rashed and Ricci, William. (2006). "Characterization of Mechanical and Electrical Properties of Epoxy-Glass Microballoon Syntactic Composites." *Ferroelectrics,* 345(1), 1-12.

Gupta, Nikhil, Singh Brar, Balraj and Woldesenbet, Eyassu. (2001). "Effect of filler addition on the compressive and impact properties of glass fibre reinforced epoxy." *Bulletin of Materials Science,* 24(2), 219-223.

Gupta, Nikhil and Woldesenbet, Eyassu. (2003). "Hygrothermal studies on syntactic foams and compressive strength determination." *Composite Structures,* 61(4), 311-320.

Gupta, Nikhil and Woldesenbet, Eyassu. (2004). "Microballoon Wall Thickness Effects on Properties of Syntactic Foams." *Journal of Cellular Plastics,* 40(6), 461-480.

Gupta, Nikhil, Woldesenbet, Eyassu and Mensah, Patrick. (2004). "Compression properties of syntactic foams: effect of cenosphere radius ratio and specimen aspect ratio." *Composites Part A: Applied Science and Manufacturing,* 35(1), 103-111.

Gupta, Nikhil, Ye, Raymond and Porfiri, Maurizio. (2010). "Comparison of tensile and compressive characteristics of vinyl ester/glass microballoon syntactic foams." *Composites Part B: Engineering,* 41(3), 236-245.

Guru, K., Mishra, S. B. and Shukla, K. K. (2015). "Effect of temperature and functionalization on the interfacial properties of CNT reinforced nanocomposites." *Applied Surface Science,* 349, 59-65.

Harsha, A. P. and Jha, Sanjeev Kumar. (2008). "Erosive wear studies of epoxy-based composites at normal incidence." *Wear,* 265(7), 1129-1135.

Hartwig, G. (1979). Mechanical and Electrical Low Temperature Properties of High Polymers. In A. F. Clark, R. P. Reed & G. Hartwig (Eds.), *Nonmetallic Materials and Composites at Low Temperatures* (pp. 33-50). Boston, MA: Springer US.

Hemalata, Jena, Kumar, Pradhan Arun and Kumar, Pandit Mihir. (2016). "Study of Solid Particle Erosion Wear Behavior of Bamboo Fiber Reinforced Polymer Composite with Cenosphere Filler." *Advances in Polymer Technology,* 37(3), 761-769.

Hu, Guohe and Yu, Demei. (2011). "Tensile, thermal and dynamic mechanical properties of hollow polymer particle-filled epoxy syntactic foam." *Materials Science and Engineering: A,* 528(15), 5177-5183.

Huang, J. S. and Gibson, L. J. (1993). "Elastic moduli of a composite of hollow spheres in a matrix." *Journal of the Mechanics and Physics of Solids,* 41(1), 55-75.

Hull, D. and Clyne, T. W. (1996), *An Introduction to Composite Materials*, 2 edition. Cambridge University Press, Cambridge.

Hutchings, I. M. (1992). "Ductile-brittle transitions and wear maps for the erosion and abrasion of brittle materials." *Journal of Physics D: Applied Physics,* 25(1A), A212.

Imani, Abolhassan, Zhang, Hui, Owais, Mohammad, Zhao, Jun, Chu, Pengfei, Yang, Jinglei and Zhang, Zhong. (2018). "Wear and friction of epoxy based nanocomposites with silica nanoparticles and wax-containing microcapsules." *Composites Part A: Applied Science and Manufacturing,* 107, 607-615.

Jayavardhan, M. L. and Doddamani, Mrityunjay. (2018). "Quasi-static compressive response of compression molded glass microballoon/HDPE syntactic foam." *Composites Part B: Engineering,* 149, 165-177.

Jena, Hemalata, Pandit, Mihir Kumar and Pradhan, Arun Kumar. (2013). "Effect of cenosphere on mechanical properties of bamboo–epoxy composites." *Journal of Reinforced Plastics and Composites,* 32(11), 794-801.

Jena, Hemalata, Pradhan, Arun Kumar and Pandit, Mihir Kumar. (2016). "Study of Solid Particle Erosion Wear Behavior of Bamboo Fiber Reinforced Polymer Composite with Cenosphere Filler." *Advances in Polymer Technology,* 37, 761-769.

Jia, Bin-Bin, Li, Tong-Sheng, Liu, Xu-Jun and Cong, Pei-Hong. (2007). "Tribological behaviors of several polymer–polymer sliding combinations under dry friction and oil-lubricated conditions." *Wear,* 262(11–12), 1353-1359.

Jia, Zian, Li, Tiantian, Chiang, Fu-pen and Wang, Lifeng. (2018). "An experimental investigation of the temperature effect on the mechanics of carbon fiber reinforced polymer composites." *Composites Science and Technology,* 154, 53-63.

Jian, Gu, Gaohui, Wu and Xiao, Zhao. (2009). "Effect of surface- modification on the dynamic behaviors of fly ash cenospheres filled epoxy composites." *Polymer Composites,* 30(2), 232-238.

Kanchanomai, C., Noraphaiphipaksa, N. and Mutoh, Y. (2011). "Wear characteristic of epoxy resin filled with crushed-silica particles." *Composites Part B: Engineering,* 42(6), 1446-1452.

Kato, Koji. (2000). "Wear in relation to friction — a review." *Wear,* 241(2), 151-157.

Kim, J. I., Ryu, S. H. and Chang, Y. W. (2000). "Mechanical and dynamic mechanical properties of waste rubber powder/HDPE composite." *Journal of Applied Polymer Science,* 77(12), 2595-2602.

Kulkarni, S. M. and Kishore. (2002). "Effect of contact at the interface on the compressive properties of fly ash-epoxy composites." *The Journal of Adhesion,* 78(2), 155-166.

Kumar, S. Santhosh and Hiremath, Somashekhar S. (2014). "Microstructure and Mechanical Behavior of Nanoparticles Reinforced Metal Matrix Composites – A Review." *Applied Mechanics and Materials,* 592-594, 939-944.

Labella, Matthew, Zeltmann, Steven E., Shunmugasamy, Vasanth Chakravarthy, Gupta, Nikhil and Rohatgi, Pradeep K. (2014). "Mechanical and thermal properties of fly ash/vinyl ester syntactic foams." *Fuel,* 121, 240-249.

Lawrence, E. Nielsen. (1966). "Simple theory of stress- strain properties of filled polymers." *Journal of Applied Polymer Science,* 10(1), 97-103.

Lin, Tien Chih, Gupta, Nikhil and Talalayev, Anton. (2009). "Thermoanalytical characterization of epoxy matrix-glass microballoon syntactic foams." *Journal of Materials Science,* 44(6), 1520-1527.

Lord, Harold W. and Dutta, Piyush K. (1988). "On the Design of Polymeric Composite Structures for Cold Regions Applications." *Journal of Reinforced Plastics and Composites,* 7(5), 435-458.

Mallik, Sabuj, Ekere, Ndy, Best, Chris and Bhatti, Raj. (2011). "Investigation of thermal management materials for automotive electronic control units." *Applied Thermal Engineering,* 31(2), 355-362.

Manakari, Vyasaraj, Parande, Gururaj, Doddamani, Mrityunjay, Gaitonde, V. N., Siddhalingeshwar, I. G., Kishore, Shunmugasamy, Vasanth Chakravarthy and Gupta, Nikhil. (2015). "Dry sliding wear of epoxy/cenosphere syntactic foams." *Tribology International,* 92, 425-438.

Mathew, G., M.- Y., Huh, M., Rhee J., M.- H., Lee and C., Nah. (2004). "Improvement of properties of silica- filled styrene- butadiene rubber composites through plasma surface modification of silica." *Polymers for Advanced Technologies,* 15(7), 400-408.

Miyazaki, N. and Takeda, N. (1993). "Solid Particle Erosion of Fiber Reinforced Plastics." *Journal of Composite Materials,* 27(1), 21-31.

Mohan, N., Natarajan, S., Kumaresh Babu, S. P., Siddaramaiah, S. and Lee, Joong Hee. (2012). "Studies on Erosive Wear Behavior of UHMWPE-Filled Aramid–Epoxy Hybrid Composites." *Materials and Manufacturing Processes,* 27(4), 430-435.

Mondal, D. P., Das, S. and Jha, Nidhi. (2009). "Dry sliding wear behaviour of aluminum syntactic foam." *Materials & Design,* 30(7), 2563-2568.

Nabil, A. N. Alkadasi, G.Hundiwale, D. and Kapadi, U. R. (2004). "Effect of coupling agent on the mechanical properties of fly ash–filled polybutadiene rubber." *Journal of Applied Polymer Science,* 91(2), 1322-1328.

Nikhil, Gupta and Ruslan, Nagorny. (2006). "Tensile properties of glass microballoon- epoxy resin syntactic foams." *Journal of Applied Polymer Science,* 102(2), 1254-1261.

Norbert, Platzer. (1988). "Handbook of fillers for plastics." *Journal of Polymer Science Part C: Polymer Letters,* 26(6), 274-274.

Patnaik, Amar, Satapathy, Alok, Chand, Navin, Barkoula, N. M. and Biswas, Sandhyarani. (2010). "Solid particle erosion wear characteristics of fiber and particulate filled polymer composites: A review." *Wear,* 268(1), 249-263.

Pattanaik, Ashutosh, Satpathy, Mantra Prasad and Mishra, Subash Chandra. (2016). "Dry sliding wear behavior of epoxy fly ash composite with Taguchi optimization." *Engineering Science and Technology, an International Journal,* 19(2), 710-716.

Pool, K. V., Dharan, C. K. H. and Finnie, I. (1986). "Erosive wear of composite materials." *Wear,* 107(1), 1-12.

Poveda, Ronald L., Dorogokupets, Gleb and Gupta, Nikhil. (2013). "Carbon nanofiber reinforced syntactic foams: Degradation mechanism for long term moisture exposure and residual compressive properties." *Polymer Degradation and Stability,* 98(10), 2041-2053.

Prusty, Rajesh Kumar, Rathore, Dinesh Kumar, Shukla, Meet Jayesh and Ray, Bankim Chandra. (2015). "Flexural behaviour of CNT-filled glass/epoxy composites in an in-situ environment emphasizing temperature variation." *Composites Part B: Engineering,* 83, 166-174.

Ramakrishna, H. V., Priya, S. Padma and Rai, S. K. (2006). "Utilization of Granite Powder as Filler in Epoxy Phenol Cashew Nut Shell Liquid-toughened Epoxy Resin

for Impact and Compression Strength." *Journal of Reinforced Plastics and Composites,* 25(3), 227-234.

Ranjan, Pati Pravat and Alok, Satapathy. (2015). "A Study on Processing, Characterization and Erosion Wear Response of Linz–Donawitz Slag Filled Epoxy Composites." *Advances in Polymer Technology,* 34(4).

Ranney, M W, Berger, S E and Marsden, J G. (1974), *Interfaces in Polymer Matrix Composites,* 1st edition. Academic press, New York.

Rao, K. Sudarshan, Varadarajan, Y. S. and Rajendra, N. (2015). "Erosive Wear Behaviour of Carbon Fiber-reinforced Epoxy Composite." *Materials Today: Proceedings,* 2(4), 2975-2983.

Rao, R. N. and Das, S. (2011). "Effect of sliding distance on the wear and friction behavior of as cast and heat-treated Al–SiCp composites." *Materials & Design,* 32(5), 3051-3058.

Rashid, B., Leman, Z., Jawaid, M., Ghazali, M. J., Ishak, M. R. and Abdelgnei, M. A. (2017). "Dry sliding wear behavior of untreated and treated sugar palm fiber filled phenolic composites using factorial technique." *Wear,* 380-381, 26-35.

Ray, Dipa and Gnanamoorthy, R. (2007). "Friction and Wear Behavior of Vinylester Resin Matrix Composites Filled with Fly Ash Particles." *Journal of Reinforced Plastics and Composites,* 26(1), 5-13.

Ray, Dipa, Sarkar, B. K., Das, S. and Rana, A. K. (2002). "Dynamic mechanical and thermal analysis of vinylester-resin-matrix composites reinforced with untreated and alkali-treated jute fibres." *Composites Science and Technology,* 62(7), 911-917.

Rivera, J. and Karbhari, V. M. (2002). "Cold-temperature and simultaneous aqueous environment related degradation of carbon/vinylester composites." *Composites Part B: Engineering,* 33(1), 17-24.

Rugele, Kristine, Lehmhus, Dirk, Hussainova, Irina, Peculevica, Julite, Lisnanskis, Marks and Shishkin, Andrei. (2017). "Effect of Fly-Ash Cenospheres on Properties of Clay-Ceramic Syntactic Foams." *Materials,* 10(7), 828.

Sachinkumar, Narendranath, S. and Chakradhar, D. (2018). "Study on microstructure and tensile properties of fly ash AMCs welded by FSW." *AIP Conference Proceedings,* 1943(1), 020118.

Sanchez Saez, S., Gomez del Rio, T., Barbero, E., Zaera, R. and Navarro, C. (2002). "Static behavior of CFRPs at low temperatures." *Composites Part B: Engineering,* 33(5), 383-390.

Sankaran, S., Sekhar, K. Ravi, Raju, Govinda and Kumar, M. N. Jagdish. (2006). "Characterization of epoxy syntactic foams by dynamic mechanical analysis." *Journal of Materials Science,* 41(13), 4041-4046.

Satapathy, Alok, Patnaik, Amar and Pradhan, Manoj Kumar. (2009). "A study on processing, characterization and erosion behavior of fish (Labeo-rohita) scale filled epoxy matrix composites." *Materials & Design,* 30(7), 2359-2371.

Seidel, Arza. (2012), *Fillers*, 4th edition. John Wiley & Sons, New York.

Shahapurkar, Kiran, Garcia, Carlos D., Doddamani, Mrityunjay, Mohan Kumar, G. C. and Prabhakar, Pavana. (2018). "Compressive behavior of cenosphere/epoxy syntactic foams in arctic conditions." *Composites Part B: Engineering,* 135, 253-262.

Shalwan, A. and Yousif, B. F. (2014). "Influence of date palm fibre and graphite filler on mechanical and wear characteristics of epoxy composites." *Materials & Design,* 59, 264-273.

Shekhar, B. (2012). "Roadmap to 13 Million Tons." *Plastindia in-house journal,* 37, 6-11.

Shunmugasamy, Vasanth Chakravarthy, Pinisetty, Dinesh and Gupta, Nikhil. (2012). "Thermal expansion behavior of hollow glass particle/vinyl ester composites." *Journal of Materials Science,* 47(14), 5596-5604.

Shunmugasamy, Vasanth Chakravarthy, Pinisetty, Dinesh and Gupta, Nikhil. (2013). "Viscoelastic properties of hollow glass particle filled vinyl ester matrix syntactic foams: effect of temperature and loading frequency." *Journal of Materials Science,* 48(4), 1685-1701.

Siddhartha and Gupta, Kuldeep. (2012). "Mechanical and abrasive wear characterization of bidirectional and chopped E-glass fiber reinforced composite materials." *Materials & Design,* 35, 467-479.

Singh, Akant Kumar and Siddhartha. (2015). "Leverage of cenosphere filler size on mechanical and dry sliding wear peculiarity of polyester composites." *Journal of Composite Materials,* 49(22), 2789-2802.

Smith, Brooks, Szyniszewski, Stefan, Hajjar, Jerome, Schafer, Benjamin and Arwade, Sanjay. (2012). "Characterization of Steel Foams for Structural Components." *Metals,* 2(4), 399.

Srivastava, V. K. and Pawar, A. G. (2006). "Solid particle erosion of glass fibre reinforced flyash filled epoxy resin composites." *Composites Science and Technology,* 66(15), 3021-3028.

Srivastava, V. K. and Shembekar, P. S. (1990). "Tensile and fracture properties of epoxy resin filled with flyash particles." *Journal of Materials Science,* 25(8), 3513-3516.

Sundararajan, G., Roy, M. and Venkataraman, B. (1990). "Erosion efficiency-a new parameter to characterize the dominant erosion micromechanism." *Wear,* 140(2), 369-381.

Swetha, C. and Kumar, Ravi. (2011). "Quasi-static uni-axial compression behaviour of hollow glass microspheres/epoxy based syntactic foams." *Materials & Design,* 32(8), 4152-4163.

Tagliavia, G., Porfiri, M. and Gupta, N. (2009). "Vinyl Ester—Glass Hollow Particle Composites: Dynamic Mechanical Properties at High Inclusion Volume Fraction." *Journal of Composite Materials,* 43(5), 561-582.

Tagliavia, G., Porfiri, M. and Gupta, N. (2010). "Analysis of flexural properties of hollow-particle filled composites." *Composites Part B: Engineering,* 41(1), 86-93.

Tagliavia, G., Porfiri, M. and Gupta, N. (2010). "Analysis of hollow inclusion–matrix debonding in particulate composites." *International Journal of Solids and Structures,* 47(16), 2164-2177.

Thakur, Sunil and Chauhan, Santram. (2014). "Effect of micron and submicron size cenosphere particulate on mechanical and tribological characteristics of vinylester composites." *Proceedings of the Institution of Mechanical Engineers, Part J: Journal of Engineering Tribology,* 228(4), 415-423.

Thongsang, S. and Sombatsompop, N. (2006). "Effect of NaOH and Si69 treatments on the properties of fly ash/natural rubber composites." *Polymer Composites,* 27(1), 30-40.

Woldesenbet, Eyassu, Gupta, Nikhil and Jerro, H. Dwayne. (2005). "Effect of Microballoon Radius Ratio on Syntactic Foam Core Sandwich Composites." *Journal of Sandwich Structures & Materials,* 7(2), 95-111.

Wouterson, Erwin M., Boey, Freddy Y. C., Hu, Xiao and Wong, Shing-Chung. (2005). "Specific properties and fracture toughness of syntactic foam: Effect of foam microstructures." *Composites Science and Technology,* 65(11), 1840-1850.

Wright, W. W. (1991). "International encyclopedia of composites." *Polymer International,* 25(2), 132-132.

Yu, Ming, Zhu, Ping and Ma, Yingqi. (2012). "Experimental study and numerical prediction of tensile strength properties and failure modes of hollow spheres filled syntactic foams." *Computational Materials Science, 63*, 232-243.

Yusriah, L and Mariatti, M. (2013). "Effect of hybrid phenolic hollow microsphere and silica-filled vinyl ester composites." *Journal of Composite Materials, 47(2),* 169-182.

Zeltmann, Steven Eric, Gupta, Nikhil, R, Bharath Kumar B and Doddamani, Mrityunjay. (2016). "Dynamic mechanical analysis of cenosphere/HDP E syntactic foams". *American Society for Composites, 31st Technical Conference* Williamsburg, Virginia, USA.

Zeltmann, Steven Eric, Poveda, Ronald L. and Gupta, Nikhil. (2015). "Accelerated environmental degradation and residual flexural analysis of carbon nanofiber reinforced composites." *Polymer Degradation and Stability,* 121, 348-358.

Zhang, Liying and Ma, J. (2010). "Effect of coupling agent on mechanical properties of hollow carbon microsphere/phenolic resin syntactic foam." *Composites Science and Technology, 70(8),* 1265-1271.

Zhang, Liying, Roy, Sunanda, Chen, Ye, Chua, Eng Kee, See, Kye Yak, Hu, Xiao and Liu, Ming. (2014). "Mussel-Inspired Polydopamine Coated Hollow Carbon Microspheres, a Novel Versatile Filler for Fabrication of High Performance Syntactic Foams." *ACS Applied Materials & Interfaces, 6(21),* 18644-18652.

Zhu, Jiahua, Wei, Suying, Ryu, Jongeun, Budhathoki, Mahesh, Liang, Gang and Guo, Zhanhu. (2010). "In situ stabilized carbon nanofiber (CNF) reinforced epoxy nanocomposites." *Journal of Materials Chemistry, 20(23),* 4937-4948.

LIST OF PUBLICATIONS

INTERNATIONAL JOURNALS

1. <u>Kiran Shahapurkar</u>, Carlos Garcia, Mrityunjay Doddamani, G.C.Mohan Kumar and Pavana Prabhakar (2018),"Compressive behavior of cenosphere/epoxy syntactic foams in arctic conditions" *Composite Part B*, 135, 253-262. (**Elsevier, 4.920**)

2. <u>Kiran Shahapurkar</u>, Mrityunjay Doddamani, G.C. Mohan Kumar and Nikhil Gupta (2018), "Effect of cenosphere filler surface treatment on the erosion behaviour of epoxy matrix syntactic foams" *Polymer Composites*. (Accepted for publication) (**Wiley, 2.324**)

3. Carlos Garcia, <u>Kiran Shahapurkar</u>, Mrityunjay Doddamani, G.C.Mohan Kumar and Pavana Prabhakar (2018) "Flexural behavior of surface modified cenosphere/epoxy syntactic foams in arctic environment" *Composite Part B*, 151, 265-273. (**Elsevier, 4.920**)

4. <u>Kiran Shahapurkar</u>, Mrityunjay Doddamani and G.C. Mohan Kumar (2018) "Influence of surface modification on wear behavior of fly ash cenosphere/epoxy syntactic foam" *Wear*, (Under Review) (**Elsevier, 2.531**)

INTERNATIONAL CONFERENCES

1. <u>Kiran Shahapurkar</u>, Mrityunjay Doddamani, G.C. Mohan Kumar (2016) "Mechanical behavior of cenosphere/epoxy syntactic foam composites" *International Symposium for Research Scholars*, December 21-23, 2016, Indian Institute of Technology Madras, Chennai, India.

2. <u>Kiran Shahapurkar</u>, Mrityunjay Doddamani, G.C. Mohan Kumar (2017) "Tribological response of cenosphere/epoxy syntactic foams" *International Conference on Composite and Nano engineering*, July 16-20, 2017, Rome, Italy.

3. <u>Kiran Shahapurkar</u>, G.C. Mohan Kumar and Mrityunjay Doddamani (2017) "Quasi static compressive response of cenosphere/epoxy Syntactic foams" *26th International Conference on Processing and Fabrication of Advanced*

Materials, October 16-21, 2017, Chonbuk National University, Jeonju, South Korea.

4. <u>Kiran Shahapurkar</u>, Mrityunjay Doddamani and G.C. Mohan Kumar (2017) "Analysis of tensile properties of cenosphere/epoxy Syntactic foams" *International Conference on Advances in Polymer Science and Technology*, November 23-25, 2017, Indian Institute of Technology, New Delhi, India.

5. <u>Kiran Shahapurkar</u>, Mrityunjay Doddamani and G.C. Mohan Kumar (2017). "Quasi static compressive response of cenosphere/epoxy Syntactic foams." *International Conference on Advances in Materials and Processing: Challenges and Opportunities*, November 29-December 02, 2017 Indian Institute of Technology, Roorkee, India.

6. <u>Kiran Shahapurkar</u>, Mrityunjay Doddamani and G.C. Mohan Kumar (2018). "Tensile behavior of cenosphere/epoxy Syntactic foams." *International Conference on Design, Materials & Manufacture - IcDeM 2018*, January 29-31, 2018 National Institute of Technology Karnataka, Surathkal, India. DOI: 10.1063/1.5029676

7. <u>Kiran Shahapurkar</u>, Mrityunjay Doddamani and G.C. Mohan Kumar (2018). "Flexural response of Cenosphere/Epoxy Syntactic Foams" *7th International Engineering Symposium (IES2018)*, March 06-13, 2018 Kumamoto University, Kumamoto, Japan.

8. <u>Kiran Shahapurkar</u>, Mrityunjay Doddamani and G.C. Mohan Kumar (2018). "Erosion response of cenosphere/epoxy syntactic foams." *International Conference on Composite and Nano engineering*, July 15-21, 2018, Paris, France (Accepted).

BIO-DATA

1. Name   : Kiran Shahapurkar

2. Father's Name   : Hanmant Shahapurkar

3. Date of Birth   : 15th December 1988

4. Nationality   : Indian

5. Marital Status   : Single

6. Address   : Department of Mechanical Engineering

                           National Institute of Technology Karnataka

                           Surathkal, PO Srinivasnagar 575 025

                           Karnataka, India.

7. Mobile Number   : +91 9663732673

8. E-mail id.   : *kiranhs1588@gmail.com*

9. Educational Qualification :

Qualification	University/Board	Year of Passing
Ph.D. (Mechanical Engineering)	National Institute of Technology Karnataka	Pursuing
M.Tech. (Mechanical Engineering)	Visvesvaraya Technological University, Belgaum	2014
B.E. (Mechanical Engineering)	Visvesvaraya Technological University, Belgaum	2012